DEVELOPMENT OF A BIO-NANOPARTICLE DNA-BASED BIOSENSOR FOR TUBERCULOSIS DETECTION USING ISOTHERMAL AMPLIFICATION

By

Edith Torres-Chavolla

A DISSERTATION

Submitted to
Michigan State University
in partial fulfillment of the requirements
for the degree of

DOCTOR OF PHILOSOPHY

Biosystems Engineering

2011

ABSTRACT

DEVELOPMENT OF A BIO-NANOPARTICLE DNA-BASED BIOSENSOR FOR TUBERCULOSIS DETECTION USING ISOTHERMAL AMPLIFICATION

By

Edith Torres-Chavolla

Tuberculosis (TB) is the world's second deadliest infectious disease and it has been identified as a leading cause of death among HIV-positive patients. The standard test for TB diagnosis is smear sputum microscopy, which is not able to identify half of the positive TB infections. Several molecular based techniques have been explored for the rapid detection of *Mycobacterium tuberculosis*, but they require highly specialized equipment, which makes them expensive and difficult to implement in resource-constrained peripheral laboratories. The main objective of the dissertation was to develop a portable, bio-nanoparticle DNA based biosensor to detect *M. tuberculosis* using dextrin coated gold nanoparticles as electrochemical labels and isothermal helicase-dependent thermophilic amplification (tHDA). The gold nanoparticles were synthesized using a novel alkaline, dextrin driven alternative to the citrate-coated gold nanoparticles. Particles were obtained with a diameter between 5.9 and 16.8 nm and the effects of dextrin concentration, temperature, and pH over diameter and production rate were evaluated. The dextrin coated gold nanoparticles were functionalized with DNA probes and used as electrochemical labels for the DNA biosensor. The tHDA reaction was successfully optimized to amplify a specific fragment of *M. tuberculosis* (from the *IS6110* gene) in a regular heating block. Therefore, a thermocycler is not required for the DNA amplification, like in PCR. The obtained detection limit of the DNA biosensor was 0.01ng/µl of isothermally amplified DNA fragments using synthetic targets.

AKNOWLEDGEMENTS

I want to express my deepest gratitude and appreciation to everyone who contributed to the successful completion of this dissertation. Thank you very much to:

- Dr. Evangelyn Alocilja for being my mentor, for her guidance and support during my PhD, for her friendship, and most of all for believing in me since the very first day.
- The committee members for their guidance and support during my academic program: Dr. Bradley Marks, Dr. John Gerlach, and Dr. Joan Rose. Special thanks to Dr. Ericka Flores and Dr. Rosalba Gutierrez from Mexico for their support and encouragement during my undergraduate and graduate studies.
- Present and past members of the Alocilja's research group, especially Michael Anderson for his help and collaboration to the project, and the undergraduate students that I had the pleasure to work with: Romali Ranasinghe, Brian A. Castro, and Ryan Pawloski. I sincerely appreciate their help and contribution to the research project.
- Dr. Alicia Pastor-Lecha from the MSU Center for Advance Microscopy for her valuable help and guidance on TEM, and more importantly her friendship. Gracias Alicia.
- The Mexican Council of Science and Technology (CONACYT) for the PhD fellowship support.
- The funding agencies that support the Nano-biosensors laboratory research.
- The faculty and staff from the Biosystems & Agricultural Engineering department, especially Dr. Bakker-Arkema for his support and encouragement, Dr. James Steffe, and Barb Delong for their help during my graduate program.

- My family in MSU: Anne Serotkin and her family, Isis Tomik and the Fernandez-Torres family, the MSU Latin American Community, Lourdes Martinez, Cecilia Martinez, Itza Mendoza, Zenaida Moreno and Ana Becerril. I could not have done it without their help, friendship, and unconditional support. Thank you very much.
- And last but not least, to my dear family: my parents Victoria and Gilberto, my two sisters Lorena and Erika, and my brother David for their love, support, and encouragement. They are my strength. Thank you also to my friends in Mexico: Karla Duenas, Adriana Perez, Monika Barajas, Alma Barba, Norma Flores, and Lucila Trigueros for their unconditional support and friendship. **Muchas Gracias a todos!**

Edith Torres-Chavolla.

TABLE OF CONTENTS

LIST OF TABLES

LIST OF FIGURES

ABBREVIATIONS

AFB: Acid-fast bacilli

AIDS: Acquired immune deficiency syndrome

ANOVA: Analysis of variance

ATCC: American type culture collection

AuNPs: Gold nanoparticles

BCG: Bacillus Calmette-Guérin

BLASTN: Basic local alignment search tool (nucleotides)

CFP10: Culture filtrate protein 10

CFU: Culture forming units

DNA: Deoxyribonucleic acid

dNPT: Deoxyribonucleotide triphosphate

DPV: Differential pulse voltammetry

dsDNA: Double stranded DNA

DST: Drug susceptibility testing

DTT: Dithiothreitol

ELISA: Enzyme-linked immunosorbent assay

ESAT6: Early secretory antigen target 6

FAM: Fluorescein amidite

FM: Fluorescence microscope

HIV: Human immunodeficiency virus

HTB: Hickey-Tresner broth

IGRA: Interferon-gamma release assay (also known as INF-γ)

LAM: Lipoarabinomannan

LAMP: Loop-mediated isothermal amplification

LTBI: Latent tuberculosis infection

MDR-TB: Multidrug-resistant tuberculosis

MGIT: Mycobacteria growth indicator tube

MNPs: Magnetic nanoparticles

MODS: Microscopic-observation drug-susceptibility

MPs: Magnetic particles

Mtb: *Mycobacterium tuberculosis*

MTC: *Mycobacterium tuberculosis* complex

NAATs: Nucleic acid amplification tests

NADH: Nicotinamide adenine dinucleotide plus hydrogen

NID: Neglected infectious diseases

NMR: Nuclear magnetic resonance

PBS: Phosphate buffered saline

PCR: Polymerase chain reaction

POC: Point-of-care

PPD: Purified protein derivative

QDs: Quantum dots.

RFLP: Restriction fragment length polymorphism analysis

RIF: Rifampicin

SDA: Strand displacement amplification

SPCE: Screen printed carbon electrode

ssDNA: Single stranded DNA

Sulfo-SMCC: Sulfosuccinimidyl 4-*N*-maleimidomethyl cyclohexane-1-carboxylate

TB: Tuberculosis

TEM: Transmission electron microscopy

tHDA: Isothermal helicase-dependent thermophilic amplification

Tm: Melting temperature

TMA: Transcription-Mediated Amplification

VOCs: Volatile organic compounds

WHO: World health organization

XDR-TB: Extensively drug-resistant tuberculosis

Chapter 1

Introduction

Infectious diseases are still the number one cause of deaths in developing countries. Annually, around one million people die from malaria, 2.9 million from enteric infections and 5 million from AIDS and tuberculosis *(1)*. The development of better and widely available diagnostic tests would greatly contribute to the control of many infectious diseases, particularly in limited-resource settings. Better diagnostics may improve case-finding, case-management, and disease surveillance (*1*). Furthermore, drug resistant monitoring is fundamental to the control and reduction of infectious disease burden around the world, which requires constant testing, particularly in populations where the diseases are endemic.

The development and improvement of diagnostics for neglected infectious diseases (NIDs) does not represent commercial interest for diagnostic companies, since most people affected by them live in the poorest countries and can not afford to pay for cutting-edge diagnostic tests (*2*). For example, tuberculosis (TB) is the world's second deadliest infectious disease (1.7 million people die every year) (*3*), and the standard TB diagnostic technology in developing countries continues to be the sputum smear microscopy; which was developed in the 1880s and has remained almost the same since then. Despite its convenience, it has a low sensitivity ($\sim 10^3$ cells/ml), and half of all TB active cases are not detected with this technique. Besides, smear-negative TB disease is highly common in HIV co-infected patients (*4*). Among the novel and nonconventional detection methodologies are the nucleic acid amplification tests (NAATs). These have been extensively explored for active TB diagnosis. NAATs have high specificity and

sensitivity, and can provide same day results (detection time: from 2-8 h on processed specimens). However, NAATs require highly specialized personnel, expensive equipment, and are used only in proficient laboratories that can afford reference reagents to monitor the assay performance. Therefore, they are suitable for reference laboratories, but difficult to use in peripheral laboratories with limited resources (*5-7*).

Recently, nanomaterials (nanoparticles, nanotubes and nanowires) have been introduced to enhance molecular detection platforms, creating an entire new field in development called nanodiagnostics. Sensitivity enhancement has been achieved with the use of nanoparticles as tags or labels, especially in electrochemical DNA based technologies (*8-9*). Biosensors represent a promising alternative for the development of portable, easy to use and inexpensive testing devices that can be used in limited resource settings to detect infectious diseases.

The present dissertation describes the development of a DNA-based electrochemical biosensor for tuberculosis detection using dextrin coated gold nanoparticles and isothermal helicase-dependent amplification. Chapter 2 presents a literature review of relevant materials to the research project, including tuberculosis detection, isothermal amplification techniques, biosynthesis of gold nanoparticles, and gold nanoparticle-DNA based detection methodologies. Two different approaches were evaluated for the biosynthesis and functionalization of gold nanoparticles and are presented in chapter 3. The first approach used a microorganism (*Thermomonospora curvata*) for the gold nanoparticle production. The second approach used dextrin as a capping agent for the alkaline biosynthesis of gold nanoparticles. Chapter 4 describes the design and development of the nanoparticle based electrochemical DNA biosensor for tuberculosis detection using synthetic targets, including the development and application of the isothermal target DNA amplification protocol. Finally, Chapter 5 presents a recommendation

of future research work derived from this dissertation. The following sections of the introduction describe the hypothesis, objectives and novelty of the project.

1.1 Hypotheses

The research presented in this dissertation was based on the following hypotheses:

- Gold nanoparticles can be synthesized at alkaline pHs in a single step reaction using biomolecules as reduction and capping agents.
- Oligo-functionalized dextrin coated gold nanoparticles can be used as electrochemical labels to translate DNA hybridization events into electrochemical signals.
- Amplification of IS*6110* DNA fragment from *Mycobacterium tuberculosis* can be accomplished at a single temperature.
- Isothermally amplified DNA products can be detected by a nanoparticle based biosensor platform.

1.2 Research objectives

The overall objective of this dissertation is to develop a DNA biosensor to detect *M. tuberculosis* using a single temperature for DNA amplification and dextrin coated gold nanoparticles for signal identification.

The specific objectives are:

- To synthesize gold nanoparticles using bacteria and carbohydrates as alternatives to the conventional citrate method.
- To functionalize biosynthetic gold nanoparticles with DNA probes (oligonucleotides).

- To design and develop an isothermal amplification protocol to specifically amplify a DNA fragment of the IS*6110* gene of *Mycobacterium tuberculosis*.
- To develop an electrochemical detection system based on dextrin coated gold nanoparticle detection using SPCE.

1.3 Research novelty and significance

The novelty of the research presented in this dissertation relies on the use of a novel dextrin coated gold nanoparticle as an electrochemical label on a DNA-based biosensor platform. Several DNA-based detection strategies have been explored using gold nanoparticles as tags, labels or carriers for additional labeling molecules, to improve the sensitivity of the detection system. Nevertheless, the use of biosynthetic gold nanoparticles for these applications remains unexplored. To the best of our knowledge, this is the first report of successful dextrin coated gold nanoparticle functionalization with DNA probes, and is the first report that utilizes these gold nanoprobes for the hybridization and electrochemical detection of a specific target DNA sequence using a biosensor platform.

Commonly, DNA-based biosensors require pre-detection steps (sample preparation), which include target amplification using PCR. This technique requires the use of a thermocycler, which increases the cost of the detection systems and increases the difficult of the utilization and implementation of biosensing platforms in limited resource settings. Therefore, isothermal amplification alternatives have been recently proposed and explored that do not require the use of a thermocycler for target DNA preparation. The research presented in this dissertation demonstrates the first application of isothermal helicase-dependent amplification (tHDA) on a

DNA-based biosensor for tuberculosis detection. A summary of the novelty of the research presented in this dissertation by comparison with current literature is presented in Table 1-1.

Table 1-1. Research contribution to the literature and novelty of the dissertation project.

SUBJECT	REFERENCES		
Biosynthesis of AuNP	Ahmad et al., 2003	Mohanpuria et al., 2007	Bharde et al., 2007
One step GlycoAuNP biosynthesis	**Anderson et al., 2010**		
Dextrin coated AuNP DNA functionalization	**Anderson et al., 2010**		
Application of dextrin coated AuNP in biosensing	**Torres-Chavolla et al., 2011**		
NP-based electrochemical biosensor	Wang et al., 2005	Castañeda et al., 2007	Guo and Dong, 2009
tHDA for microbial detection	Chow et al., 2008	Goldmeyer et al., 2008	Andersen et al., 2009
NP-based electrochemical biosensor for TB DNA detection using isothermal amplification (tDHA)	**Torres-Chavolla and Alocilja, 2011**		

Note: Gray blocks represent the papers published from this dissertation.

References

1.4 References

1. Mabey, D., Peeling, R. W., Ustianowski, A. & Perkins, M. D. Tropical infectious diseases: Diagnostics for the developing world. *Nature Reviews Microbiology* **2**, 231-240 (2004).

2. Joseph, M. N., Sylvain, B. & Giorgio, R. "Piggy-Backing" on Diagnostic Platforms Brings Hope to Neglected Diseases: The Case of Sleeping Sickness. *PLoS Neglected Tropical Diseases* **4**, e715 (2010).

3. WHO Global Tuberculosis Control 2009. Epidemiology, Strategy, and Financing. http://www.who.int/tb/publications/global_report/2009/pdf/full_report.pdf. 2009.

4. Perkins, M. D., Roscigno, G. & Zumla, A. Progress towards improved tuberculosis diagnostics for developing countries. *The Lancet* **367**, 942-943.

5. Pai, M. & O'Brien, R. New diagnostics for latent and Active Tuberculosis: State of the art and future prospective. *Seminars in Respiratory and Critical Care Medicine* **29**, 560-568 (2008).

6. Palomino, J. C. Nonconventional and new methods in the diagnosis of tuberculosis: feasibility and applicability in the field. *European Respiratory Journal* **26**, 339-350 (2005).

7. Somoskovi, A., Gutierrez, C. M. & Salfinger, M. Laboratory diagnosis of tuberculosis: novel and nonconventional methods. *Reviews in Medical Microbiology* **19**, (2008).

8. Jain, K. K. Nanotechnology in clinical laboratory diagnostics. *Clinica Chimica Acta* **358**, 37-54 (2005).

9. Jain, K. K. Applications of Nanobiotechnology in Clinical Diagnostics. *Clinical Chemistry* **53**, 2002-2009 (2007).

Chapter 2

Literature review

2.1 Tuberculosis

Tuberculosis (TB) is the world's second deadliest infectious disease (1.7 million people die every year). Approximately 9.2 million new cases of TB occur each year worldwide. TB has been identified as a leading cause of death among HIV-positive patients (1.37 million people per year infected with HIV are co-infected with TB) (*1*). Africa and Southeast Asia have the highest incidence (Table 2-1). TB is an airborne infectious disease caused by *Mycobacterium tuberculosis* (Mtb). Infection is spread through aerosols released in the air by a contagious person. Mtb is an aerobic, rod-shape bacterium (as observed with Ziehl-Neelsen staining or acid-fast staining), that belongs to the *Micobacteriaceae* family (*2*). Mtb is a facultative intracellular (macrophages) pathogen that has a slow generation time (15-20h) which may contribute to its virulence. In optimal in vitro growing conditions, it takes from 1-6 weeks to get visual colonies in selective agar media (*2*).

The bacilli cell wall is composed of an extensive array of complex lipidoglycans (mycolic acids, trehalose dimycolate [cord factor], and sulfolipids) (*2,3*). Mtb possesses the ability to parasite the macrophages of its host. After phagocytosis by the macrophage, the Mtb is retained within a phagocytic vacuole until the host cell dies through necrosis or apoptosis (*4*). The infected macrophages together with lymphocytes, produced by a localized pro-inflammatory response, will form the granuloma or tubercle that gives the name to the disease.

Table 2-1. Estimated incidence and mortality of TB and HIV-TB co-infection in 2007[1]. Summary by WHO region.

	Incidence*				Mortality*				•
	TB		HIV-TB		TB		HIV-TB		
REGION	Number	Rate+	Number	Rate+	Number	Rate+	Number	Rate+	(%)
AFR	2 879 434	363	1 080 328	136	734 891	93	377 535	48	38
AMR	294 636	32	33 356	4	40 616	4	7 892	< 1	11
EMR	582 767	105	20 517	4	104 300	19	7 726	1	3.5
EUR	431 518	49	42 322	5	63 765	7	8 096	< 1	9.8
SEAR	3 165 139	181	146 042	8	537 616	31	40 465	2	4.6
WPR	1 919 306	108	51 483	3	290 546	16	14 503	< 1	2.7
GLOBAL	**9 272 799**	**139**	**1 374 048**	**21**	**1 771 733**	**27**	**456 218**	**7**	**15**

AFR=Africa, AMR=The Americas, EMR=Eastern Mediterranean, EUR=Europe, SEAR=South-East Asia, WPR=Western Pacific.

• HIV prevalence in incident TB cases; * number of cases or deaths per year; + per 100,000 population per year

[1] WHO Global Tuberculosis Control 2009 http://www.who.int/tb/publications/global_report/2009/pdf/full_report.pdf
WHO Global Tuberculosis Database http://apps.who.int/globalatlas/dataQuery/default.asp

This stage of the infection is classified as "latent" TB, during which there are no symptoms and the host does not transmit the infection. It is estimated that approximately one-third of the world's population is currently infected with TB. Of these latent TB cases, only 5-10% become sick ("active" TB). The disease becomes active when the immune status of the host changes and the center of the contained granuloma spills viable, infectious bacilli into the pulmonary cavities (airways) (*4*).

Pulmonary tuberculosis represents around 85% of TB cases. Extrapulmonary tuberculosis is less common (15%). This form of infection includes: lymph node, pleural, genitourinary, skeletal, central nervous system, abdominal, and pericardial tuberculosis. Epidemic rates of extrapulmonary cases have increased since the HIV epidemic. Immuno-compromised patients are more susceptible to develop extrapulmonary TB. The immune system fails to contain *M. tuberculosis*, producing TB bacillemia and subsequent dissemination to non-pulmonary sites (*5*).

Cutaneous tuberculosis (another form of TB) can be classified according to the transmission and propagation mechanism by (i) direct inoculation (ii) through contiguous infection, or (iii) hematogenous dissemination. The direct inoculation usually occurs within health care or laboratory personnel that have been accidentally exposed with a contaminated material. Another form of the disease occurs within people that are exposed to *Mycobacterium tuberculosis* through a household member with pulmonary TB. Contiguous infection and hematogenous dissemination are produced by the propagation of TB from an active focus from deep tissue (commonly lymph node or bone) (*6*).

Besides person-to-person aerosol transmission, other route of TB infection could be the consumption of un-pasteurized contaminated milk from cattle infected with *M. bovis* (animal-to-human transmission) (*7*). Bovine tuberculosis is caused by *M. bovis*, which is a member of the

Mycobacterium tuberculosis complex (MTC)[2]. All the members of this group can potentially cause TB in humans. *M. bovis* hosts include not only cattle, but also other domestic livestock (goats, deer, buffaloes, camels and llamas) as well as numerous wild animal species (*8*). Aerosol transmission of the disease could also occur between infected animals and humans.

High incidence and mortality rates of TB are exacerbated by multidrug-resistant and extensively drug-resistant TB cases. Multidrug-resistant TB (MDR-TB) is described as TB infection caused by an Mtb strain that is resistant to at least isoniazid and rifampicin, the two most powerful first-line anti-TB drugs. MDR-TB has to be treated with second-line anti-TB drugs (which are more expensive and produce more adverse reactions) during extensive chemotherapy (approximately two years) (*4*). Extensively drug-resistant TB (XDR-TB) is caused by an Mtb strain that is resistant to at least rifampicin and isoniazid among the first-line anti-TB drugs; any member of the quinolone family; and at least one of the following second-line anti-TB injectable drugs: Kanamycin, capreomycin or amikacin (*9*).

Exact incidence rates for drug resistant TB are currently unknown but it has been estimated that more than 400,000 new cases of MDR-TB occur each year and XDR-TB has been reported worldwide (*10*). Rifampicin resistance mutations are mainly located in an 81-bp region within the *rpoB* gene. Approximately 95% of RIF-resistant strains have mutations in this region (*11*). Some codons within this location are more frequently associated with resistance-encoding mutations, especially 531, 526 and 516 (*12*). Isoniazid mutations are commonly located in four different genes (*katG*, *inhA*, *ahpC* and *oxyR*) (*12*) which increase the complexity of detection. It has been estimated that approximately 80% of rifampicin-resistant cases are also MDR-TB;

[2] Mycobacterium tuberculosis complex includes: *M. tuberculosis*, *M africanum* (subtypes I and II), *M. bovis*, attenuated *M. bovis* (BCG vaccine strain), *M. bovis* subsp. *caprae*, *M. microti*, *M. canettii, M. pinnipedii.*

therefore, rifampicin resistance can potentially be used as marker to detect MDR-TB for screening purposes (*13*,*14*). TB diagnosis depends on sputum smear microscopy (to detect the presence of the microorganism), culture, tuberculin skin test, and chest radiography. The following sections describe the traditional, nonconventional, and novel alternatives for the detection and identification of Mtb.

2.1.1 Traditional methods of detection

The standard TB diagnostic technology in developing countries continuous to be the sputum smear microscopy; it was developed in the 1880s and has remained almost the same since then. It relies on the presence of acid-fast bacilli (AFB) in stained smears. Despite its convenience; it can not differentiate between MTC strains and other non-turberculosis mycobacteria (*15*), it has a low sensitivity (sputum must contain 5000-10,000 bacilli/ml to be detectable by microscopy), and half of all active cases of TB are not detected with this technique (*16*). Besides, smear-negative TB disease is highly common in HIV co-infected patients (*17*). Some modifications to the bacilloscopy have been explored to improve its sensitivity including sputum liquefaction and concentration using sodium hypochlorite and centrifugation. Fluorescence microscopy has shown to improve the rate of detection, but the main disadvantage of using fluorescence is the need of a special detector in the microscope, which increases the cost of the assay (*17*). Some alternatives to design a cheaper fluorescence microscope (FM) are under development, including the design of low-cost ultrabright light-emitting diodes with long lifespan to replace expensive lamps currently used in FM (*18*).

Culture (growth) detection remains to be one of the gold standards for TB detection. It is not only a TB detection methodology, but also provides material (isolates) for further identification

and testing like drug susceptibility or genetic characterization. Common media for Mtb culture includes Löwensten-Jensen (LJ) medium and Middlebrook agar (*19*). The sputum samples have to be purified and liquefied before media inoculation; after the purification, the samples are incubated for growth for several weeks (6-8). After growth, the isolates are characterized using biochemical tests. The entire procedure is very laborious and time consuming. Additionally, biosafety level 3 facilities are required for Mtb growth and isolation, therefore the routinary use of culture in TB diagnostic is privative for limited-resource settings. Some alternatives have been explored to reduce the time necessary for culture, including radiometric (BACTEC TB-460® Becton Dickinson) and fluorescence based assays (MGIT® Becton Dickinson). These alternatives have reduced the culture time from weeks to 9-12 days (*20*). The mycobacteria growth indicator tube (MGIT) is based on a modified Middlebrook broth containing a fluorescence indicator that is activated by Mtb oxygen consumption. This has been used in automated systems that can incubate the sample and read the fluorescence in the same equipment (BACTEC MGIT 960 system). Sensitivity improvement and shorter incubation times have been obtained with this system (*19-21*); however, the cost-effect and impact of the system in limited-resource settings has not been studied or evaluated (*20*).

Drug susceptibility testing (DTS) in solid media requires between 28-42 days for identification. The use of liquid culture alternatives, like the ones described above (BACTEC and MGIT) can reduce this time to 10 days (*18*). The microscopic-observation drug-susceptibility (MODS) is a modification of the common bacilloscopy that incorporates antimicrobial drugs and a growth stage to identify MDR-TB. It uses an inverted light microscope and Middlebrook broth media modified with the antimicrobial agents for DTS. MODS has shown better sensitivity (97.8%) than the culture itself. It also reduced the time needed for

positive culture and susceptibility test (7 days) when compared with automated mycobacterial culture and LJ culture (*18*).

2.1.2 Immunological based detection systems

The immunological assays are based on the detection of specific antibodies that are produced by the immune system when TB infection is present; most commonly based on enzyme-linked immunosorbent assay (ELISA). Serological tests are usually less expensive than traditional methods and easy to use, which make them suitable for limited-resource settings (*16*); nevertheless, most of the TB antigen-antibody based assays commercially available have not shown adequate accuracy and have low sensitivity (16-57%) (*16,22,23*). The first developed serological assays used partially purified antigens which showed poor specificity. The second generation used highly purified native or recombinant antigens, which increased the specificity but lowered the sensitivity (*20*). Specificity ranges between 62-100% have been reported (*23,24*). Additionally, it has been found that the immunological response to TB is not homogeneous. It depends on several factors like, previous exposure to non-tuberculosis mycobacteria, HIV co-infection and BCG vaccination, among others. It has also been estimated that around 30% of smear-positive pulmonary TB patents do not have detectable antibody levels that can be identified with the antigens used in current assays (*16,20,22*).

The tuberculin skin test (TST) is commonly used to detect latent TB infection (LTBI). It uses a purified protein derivative (PPD) which is a crude mixture of antigens with the limitation that some of them are shared among Mtb, BCG, and non-TB mycobacteria. Therefore, it has low specificity among BCG vaccinated populations (*18,20*). Recently, the interferon-gamma release assay (INF-γ or IGRA) has been introduced for LTBI detection. IGRAs are *in vitro* blood tests

based on the use of mycobacterial antigens to stimulate T-cells. If the cells have been previously exposed to TB antigens, they will produce INF-γ when they are re-exposed to these antigens. The most commonly used antigens for this assay are the early secretory antigen target 6 (ESAT6) and the culture filtrate protein 10 (CFP10). These two antigens are specific to Mtb. Commercially available INF-γ assays include the QuantiFERON-TB® assay (Cellestis Ltd) and the T SPOT-TB test (Oxford Immunotec) (*18,20*). Although IGRAs have high specificity (75-90%) and previous BCG vaccination does not cause interference, they can not differentiate between active and latent TB. Overall they are useful for LTBI detection and may have some potential application in active TB diagnosis in low-incidence settings and selected population groups (children, immunocompromised patients, and individuals with smear-negative extra pulmonary TB) (*18,24*).

Among the promising new developments in immuno-based assays are the antigen detection-based tests. Instead of searching for antibodies produced in TB patients, which are depending on immuno-supression and other factors; the presence of specific TB antigens in sputum, serum, and urine can be evaluated. The lipoarabinomannan (LAM) is a heat-stable glycolipid that has been found in the urine of ~80% of culture-confirmed TB cases in several studies (*25,26*). Based on these findings, a prototype for a commercially available urine test is under development (*18*).

2.1.3 Molecular based detection systems

Among the novel and nonconventional detection methodologies are the nucleic acid amplification tests (NAATs). These have been extensively explored for active TB diagnosis. NAATs have high specificity and sensitivity, and can provide same day results (detection time: from 2-8 h on processed specimens). The molecular detection methodologies are based on the

selection and design of oligonucleotides (primers and probes) to specifically hybridize and/or amplify a particular DNA fragment that can be specific to *M. tuberculosis* or present exclusively in MTC members, which allows the differentiation between TB mycobacteria and non-TB mycobacteria. Therefore, DNA based methodologies have very high specificity (varying between 90-99%). Table 2-2 shows representative examples of target genes or DNA fragments that are commonly used for the specific identification of Mtb in both in-house and commercial molecular assays.

Table 2-2. Common specific genes used for the DNA-based detection and identification of tuberculosis species.

Gene	Target TB specie(s) and applications	References
hsp65	Mycobacterium species identification	(*27*,*28*)
secA1		(*29*)
IS*6110*	MTC complex identification	(*30-33*)
IS*1561*		(*34*)
IS*1081*		(*35*)
cfp32		(*28*,*36*)
rpo B	Mtb - rifampicin resistance	(*11*,*37*,*38*)
katG *katC*	Mtb - isoniazid resistance	(*37*,*39*,*40*)
inhA		(*37*,*39*,*40*)
kasA		(*41*,*42*)
oxyR	Mtb - isoniazid resistance MTC complex identification	(*43*)
gyrB *gyr A*	Mtb - fluoroquinolones resistance MTC complex identification	(*44*,*45*)
rrs *rpsL*	Mtb – streptomycin resistance	(*46*)
pncA	Mtb – pyrazinamide resistance MTC complex identification	(*43*)
embB	Mtb – ethambutol resistance	(*46*)

Sensitivity rates of a TB PCR-based assay (DNA amplification) have been reported between 90-100% for smear positive, and 60-70% for smear negative, culture positive sputum samples (*16*,*47*). Although the sensitivity is lower than microbial culture (up to 98%); it can be optimized with sample preparation treatments (*16*). The sensitivity of nucleic acid based technologies also depends on the type of specimen (sample) that is used for the DNA identification; it ranges from 60-99% for respiratory specimens and 30-85% for extra pulmonary specimens (*15*). Overall the sensitivity of DNA based detection methodologies decreases with smear-negative samples for both pulmonary and extra pulmonary species. One of the main advantages of DNA based technologies is that they can identify the presence or absence of the microorganism to detect non-pulmonary TB (i.e. tuberculosis of the central nervous system) in samples where the number of microorganisms is commonly low (i.e., cerebrospinal fluid) and the visualization with microscopy becomes more challenging (*15*). There are several commercially available tests based on nucleic acid amplification (Table 2-3).

Table 2-3. Representative commercially available NAAT's for the direct detection of Mtb.

Test	Technology	Sensitivity* (%)		Specificity (%)	References
		Re	Ex	Overall	
Amplicor® (Roche)	PCR	83-97	27-85	91-100	(*48*,*49*)
AMTD® (Gen-Probe)	Transcription-Mediated Amplification (TMA)	86-98	74-100	92-100	(*49*,*50*)
BD Probe Tec® (Becton)	Strand displacement Amplification (SDA)	60-100	33-86	99-100	(*49*,*51*)
GenoType® (Hain Lifescience)	TMA	61-99		99-100	(*49*)

Re = Respiratory specimens. Ex = Extra pulmonary specimens. *Ranges include smear positive and smear negative samples.

Several molecular approaches have been used for the identification of MTC strains. These methodologies are not for direct detection. They require previous steps of growth or amplification and are used to identify mycobacteria strains. Some examples include nucleic acid probe hybridization, restriction fragment length polymorphism analysis (RFLP) of the *hsp65* gene (*27*), solid phase hybridization (line-probe assay) (*52*), single nucleotide polymorphism (SNP) (*43*), and DNA sequencing (*53*). These methodologies are based on the identification of molecular differences between the MTC species, which allows specific strain identification. Some examples of commercially available tests based on these methodologies include: GenoType® MTBC (Hain Lifescience), AccuProbe® (Gen-Probe), and INNO-LiPA® Mycobacteria assay (Innogenetics) (*15*).

Molecular methods to detect drug resistance Mtb (MDR-TB) are based on identifying the presence or absence of point mutation in specific genetic regions which are known to produce resistivity (*12*). These nucleic acid hybridization methodologies are based on the recognition of a genetic region of the clinical strand (target) with a specific oligonucleotide probe. If a mismatch occurs in some nucleotide position due to the presence of mutation, the hybridization thermodynamics change (*12*). Hybridization probes are designed to bind mismatched (mutated) sequences or perfectly matched sequences (rifampicin-sensitive sequence) (*54*). DNA MDR-TB detection methodologies include: sequencing (*12*), real-time PCR (*54*), allele specific PCR (*55*), microarrays (*54*), and line probe assays (*9,37*). Line-probe assays are strip-based test that use PCR and reverse hybridization probes. Commercially available examples include the INNO-LiPA Rif.TB® kit (Innogenetics) and the GenoType MTBDR plus® assay (Hain Lifescience). Specificity and sensitivity values between 95-99% have been recently reported for the GenoType assay to detect rifampicin resistance in smear-positive sputum samples when compared with

conventional drug susceptibility testing (DST) (*37*). The WHO recently endorsed the line-probe assays for MDR-TB screening, but to be used only with culture isolates and smear-positive samples. It is not recommended to replace conventional culture and DST (*9*,*18*). Similar approach as the ones described to detect rifampicin and isoniazid resistance has been explored for the detection of other single point mutations that confer resistance to other antibiotics (Table 2-2), including the ones who cause XDR-TB (*46*).

In summary, molecular based assays have high specificity and sensitivity, and can provide same day results. However, DNA amplification assays require highly specialized personnel, expensive equipment, and are used only in proficient laboratories that can afford reference reagents to monitor the assay performance. Therefore, they are suitable for reference and peripheral laboratory implementation, but difficult to use in settings with limited resources (*15*,*18*,*20*).

2.1.4 Biosensor platforms for tuberculosis detection

Biosensors can be defined as analytical devices that integrate a biological receptor (sensing element) with a transducer to quantify the interaction between receptor and target, and translate this biochemical interaction into an optical or electrical signal (Figure 2-1). Based on different sensing elements, the biosensor can be divided into immuno-sensor, DNA sensor, cell-based biosensor, aptasensor, enzyme-based sensor, and other combinations. DNA based biosensors usually relies on the immobilization of a single-strand DNA (ssDNA) probe onto a surface to recognize its complementary DNA target sequence by hybridization. Transduction of the DNA hybridization can be measured electronically (*56*), optically (*57-59*), electrochemically (*60-62*), or by using mass-sensitive devices (*63*). The following paragraphs describe some of the most

representative examples of TB biosensors recently published that have been evaluated and validated using real samples. A special summary of gold nanoparticle electrochemical-based biosensors for TB is reviewed in chapter 5.

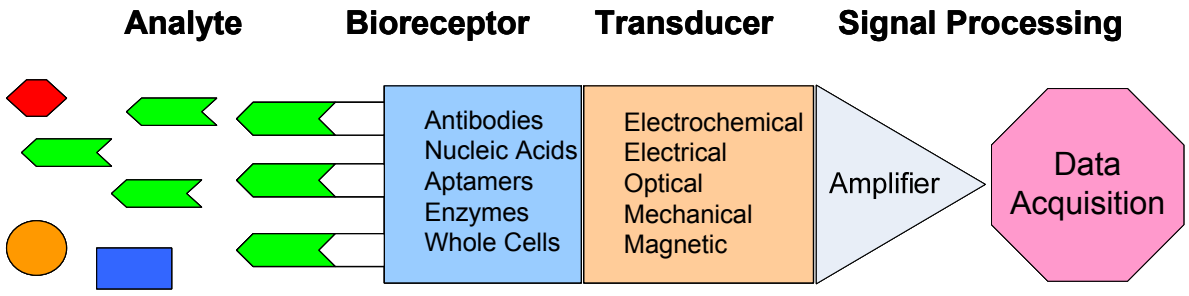

Figure 2-1. Schematic representation of a biosensor and its components. (For interpretation of the references to color in this and all other figures, the reader is referred to the electronic version of this dissertation).

In 2009, Lee and collaborators (*64*) published a TB biosensor platform in which magnetic nanoparticles (MNPs) functionalized with anti-BCG monoclonal antibodies were used for mycobacteria concentration into a microfluidic chamber; and nuclear magnetic resonance (NMR) was used for detection. The obtained sensitivity using BCG as a surrogate for *M. tuberculosis* was 20 CFU/ml in sputum. The detection time was 30 min. The portable device has an NMR-filter that enhances the detection sensitivity. The filter captures the bacteria from large sample volumes and enables on-chip separation of bacteria from unbound MNPs. The captured BCG cells are then resuspended by reversing the flow direction. The platform was evaluated using spiked sputum samples, and the results were compared with standard TB diagnostic tests. After sputum liquefaction (sample preparation) 1 ml of each sample was passed, filtered and detected

through the system. The lab-on-chip platform could potentially be used for the TB detection at the point-of-care level.

In 2010, Gazouli and collaborators (*65*) reported the detection of unamplified TB DNA using quantum dots (QDs) and magnetic particles (MPs). QDs were labeled with DNA probes that specifically hybridized to a fragment of the IS*6110* gene (for *M. tuberculosis* detection) and IS*900* gene (for *M. avium* subsp. *paratuberculosis* detection). The QDs where used as transducers for the sandwich hybridization reaction into a fluorescent signal. The MPs where functionalized with a DNA probe targeting a fragment of the 23S rRNA gene (*Mycobacterium* ssp. capture) and used to concentrate and isolate the DNA targets. For the fluorescence identification, a simple UV light apparatus was used for direct visualization. The detection limit in pure cultures was 12.5 ng/20μl sample volume. The detection system was evaluated using isolates from bronchoalveolar specimens among other specimens. The overall accuracy of the QD method when compared to real-time PCR was from 70-90% depending on the sample type. The entire detection procedure was conducted in 2 hours. This methodology can be used as an alternative for TB detection at the point-of-care level.

2.1.5 Development of point-of-care diagnostics

TB diagnostics and detection are performed at three different levels within the health care system: 1) Reference (central) laboratory, which is usually a national laboratory that performs highly specialized TB assays (including gold standards and molecular approaches) for genotypification and identification, 2) Regional (peripheral) laboratory, which usually performs smear microscopy and TB culture in some cases, and 3) Health center, which is a clinical facility that does not perform mycobacteriology testing. This is the stage that is completely focused on

patient care and is in this first-entrance or point-of-care facilities where new rapid, easy to use, inexpensive and accurate detection tools, that do not required highly trained personal or a laboratory facility, are needed the most. Examples of this type of test include urine-based, breath-based, or skin-based detection assays; which are non-invasive and easy to perform without the need of specialized trained personal or a microbiology laboratory. Some of these platforms are currently being developed (*17*,*18*,*66*). Point-of-care (POC) TB tests are crucial in the control and prevention of TB, particularly in endemic countries with limited resources. The low detection rate among the TB infected population is one of the main limitations in TB control. It has been estimated that an accurate POC single-visit test with only 85% sensitivity and 97% specificity could save 392,000 lives per year (or 22.4% of the current annual deaths) if widely implemented (*66*,*67*). A less specific but still sensitive test could be used for screening and positive results could be selected for further testing.

The ideal POC test would have to be equipment free, minimum reagents, able to be performed with no electricity, and resistant to high ambient temperatures and humidity. Direct detection of the microorganism at the POC level by bacilloscopy or culture is not feasible; therefore, secondary detection molecules (nucleic acids, components of the cell wall, and secreted proteins or metabolites) are better alternatives for TB POC detection (*66*). Metabolic biomarkers have been explored in order to develop a TB test based on the detection of volatile organic compounds (VOCs) in breath or in the head space of clinical specimens. It has been recently reported that there might be measurable VOCs that are predictive of TB and specific to the MTC (*68*).

A recent example towards POC test development and implementation is the automated system GeneXpert® (Cepheid). The apparatus is based on a microfluidic platform that performs

the three main steps of a NAAT in one equipment: sample preparation and DNA extraction; DNA amplification; and detection of amplified product. The entire process is performed in a single cartridge, it uses real-time PCR and can identify Mtb and rifampicin resistance in less than 120 minutes (*18*). The test has been evaluated in clinical settings and it was recently endorsed by the WHO with the objective of making the technology available at discounted prices for countries with limited resources. The equipment is rapid and easy to use, but still remains laboratory based (non-portable). The approximate cost of the instrument has been estimated to be US$17,000 and the cost per test (cartridge) around US$16 each. This could limit its implementation in POC settings with limited resources where TB is endemic (*66*).

Among the technologies that have promising applications in the development of POC TB diagnostics are the isothermal DNA amplification based tests and the nanotechnology application for TB biomarkers detection (*66*). Isothermal amplification techniques are an alternative to traditional PCR amplification (which requires a thermocycler) that can be performed in a regular thermoblock or water bath at a single temperature. The main disadvantage for POC application of isothermal DNA amplification procedures is that the DNA still needs to be extracted from the specimen (sputum), and this sample preparation step remains laboratory based. Improvements in the simplification of DNA isolation techniques from sputum are still in need for the adoption of molecular based technologies at the POC level. Another alternative is the development of direct detection isothermal tests that do not require DNA isolation or at least simplify the sample processing procedure. For this purpose, a urine test could provide an easy-to-process sample. Transrenal mycobacterial DNA has been recently proposed as potential detection target for the development of rapid TB diagnostics. This application is still under development (*69*).

Recently, the use of nanomaterials to enhance TB diagnostics started to be explored. Nanoparticles can enhance the sensitivity of detection platforms when used as tags or labels that amplify the detection signal. They can also be used as alternatives to isolate and concentrate bacterial DNA from the samples. The following sections describe in detail the advances in both isothermal DNA amplification and nanoparticle based detection technologies as well as their application in biosensor platforms.

2.2 Isothermal nucleic acid amplification techniques

The polymerase chain reaction (PCR) is one of the most widely used techniques in molecular biology laboratories. Developed in 1983, it is now robust and versatile with diverse applications for the study of oligonucleotides and recombinant DNA technologies (*70*). PCR is an *in vitro* cyclic replication that allows the amplification of a specific DNA or RNA fragment. The amplified target (~10^6 copies) can be used for further analysis of the specific sequence or for identification. The methodology is conducted in a thermocylcer that allows the automatic cyclic changes in temperature required. Both the technology and the thermocyclers are subject to licensing which increases the cost of detection protocols when applied to clinical diagnostics. Isothermal amplification techniques have been recently developed as an alternative to PCR for target DNA amplification and detection without the use of a thermocycler (*71*). This alternative not only reduces the cost of the overall detection system, but also allows the use and implementation of molecular diagnostic platforms without the expensive requirements of a molecular biology laboratory. The following sections describe some isothermal amplification approaches that have been proposed for the detection of infectious diseases.

2.2.1 Strand displacement amplification (SDA)

Strand displacement amplification is based on the use of a restriction enzyme (endonuclease) that cut the original target DNA in specific sites and the ability of a 5'-3' exonuclease-deficient DNA polymerase to extend the 3' end at the edge of the cut and displace the downstream strand. The displaced strand serves as a template for subsequent polymerase reactions resulting in exponential amplification of the target DNA (*72,73*). The first enzymatic cleavage of the original DNA generates a specific fragment for the amplification. The DNA has to be denatured at 95°C before the primers are annealed at 37°C. After the target fragment is denatured, the single-stranded target DNA binds to an SDA primer that contains a recognition sequence for the second restriction enzyme that will generate the 3' edges needed for subsequent polymerase amplifications. The target sequence should not contain a recognition sequence for the second restriction enzyme used in SDA. This is a limitation for amplification protocol design. Besides, still two temperatures are needed for amplification and two restriction enzymes are required which increases the cost of the protocol. SDA protocols have been successfully developed for the isothermal amplification of genomic Mtb DNA (*72,73*). Additionally, a semi automated commercially available system currently uses SDA for amplification and identification of Mtb (BDProbeTec MTB Test from Becton Dickinson) (*74,75*).

2.2.2 Loop-mediated isothermal amplification (LAMP)

Loop-mediated isothermal amplification is based on the auto generation of single strand target DNA (ssDNA) sequences with stem-loops at each end that serve as the starting structure for the amplification. LAMP also relies in strand displacement reactions which are performed at a constant temperature using a DNA polymerase with strand displacement activity (*76,77*). The

loop formation and further amplification require the use of six different specific primers that bind within the target region of interest. LAMP does not require of an initial denaturation step (94-95°C) to generate ssDNA or enzymatic cleavage. In order to generate ssDNA for the amplification, one of the LAMP primers anneals to the antisense sequence (3' --- 5') of the double stranded DNA (dsDNA) at around 65°C and the *Bst* DNA polymerase (with strand displacement activity) initiates the synthesis of a DNA strand complementary to the template starting from the 3' end of the primer. A secondary primer displaces again the complementary strand releasing a single strand with a stem-loop structure at the 5' end. For the loop formation, the ends of the LAMP primers that participate in this stage (external primers) have to be complementary. The final product of this stage is a structure with stem-loops at each end that will serve as a template for further DNA synthesis and strand displacement cycles (exponential cyclic amplification) using the rest of the primers (internal primers) (Figure 2-2).

The cycling reaction is usually conducted within an hour (*76*,*77*). Specific primer design is crucial for LAMP performance. The primers have to be designed to avoid secondary structure formations (complementary primers) that could produce a false synthetic target (false positive results). The distance between primers needs to be carefully considered as well as the melting temperature for each primer region, which should be approximately the same for all primers in order to keep the reaction at one single temperature. The main advantages of LAMP is that can be performed completely isothermally, it does not require restriction enzymes and is a single-tube reaction. The main disadvantage is the use of a complex multi-primer set that has to hybridize within a specific region. For small target fragments (between 100-200 bp) this could represent a problem.

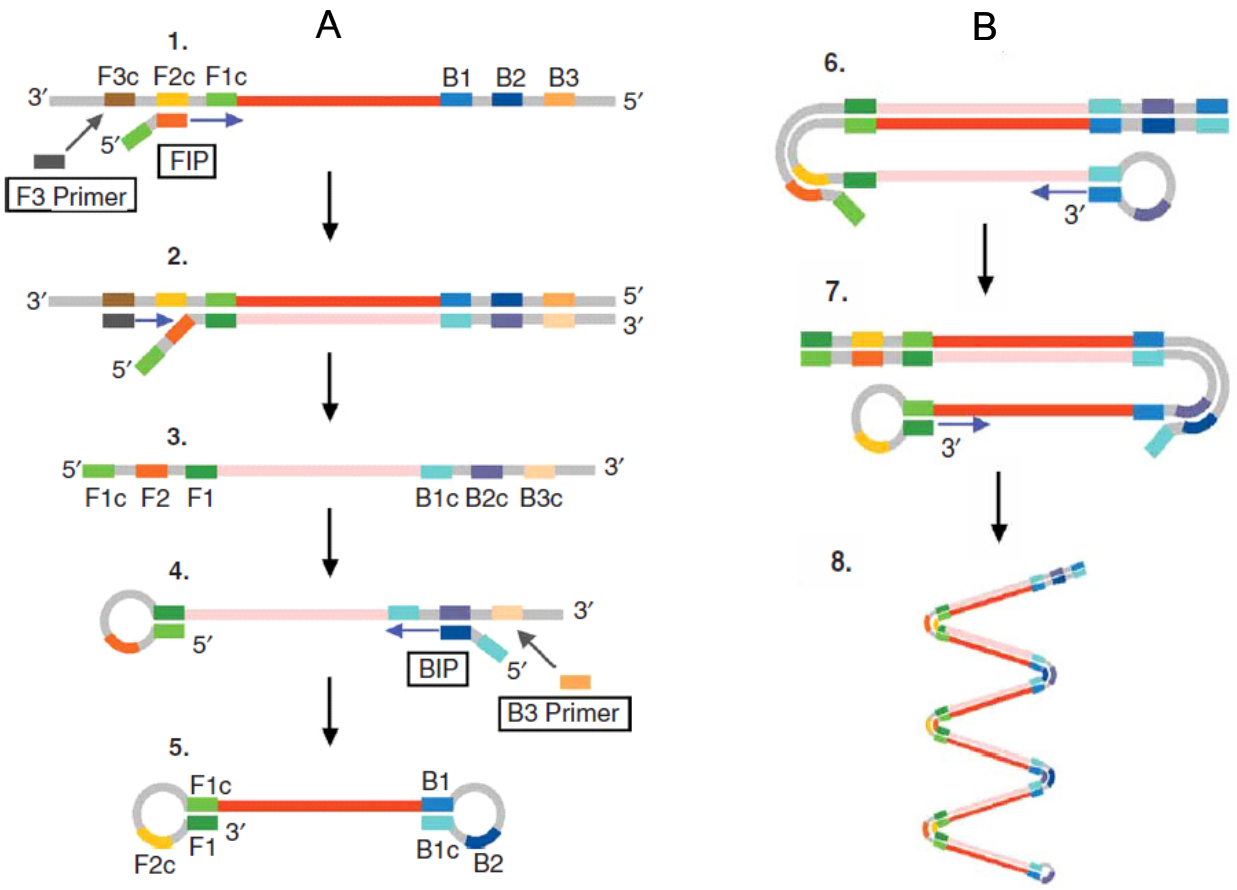

Figure 2-2. Schematic representation of LAMP main steps (simplified version). (A) Strand displacement stage. F3, F2, F1, B1, B2 and B3 are specific regions within the target that are selected for primer design; "c" means complementary, therefore F1c is complementary to F1. FIP and BIP are internal primers and F3 primer and B3 primer are external primers. The synthesis starts with the internal primer alignment and elongation to create the complementary strand (steps 1 and 2). The external primer aligns then and strand displacement DNA synthesis takes place (steps 3 and 4). Because of the way the internal primers are design, the displace strand has two complementary sections at both 5' and 3' ends that can hybridize and create a loop producing the dumbbell-like structure (step 5). (B) Cyclic amplification stage. Steps 1-5 are repeated using the dumbbell-like structure as template (steps 7-8) producing a self assembled structure (step 8.) (adapted from (*78*)).

LAMP protocols for the detection and identification of MTC strains and Mtb have been recently developed (*79*,*80*). In one of the reports, the addition of SYBR Green to amplified products (which is a fluorescent marker that binds to dsDNA) allowed visual identification of positive amplification (*79*). These TB detection protocols have been successfully used to identify Mtb from sputum culture isolates, which requires extensive sample preparation steps. The utility of the technique for direct amplification of DNA isolated from sputum is still under evaluation.

2.2.3 Thermophilic helicase-dependent isothermal amplification (tHDA)

Thermophilic helicase-dependent isothermal amplification utilizes a thermostable UvrD helicase to unwind the double stranded DNA (dsDNA) and generate single stranded templates that are used for further polymerase amplification (Figure 2-3) (*81*). The dsDNA separation and amplification are performed at the same temperature (60-65°C) which makes this technique suitable for development of point-of-care microbial detection systems, since a thermocycler is not required for DNA denaturation (95°C) and amplification (*82*,*83*). tHDA is a single tube reaction that only requires a pair of primers for the amplification (like PCR) and it does not require pre-enzymatic digestion of the target DNA, which simplifies the number of reactants and steps needed for amplification. tHDA protocols have been developed for the detection of several pathogens including: *Helicobacter pylori* (*84*), *Clostridium difficile* (*85*), *S. aureus* (*86*), *N. gonorrhoeae* (*81*), HIV-1 (*87*). tHDA has also been used in microfluidic chips with integrated sample preparation and amplification to detect *E. coli* (*88*,*89*) and for the multiplex detection of *S. aureus* and *N. gonorrhoeae* using a microarray on chip-amplification approach (*90*).

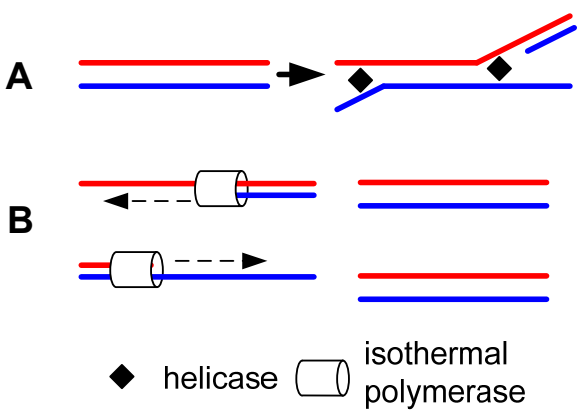

Figure 2-3. Schematic of isothermal amplification. (A) Helicase binds to dsDNA and unwinds into dsDNA and ssDNA sections. Primers bind and polymerase extends ssDNA into dsDNA; (B) New strands repeat binding and amplification.

2.3 Gold nanoparticle-based diagnostics

Nanodiagnostics is defined as the use of materials, devices or systems on the nanometer scale (10^{-9} m) to enhance detection methodologies, specially molecular diagnostics (*91*). Tests become more sensitive, flexible and faster when nanoscale particles are used as tags or labels over traditional procedures (*92,93*). Relevant areas for nanodiagnostics application include: cancer diagnosis, immunohistochemistry, genotyping, biomarker research, and detection of infectious microorganisms (*92*). Over the last decade, nanoparticles have been the most widely used nanomaterial in the development of new diagnostic devices, specially gold nanoparticles (AuNPs), quantum dots (QDs) and magnetic nanoparticles (MNPs) (*92,94*). AuNPs show unique optical properties (red SPR band at 520 nm, weakly dependent on size, but strongly changes with shape and inter-particle distance), high surface area, easy functionalization (thiol-linked ssDNA), and catalytic activity, which make them ideal candidates for biosensing enhancement (*95*).

2.3.1 Gold nanoprobe (DNA based) detection systems

One of the most explored applications of AuNPs in clinical diagnostics is the use of AuNP probes (AuNP-ssDNA probe) for the detection of DNA targets. Colorimetric assays are based on the property of AuNP to form large aggregates, when they are in close proximity, causing a reversible change in color of the AuNP suspension from red to purple (*96*,*97*). Mirkin et al. (*98*) reported the first DNA sandwich hybridization colorimetric assay using AuNPs. The methodology involves the use of two thiol-modified ssDNA probes (that hybridize different sections of the genetic target) immobilized into AuNPs; when the target is present, the hybridization of the two AuNP probes with the target results in the formation of a polymeric network which brings the AuNPs in close proximity causing a change in color from red to purple. This mechanism is known as cross-linking detection (*97*).

A different colorimetric approach (non-cross-linking) includes the aggregation of AuNPs induced by an increase in salt concentration (NaCl 2M). For this methodology, a single DNA probe (which is complementary to the DNA target) is immobilized onto the surface of AuNPs. In the presence of the target, the hybridization event between the probe and the target prevents the AuNPs aggregation when the salt concentration of the solution is increased, and the solution remains red. Non-complementary targets do not prevent AuNP salt induced aggregation, resulting in a visible change in color from red to purple (*99*).

Gold nanoprobe, colorimetric based detection protocols have been developed for TB detection (*100*,*101*). These procedures still use a PCR step for DNA amplification as part of the sample preparation before detection. Detection limit of colorimetric assays without signal amplification is in the range of nM to μM (*97*). These approaches are not sensitive enough to detect nucleic acids at the concentrations normally present in biological matrices; therefore, they

must be combined with either target amplification (PCR) or signal amplification (silver enhancement) (*102*).

Recently, bio-barcode DNA assays have been introduced as an alternative to increase sensitivity in AuNPs based detection methodologies (*103*,*104*). The barcodes are short oligonucleotides (oligos) that can be modified with several functional groups and fluorophores. For DNA detection, the target sequence is sandwiched between two specific particle-probes. One is a MNP-probe which separates the target DNA from the complex media. The second is a AuNP-probe that carries hundreds of barcode oligo sequences. Once the complex is formed (MNP-target-AuNP), it is magnetically separated from the matrix for further bio-barcode release and detection (*104*,*105*). The bio-barcode DNA is the molecule used for signal amplification, therefore several common DNA readout technologies can be used (fluorescence, electrochemistry, etc). Figure 2-4 shows a schematic representation of the bio-barcode assay using electrochemical detection of metal tracers as readout. With bio-barcode assays, DNA can be detected in ranges from femto to even zeptomolar concentration using synthetic targets (*102*,*104*,*105*). In theory, there is no need for PCR if these high levels of sensitivity are achieved. Nevertheless, the performance of this methodology has to be evaluated using real matrixes and genomic targets (*105*).

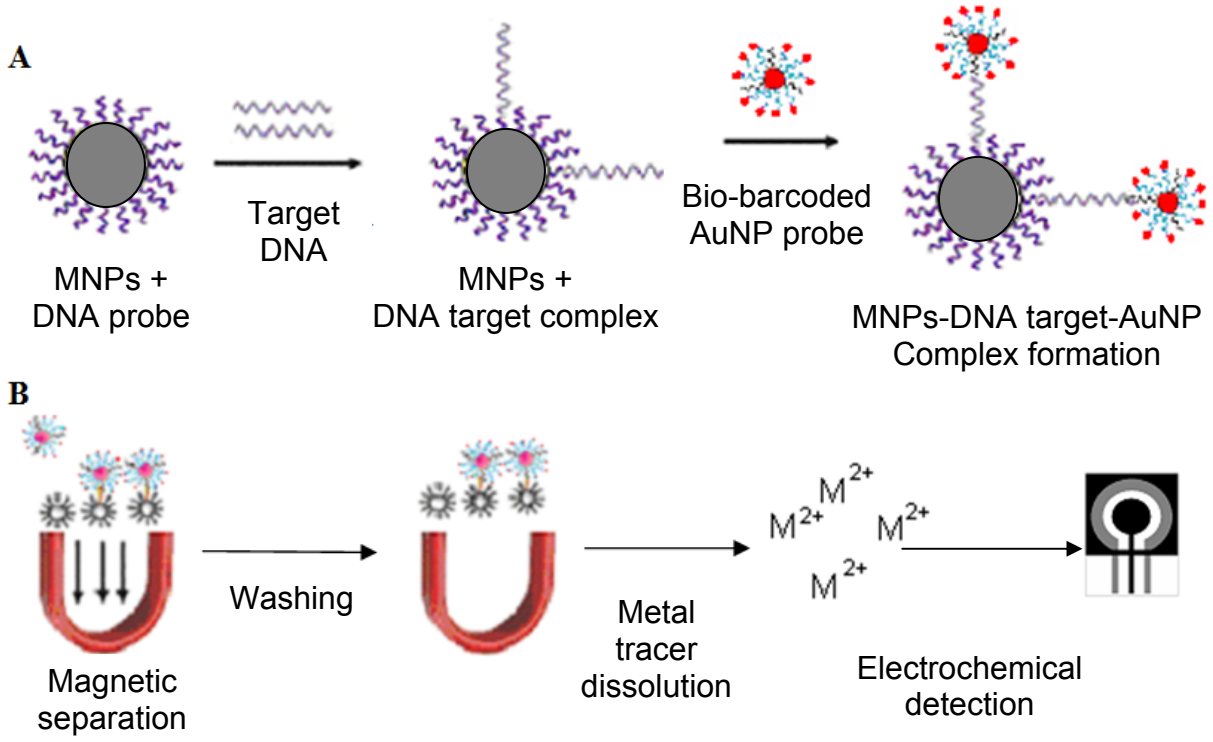

Figure 2-4. Schematic of the bio-barcode assay. (A) Formation of MNP-DNA target-AuNP sandwich structure; (B) Target complex separation and electrochemical detection (adapted from (*106*)).

2.4 Biosynthesis of magnetic and conductive nanoparticles

In the last few years, alternative biosynthetic approaches have been explored using microorganisms as bio-nano-factories to produce metal nanoparticles (*107*,*108*). One of the most studied procedures is the intracellular biosynthesis of magnetic nanoparticles using magnetotactic bacteria (*Magnetospirillum magnetotacticum*) (*109*,*110*). Recently an extracelular, aerobic alternative has been published using *Actinobacte*r sp.(*111*), which represents an advantage to the sophisticated anaerobic, fermented-based, intracellular procedure for the bacterial magnetosome formation; mechanism used by *M. magnetotacticum*. Other explorations

include the biosynthesis of cadmium sulfide, zinc sulfide, cadmium selenide, lead sulfide, silver, and gold nanoparticles (*112*).

Commonly, AuNPs are synthesized by chemical reduction of $HAuCl_4$ and the introduction of a protective agent (stabilizer). The most used method is the citrate reduction of Turkevich et al. (*113*). Stable and relatively monodispersed AuNP can be obtained by thiol-functionalization procedures (*114,115*) and other functional ligands (e.g. xanthates, disulfides, amine, phosphine and lysine) (*116*). Polysacarides like chitosan and sucrose have also been used as protective agents in "greener" approaches for the synthesis of AuNPs (*117*). Modifications to these chemical procedures allow control of AuNPs size (9-120 nm), dispersity and water solubility.

AuNPs biosynthesis procedures include the use of fungi, bacteria and actinomycetes strains (e.g. *Verticillium* sp., *Bacillus subtilis*, *Lactobacillus* sp., *Rhodococcus* sp., *Thermomonospora* sp., and *Actinobacter* spp.). A summary of representative examples is provided in Table 2-4. Majority of these procedures involve the use of microorganisms that are non-pathogenic to humans, and therefore, do not require special biosafety facilities. Some of these bio-synthetic procedures lead to the production of extracellular, homogeneus, monodisperse and water soluble AuNPs (*118,119*); which represents a non-toxic and environmentally friendly alternative to the common chemical synthesis. Possible advantages of using microorganisms instead of chemicals for nanoparticle synthesis include shape control, monodispersity, water solubility and better biocompatibility for potential applications in medical diagnostics and treatment.

To date, several aspects of the biosynthesis of magnetic and conductive nanoparticles remain unknown. The elucidation of the biochemical pathways that lead to the metal ion reduction as well as the characterization of the biogenic nanoparticles surface chemistry are necessary for better understanding and standardization of the biosynthesis (*107,108*). To the best of our

knowledge, the application of either magnetic or conductive biosynthetic nanoparticles into biosensing platforms remains unexplored.

Table 2-4. Biosynthesis of gold nanoparticles using microorganisms.

Microorganism	Particle size (nm)	Mechanism of synthesis	Reference
Actinomycetes			
Rhodococcus sp.	5-15	Intracellular	(*120*)
Thermomonospora sp	8	Extracellular	(*118*)
Bacteria			
Actinobacter sp.	50-500	Extracellular	(*119*)
Bacillus megatherium	2	Extracellular	(*121*)
E. coli	10-25	Intracellular	(*122*)
Lactobacillus sp.	20-50 and >100	Intracellular	(*123*)
Plectonema boryanum	10 and >100	Intracellular	(*124*)
Pseudomonas aeruginosa	15-30	Extracellular	(*125*)
Rhodopseudomonas capsulata	10-20	Extracellular	(*126*)
Fungi			
Colletotrichum sp.	20-40	Extracellular	(*127*)
Fusarium oxysporium	20-40	Extracellular	(*128*)
Verticillium sp.	20	Intracellular	(*129*)

2.5 Nanoparticle-based electrochemical DNA biosensors

Electrochemical biosensors have high sensitivity, miniaturization capability, and low cost when compared with fluorescent and spectroscopic detection systems. These characteristics make them suitable for decentralized testing and development of portable detection devices (*130*,*131*). Electrochemical detection of DNA can be classified into direct methods, which are based on the natural electroactivity of DNA or the changes in electrode properties (e.g. capacitance, conductivity or impedance); and indirect methods, which are based on electrochemical measurement of labels, tags or intercalators after the hybridization between the

DNA target and the specific oligonucleotide probes (*130*). Conventional labels include enzymes and redox molecules. The use of nanomaterials as electrochemical labels (e.g. nanoparticles) has led to sensitivity enhancement of the DNA detection methodologies (*130,131*).

Metal nanoparticles are defined as particles in solution, between 1-50 nm in diameter, that have a protective shell (coating material) to avoid agglomeration. Due to the small size, nanoparticles have different electrochemical properties from their bulk metal counterparts. Traditionally, nanoparticles are prepared by chemical reduction of the transition metal salt in the presence of a stabilizer agent (capping agent such as citrate or thiol) which covers the surface to provide stability, linking chemistry, appropriate charge, and solubility properties for further functionalization with biomolecules (*131*).

The new electrochemical DNA biosensor are being developed based on the use of colloidal gold tags, semiconductor quantum dot tracers, polymeric carrier beads, and magnetic beads (*132*). Some of these platforms rely on capturing the gold or silver nanoparticles to the hybridized DNA target, followed by acidic dissolution and anodic-stripping electrochemical measurement of the metal tracer. The target immobilization usually relies on the use of magnetic beads coated with DNA probes that specifically hybridize to the target sequence. With this detection system, pico and nanomolar concentrations of target DNA have been detected (*131,132*).

2.5.1 Gold nanoparticles as electrochemical label for DNA detection

The unique tunable physicochemical properties of AuNPs, plus their good biological compatibility, conducting capability, and high surface-to-volume ratio make them ideal candidates for electronic signal transduction of biological recognition events in biosensing

platforms (*117*). AuNPs have been specially applied in the development of DNA-based electrochemical biosensors. AuNPs can strongly adsorb DNA; the negative charges provided by the citrate adsorption (used in most of the synthesis processes) enhance the electrostatic adsorption between AuNPs and DNA strands. Phosphothiol groups are one of the most used DNA linkers for AuNPs immobilization (*133*). Some of the strategies to detect DNA hybridization in electrochemical systems using AuNPs include: detection of gold ions by the acidic dissolution of AuNP labels, direct detection of AuNP-DNA conjugates anchored onto the sensor surface, catalytic deposition of silver onto AuNPs (silver enhancement), and use of AuNPs as carriers or amplifiers of other electroactive labels (Figure 2-5) (*117*,*133*). Examples of electrochemical DNA-based biosensors for TB detection using gold nanoparticles are presented in chapter 5.

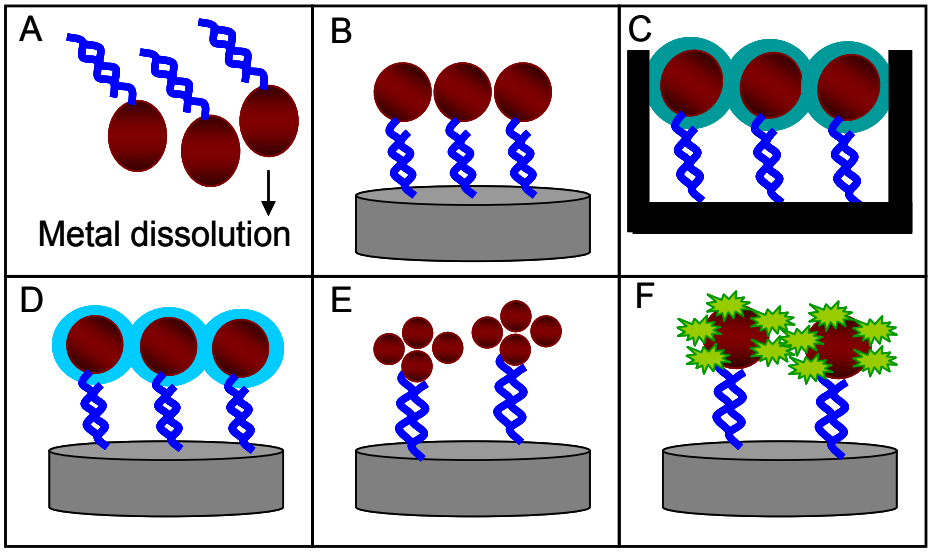

Figure 2-5. Schematic representation of strategies used for the integration of gold nanoparticles into DNA biosensors. A) Previous dissolving of AuNP by using HBr/Br2 mixture followed by Au(III) ions detection; B) direct detection of AuNPs anchored onto the surface of the sensor; C) conductometric detection, D) enhancement with silver or gold followed by detection; E) AuNPs

as carriers of other AuNPs; F) AuNPs as carriers of other electroactive labels (adapted from (*133*)).

The majority of the AuNP electrochemical detection platforms have been developed using chemical dissolution of the AuNPs in a hydrobromic acid/bromine (HBr/Br_2) solution followed by accumulation and stripping analysis of the gold ions (*133*). The HBr/Br_2 solution is highly toxic; therefore, methods based on direct electrochemical detection of AuNPs without the need of strong acidic oxidation steps are needed (*134*,*135*). In 2005, Pumera and collaborators developed a protocol based on the adsorption of AuNPs onto the surface of graphite-epoxy composite electrode, followed by the electrochemical oxidation in 0.1 M HCl at 1.25 V. The resulting gold ions were detected by differential pulse voltammetry (DPV). The reduction of $AuCl^{4-}$ ions produced a DPV peak at a potential of 0.4V which was used as the analytical signal (*135*).

In order to increase the sensitivity of the AuNP based electrochemical DNA assays, polystyrene spheres have been used as carriers of colloidal gold tags to amplify the signal. In this system, streptavidin-coated polystyrene beds were crosslinked with biotinilated AuNPs followed by catalytic enhancement of the gold tags and electrochemical detection of the dissolved gold ions (*136*). The obtained detection limit was in the range of 40 pg/mL.

Besides the use of gold as a colloidal tag, several other metal tracers have been used for signal enhancement (cadmium, lead, zinc, etc). These protocols are based on the capture of metal nanoparticle tracers followed by dissolution and stripping voltammetry measurement of the metal label (*132*). Wang et al. (*131*) have reported the use of inorganic nanocrystals (zinc sulfide,

cadmium sulfide and lead sulfide) as electrochemical labels for DNA or protein detection. Each tracer produces a distinct voltammetric peak, which is useful in the development of multiplex detection systems (*137*). These metal traces can be used to label bio-barcode DNA sequences for the electrochemical detection of DNA targets using the sandwich hybridization technique with gold and magnetic nanoparticles described above. Recently, in our laboratory, a bio-barcode electrochemical based DNA detection system using metal tracers and screen printed carbon electrodes (SPCE) has been developed for the simultaneous detection of *Salmonella enterica* ser. Enteritidis and *Bacillus anthracis* sterne strain using specific DNA target sequences amplified by PCR (*138*,*139*). Figure 2-6 shows a schematic representation of the platform. The obtained detection limit was 0.5 ng/ml of the insertion element (*Iel*) gene from *S. enteritidis* amplified product and 50 pg/ml of *pagA* gene from *B. anthracis* amplified product. The application of this technology to detect genomic DNA in real matrix conditions, without the use of PCR, represents a promising alternative for the development of point-of-care rapid diagnostics.

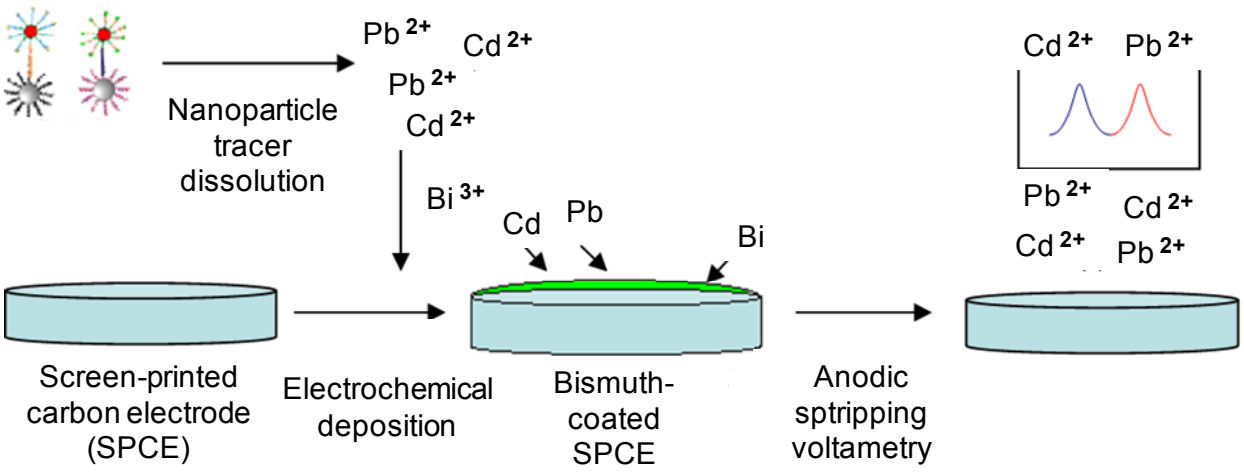

Figure 2-6. Schematic of anodic stripping voltammetry measurements of multiplex DNA targets (adapted from (*139*)).

References

2.6 References

1. WHO Global Tuberculosis Control 2009. Epidemiology, Strategy, and Financing. http://www.who.int/tb/publications/global_report/2009/pdf/full_report.pdf. (2009).

2. Brooks, G. F., Carroll, C. K., Butel, J. S. & Morse, S. A. Jawetz, Melnick, & Adelberg's Medical Microbiology. Mc Graw Hill, (2007).

3. Russell, D. G. Mycobacterium tuberculosis: here today, and here tomorrow. *Nature Reviews Molecular Cell Biology* **2**, 569-586 (2001).

4. WHO tuberculosis. Fact sheet. http://www.who.int/mediacentre/factsheets/fs104/en/. WHO (2009).

5. Tuberculosis and the Tubercle Bacillus. Cole, Eisenach, McMurray & Jacobs (eds.), pp. 15-35 (American Society for Microbiology (ASM Press), (2005).

6. Bravo & Gotuzzo Cutaneous tuberculosis. *Clinics in Dermatology* **25**, 173-180 (2007).

7. Kirk. Tuberculosis – Human and Cattle. http://www.vetmed.ucdavis.edu/vetext/INF-DA/TB1202.pdf . (2002).

8. Tuberculosis and the tubercle bacillus. Cole, Eisenach, McMurray & Jacobs (eds.), p. 537 (American Society for Microbiology (ASM Press) (2005).

9. Ling, D. I., Zwerling, A. A. & Pai, M. Rapid diagnosis of drug-resistant TB using line probe assays: from evidence to policy. *Expert Review of Respiratory Medicine* **2**, 583-588 (2008).

10. WHO. The Global MDR-TB and XDR-TB Response Plan. 2007-2008. http://whqlibdoc.who.int/hq/2007/WHO_HTM_TB_2007.387_eng.pdf. (2009).

11. Zaczek, A., Brzostek, A., ugustynowicz-Kopec, E., Zwolska, Z. & Dziadek, J. Genetic evaluation of relationship between mutations in rpoB and resistance of Mycobacterium tuberculosis to rifampin. *BMC Microbiology* **9**, 10 (2009).

12. Garcia de Viedma, D. Rapid detection of resistance in Mycobacterium tuberculosis: a review discussing molecular approaches. *Clinical Microbiology and Infection* **9**, 349-359 (2003).

13. Does rifampicin resistance reliably predict MDR-TB? Results from the Global Project FIND symposium, 4thEuropean Regional Congress of the Union http://www.finddiagnostics.org/programs/tb/links.html. (2009).

14. O'Riordan, P. *et al.* Rapid molecular detection of rifampicin resistance facilitates early diagnosis and treatment of multi-drug resistant tuberculosis: Case control study. *PLoS ONE* **3**, e3173 (2008).

15. Somoskovi, A., Gutierrez, C. M. & Salfinger, M. Laboratory diagnosis of tuberculosis: novel and nonconventional methods. *Reviews in Medical Microbiology* **19**, (2008).

16. Dinnes, J. *et al.* A systematic review of rapid diagnostic tests for the detection of tuberculosis infection. *Health Technology Assessment 2007* **11**, (2007).

17. Perkins, M. D., Roscigno, G. & Zumla, A. Progress towards improved tuberculosis diagnostics for developing countries. *The Lancet* **367**, 942-943.

18. Pai, M. & O'Brien, R. New diagnostics for latent and active tuberculosis: State of the art and future prospective. *Seminars in Respiratory and Critical Care Medicine* **29**, 560-568 (2008).

19. Hanna, B. A. *et al.* Multicenter Evaluation of the BACTEC MGIT 960 system for recovery of mycobacteria. *Journal in Clinical Microbiology.* **37**, 748-752 (1999).

20. Palomino, J. C. Nonconventional and new methods in the diagnosis of tuberculosis: feasibility and applicability in the field. *European Respiratory Journal* **26**, 339-350 (2005).

21. Tortoli, E. *et al.* Use of BACTEC MGIT 960 for recovery of Mycobacteria from clinical specimens: Multicenter study. *Journal of Clinical Microbiology* **37**, 3578-3582 (1999).

22. Bothamely, G. Serological diagnosis of tuberculosis. *The European respiratory journal. Supplement* **20**, 676-688 (1995).

23. Pottumarthy, S., Wells, V. C. & Morris, A. J. A Comparison of seven tests for serological diagnosis of tuberculosis. *Journal of Clinical Microbiology* **38**, 2227-2231 (2000).

24. Davies, P. D. O. & Pai, M. The diagnosis and misdiagnosis of tuberculosis [State of the art series. Tuberculosis. Edited by I. D. Rusen. Number 1 in the series]. *The International Journal of Tuberculosis and Lung Disease* **12**, 1226-1234 (2008).

25. Boehme, C. *et al.* Detection of mycobacterial lipoarabinomannan with an antigen-capture ELISA in unprocessed urine of Tanzanian patients with suspected tuberculosis. *Transactions of the Royal Society of Tropical Medicine and Hygiene* **99**, 893-900 (2005).

26. Tsigeweini Asgedom Tessema, B. H. G. B. S. S. B. B. Diagnostic evaluation of urinary lipoarabinomannan at an ethiopian tuberculosis centre. *Scandinavian Journal of Infectious Diseases* **33**, 279-284 (2001).

27. Chang, P. L. *et al.* Identification of individual DNA molecule of Mycobacterium tuberculosis by nested PCR-RFLP and capillary electrophoresis. *Talanta* **77**, 182-188 (2008).

28. Gopinath, K. & Singh, S. Urine as an adjunct specimen for the diagnosis of active pulmonary tuberculosis. *International journal of infectious diseases* **13**(3), 374-379 (2009).

29. Zelazny, A. M., Calhoun, L. B., Li, L., Shea, Y. R. & Fischer, S. H. Identification of Mycobacterium species by secA1 sequences. *Journal of Clinical Microbiology* **43**, 1051-1058 (2005).

30. Cousins, D. V., Skuce, R. A., Kazwala, R. R. & van Embden, J. D. A. Towards a standardized approach to DNA fingerprinting of Mycobacterium bovis. *The International Journal of Tuberculosis and Lung Disease* **2**, 471-478 (1998).

31. Dalovisio, J. R. *et al.* Comparison of the amplified Mycobacterium tuberculosis (MTB) direct test, amplicor MTB PCR, and IS6110-PCR for detection of MTB in respiratory specimens. *Clinical Infectious Diseases.* **23**, 1099-1106 (1996).

32. Fernandez, J. G. *et al.* Comparison of three immunological diagnostic tests for the detection of avian tuberculosis in naturally infected red deer (Cervus elaphus). *Journal of Veterinarian Diagnostic Investigation* **21**, 102-107 (2009).

33. Myeong-Hee, K., Hee-Young, Y., Jin-Tae, S. & Hee Joo, L. Comparison of in-house PCR with conventional techniques and Cobas Amplicor M. tuberculosis kit for detection of Mycobacterium tuberculosis. *Yonsei Medical Journal.* **49**, 537-544 (2008).

34. Huard, R. C., de Oliveira Lazzarini, L. C., Butler, W. R., van Soolingen, D. & Ho, J. L. PCR-based method to differentiate the subspecies of the Mycobacterium tuberculosis Complex on the basis of genomic deletions. *Journal of Clinical Microbiology* **41**, 1637-1650 (2003).

35. van Soolingen, D., Hermans, P. W., de Haas, P. E. & van Embden, J. D. Insertion element IS1081-associated restriction fragment length polymorphisms in Mycobacterium tuberculosis complex species: a reliable tool for recognizing Mycobacterium bovis BCG. *Journal of Clinical Microbiology* **30**, 1772-1777 (1992).

36. Huard, R. C. *et al.* The Mycobacterium tuberculosis complex-restricted gene cfp32 encodes an expressed protein that is detectable in tuberculosis patients and is positively correlated with pulmonary interleukin-10. *Infection and Immunity* **71**, 6871-6883 (2003).

37. Barnard, M., Albert, H., Coetzee, G., O'Brien, R. & Bosman, M. E. Rapid molecular screening for multidrug-resistant tuberculosis in a high-volume public health laboratory in south africa. *American Journal of Respiratory and Critical Care Medicine* **177**, 787-792 (2008).

38. Edwards, K. J., Metherell, L. A., Yates, M. & Saunders, N. A. Detection of rpoB mutations in mycobacterium tuberculosis by biprobe analysis. *Journal of Clinical Microbiology* **39**, 3350-3352 (2001).

39. Aragon, L. M. *et al.* Rapid detection of specific gene mutations associated with isoniazid or rifampicin resistance in Mycobacterium tuberculosis clinical isolates using non-fluorescent low-density DNA microarrays. *Journal of Antimicrobial Chemotherapy* **57**, 825-831 (2006).

40. Park, H. *et al.* Comparison of a conventional antimicrobial susceptibility assay to an oligonucleotide chip system for detection of drug resistance in Mycobacterium tuberculosis isolates. *Journal of Clinical Microbiology* **44**, 1619-1624 (2006).

41. Lee, A. S. G., Lim, I. H. K., Tang, L. L. H., Telenti, A. & Wong, S. Y. Contribution of kasA analysis to detection of isoniazid-resistant Mycobacterium tuberculosis in Singapore. *Antimicrobial Agents Chemotherapy* **43**, 2087-2089 (1999).

42. Sun, Y. J., Lee, A. S. G., Wong, S. Y. & Paton, N. I. Analysis of the role of Mycobacterium tuberculosis kasA gene mutations in isoniazid resistance. *Clinical Microbiology and Infection* **13**, 833-835 (2007).

43. de los Monteros, L. E. E. *et al.* Allele-Specific PCR method based on pncA and oxyR sequences for distinguishing Mycobacterium bovis from Mycobacterium tuberculosis: Intraspecific M. bovis pncA sequence polymorphism. *Journal of Clinical Microbiology* **36**, 239-242 (1998).

44. Abass, N., Suleiman, K. & El Jalii, I. Differentiation of clinical Mycobacterium tuberculosis complex isolates by their GyrB polymorphism. *Indian Journal of Medical Microbiology* **28**, 26-29 (2010).

45. Von Groll, A. *et al.* Fluoroquinolone resistance in Mycobacterium tuberculosis and mutations in gyrA and gyrB. *Antimicrobial Agents Chemotherapy* **53**, 4498-4500 (2009).

46. Gillespie, S. H. Evolution of drug resistance in Mycobacterium tuberculosis: Clinical and molecular perspective. *Antimicrobial Agents Chemotherapy* **46**, 267-274 (2002).

47. Drobniewski, F. A., Caws, M., Gibson, A. & Young, D. Modern laboratory diagnosis of tuberculosis. *Lancet Infectious Diseases* **3**, 141-147 (2003).

48. Bonington, A. *et al.* TB PCR in the early diagnosis of tuberculous meningitis: evaluation of the Roche semi-automated COBAS Amplicor MTB test with reference to the manual Amplicor MTB PCR test. *Tubercle and Lung Disease* **80**, 191-196 (2000).

49. Piersimoni, C. & Scarparo, C. Relevance of Commercial Amplification Methods for Direct Detection of Mycobacterium tuberculosis Complex in Clinical Samples. *J. Clin. Microbiol.* **41**, 5355-5365 (2003).

50. Chedore, P. & Jamieson, F. B. Rapid molecular diagnosis of tuberculous meningitis using the Gen-Probe Amplified Mycobacterium Tuberculosis Direct Test in a large Canadian public health laboratory. *The International Journal of Tuberculosis and Lung Disease* **6**, 913-919 (2002).

51. Johansen, I. S. *et al.* Improved sensitivity of nucleic acid amplification for rapid diagnosis of tuberculous meningitis. *Journal of Clinical Microbiology* **42**, 3036-3040 (2004).

52. Padilla, E. *et al.* Comparative evaluation of the new version of the INNO-LiPA mycobacteria and GenoType Mycobacterium assays for identification of Mycobacterium species from MB/BacT liquid cultures artificially inoculated with mycobacterial strains. *Journal of Clinical Microbiology* **42**, 3083-3088 (2004).

53. Turenne, C. Y., Tschetter, L., Wolfe, J. & Kabani, A. Necessity of quality-controlled 16S rRNA gene sequence databases: Identifying nontuberculous Mycobacterium species. *Journal of Clinical Microbiology* **39**, 3637-3648 (2001).

54. Tang, X., Morris, S. L., Langone, J. J. & Bockstahler, L. E. Microarray and allele specific PCR detection of point mutations in Mycobacterium tuberculosis genes associated with drug resistance. *Journal of Microbiological Methods* **63**, 318-330 (2005).

55. Mokrousov, I., Otten, T., Vyshnevskiy, B. & Narvskaya, O. Allele-specific rpoB PCR assays for detection of rifampin-resistant Mycobacterium tuberculosis in sputum smears. *Antimicrobial Agents Chemotherapy* **47**, 2231-2235 (2003).

56. Lee, T. Y. & Shim, Y. B. Direct DNA hybridization detection based on the oligonucleotide-functionalized conductive polymer. *Analytical Chemistry* **73**, 5629-5632 (2001).

57. Dubertret, B. Quantum dots - DNA detectives. *Nature Materials* **4**, 797-798 (2005).

58. Pu, K. Y., Pan, S. Y.-H. & Liu, B. Optimization of interactions between a cationic conjugated polymer and chromophore-labeled DNA for optical amplification of fluorescent sensors. *The Journal of Physical Chemistry B* **112**, 9295-9300 (2008).

59. Sassolas, A., Leca-Bouvier, B. D. & Blum, L. J. DNA biosensors and microarrays. *Chemical Reviews* **108**, 109-139 (2007).

60. de-los-Santos-Alvarez, P., Lobo-Castanon, M. J., Miranda-Ordieres, A. J. & Tunon-Blanco, P. Electrochemistry of nucleic acids at solid electrodes and its applications. *Electroanalysis* **16**, 1193-1204 (2004).

61. Drummond, T. G., Hill, M. G. & Barton, J. K. Electrochemical DNA sensors. *Nature Biotechnology* **21**, 1192-1199 (2003).

62. Weng, J. *et al.* Label-free DNA sensor by boron-doped diamond electrode using an ac impedimetric approach. *Analytical Chemistry* **80**, 7075-7083 (2008).

63. Huang, G. S., Wang, M. T. & Hong, M. Y. A versatile QCM matrix system for online and high-throughput bio-sensing. *Analyst* **131**, 382-387 (2006).

64. Lee, H., Yoon, T. J. & Weissleder, R. Ultrasensitive detection of bacteria using core–shell nanoparticles and an NMR-Filter system. *Angewandte Chemie International Edition* **48**, 5657-5660 (2009).

65. Gazouli, M. *et al.* Specific detection of unamplified mycobacterial DNA by use of fluorescent semiconductor quantum dots and magnetic beads. *Journal of Clinical Microbiology* **48**, 2830-2835 (2010).

66. McNerney, R. & Daley, P. Towards a point-of-care test for active tuberculosis: obstacles and opportunities. *Nature Reviews Microbiology* **9**, 204-213 (2011).

67. Keeler, E. *et al.* Reducing the global burden of tuberculosis: the contribution of improved diagnostics. *Nature* (2006).

68. Phillips, M. *et al.* Breath biomarkers of active pulmonary tuberculosis. *Tuberculosis* **90**(2), 145-151 (2010).

69. Green, C. *et al.* Rapid diagnosis of tuberculosis through the detection of mycobacterial DNA in urine by nucleic acid amplification methods. *The Lancet Infectious Diseases* **9**, 505-511 (2009).

70. McPherson, M. J. & Moller, S. G. *PCR. The Basics.* BIOS Scientific Publishers, New York (2000).

71. Gill, P. & Ghaemi, A. Nucleic acid isothermal amplification technologies–a review. *Nucleosides Nucleotides and Nucleic acids.* **27**, 224-243 (2008).

72. Walker, G. T., Little, M. C., Nadeau, J. G. & Shank, D. D. Isothermal in vitro amplification of DNA by a restriction enzyme/DNA polymerase system. *Proceedings of the National Academy of Sciences* **89**, 392-396 (1992).

73. Walker, G. T. *et al.* Strand displacement amplification-an isothermal, in vitro DNA amplification technique. *Nucleic Acids Researc* **20**, 1691-1696 (1992).

74. Bergmann, J. S. & Woods, G. L. Clinical evaluation of the BDProbeTec Strand Displacement Amplification assay for rapid diagnosis of tuberculosis. *Journal of Clinical Microbiology* **36**, 2766-2768 (1998).

75. Little, M. C. *et al.* Strand Displacement Amplification and homogeneous real-time eetection incorporated in a second-generation DNA probe system, BDProbeTecET. *Clinical Chemistry* **45**, 777-784 (1999).

76. Mori, Y. & Notomi, T. Loop-mediated isothermal amplification (LAMP): a rapid, accurate, and cost-effective diagnostic method for infectious diseases. *Journal of Infection and Chemotherapy.* **15**, 62-69 (2009).

77. Parida, M., Sannarangaiah, S., Dash, P. K., Rao, P. V. L. & Morita, K. Loop mediated isothermal amplification (LAMP): a new generation of innovative gene amplification technique; perspectives in clinical diagnosis of infectious diseases. *Reviews in Medical Virology* **18**, 407-421 (2008).

78. Tomita, N., Mori, Y., Kanda, H. & Notomi, T. Loop-mediated isothermal amplification (LAMP) of gene sequences and simple visual detection of products. *Nature Protocols* **3**, 877-882 (2008).

79. Iwamoto, T., Sonobe, T. & Hayashi, K. Loop-mediated isothermal amplification for direct detection of Mycobacterium tuberculosis Complex, M. avium, and M. intracellulare in sputum samples. *Journal of Clinical Microbiology* **41**, 2616-2622 (2003).

80. Pandey, B. D. *et al.* Development of an in-house loop-mediated isothermal amplification (LAMP) assay for detection of Mycobacterium tuberculosis and evaluation in sputum samples of Nepalese patients. *Journal of Medical Microbiology* **57**, 439-443 (2008).

81. Lixin, A. *et al.* Characterization of a thermostable UvrD helicase and its participation in helicase dependent amplification. *The Journal of Biological Chemistry* **280**, 28952-28958 (2005).

82. Andresen, D., Nickisch-Rosenegk, M. v. & Bier, F. F. Helicase-dependent amplification: use in OnChip amplification and potential for point-of-care diagnostics. *Expert Reviews on Molecular Diagnostics* **9**, 645-650 (2009).

83. Jeong, Y. J., Park, K. & Kim, D. E. Isothermal DNA amplification in vitro: the helicase-dependent amplification system. *Cellular and Molecular Life Sciences* **66**, 3325-3336 (2009).

84. Gill, P., Alvandi, A. H., bdul-Tehrani, H. & Sadeghizadeh, M. Colorimetric detection of Helicobacter pylori DNA using isothermal helicase-dependent amplification and gold nanoparticle probes. *Diagnostic Microbiology and Infectious Disease* **62**, 119-124 (2008).

85. Chow, W. H. *et al.* Application of isothermal helicase-dependent amplification with a disposable detection device in a simple sensitive stool test for toxigenic Clostridium difficile. *Journal of Molecular Diagnostics* **10**, 452-458 (2008).

86. Goldmeyer, J. *et al.* Identification of Staphylococcus aureus and determination of methicillin resistance directly from positive blood cultures by isothermal amplification and a disposable detection device. *Journal of Clinical Microbiology* **46**, 1534-1536 (2008).

87. Tang, W. *et al.* Nucleic acid assay system for tier II laboratories and moderately complex clinics to detect HIV in low-resource settings. *Journal of Infectious Diseases* **201**, S46-S51 (2010).

88. Mahalanabis, M., Do, J., ALMuayad, H., Zhang, J. & Klapperich, C. An integrated disposable device for DNA extraction and helicase dependent amplification. *Biomedical Microdevices* **12**, 353-359 (2010).

89. Zhang, Y. *et al.* A surface topography assisted droplet manipulation platform for biomarker detection and pathogen identification. *Lab on a Chip* **11**, 398-406 (2011).

90. Andresen, D., von Nickisch-Rosenegk, M. & Bier, F. F. Helicase dependent OnChip-amplification and its use in multiplex pathogen detection. *Clinica Chimica Acta* **403**, 244-248 (2009).

91. Jain, K. K. Nanodiagnostics: application of nanotechnology in molecular diagnostics. *Expert Review of Molecular Diagnostics* **3**, 153-161 (2003).

92. Jain, K. K. Nanotechnology in clinical laboratory diagnostics. *Clinica Chimica Acta* **358**, 37-54 (2005).

93. Jain, K. K. Applications of nanobiotechnology in clinical diagnostics. *Clinical Chemistry* **53**, 2002-2009 (2007).

94. Azzazy, H. M. E., Mansour, M. M. H. & Kazmierczak, S. C. Nanodiagnostics: A new frontier for clinical laboratory medicine. *Clinical Chemistry* **52**, 1238-1246 (2006).

95. Baptista, P. *et al.* Gold nanoparticles for the development of clinical diagnosis methods. *Analytical and Bioanalytical Chemistry* **391**, 943-950 (2008).

96. Sato, K., Hosokawa, K. & Maeda, M. Colorimetric biosensors based on DNA-nanoparticle conjugates. *Analytical Sciences* **23**, 17-20 (2007).

97. Zhao, W., Brook, M. A. & Li, Y. F. Design of gold Nanoparticle-based colorimetric biosensing assays. *Chembiochem* **9**, 2363-2371 (2008).

98. Elghanian, R., Storhoff, J. J., Mucic, R. C., Letsinger, R. L. & Mirkin, C. A. Selective colorimetric detection of polynucleotides based on the distance-dependent optical properties of gold nanoparticles. *Science* **277**, 1078-1081 (1997).

99. Doria, G., Franco, R. & Baptista, P. Nanodiagnostics: fast colorimetric method for single nucleotide polymorphism/mutation detection. *Letters in Nanobiotechnology* **1**, 53-57 (2007).

100. Baptista, P. V., Koziol-Montewka, M., Paluch-Oles, J., Doria, G. & Franco, R. Gold-nanoparticle-probe-based assay for rapid and direct detection of Mycobacterium tuberculosis DNA in clinical samples. *Clinical Chemistry* **52**, 1433-1434 (2006).

101. Soo, P. C. *et al.* A simple gold nanoparticle probes assay for identification of Mycobacterium tuberculosis and Mycobacterium tuberculosis complex from clinical specimens. *Molecular and Cellular Probes* **23**, 240-246 (2009).

102. Wilson, R. The use of gold nanoparticles in diagnostics and detection. *Chemical Society Reviews* **37**, 2028-2045 (2008).

103. Nam, J. M., Thaxton, C. S. & Mirkin, C. A. Nanoparticle-based bio-bar codes for the ultrasensitive detection of proteins. *Science* **301**, 1884-1886 (2003).

104. Nam, J. M., Stoeva, S. I. & Mirkin, C. A. Bio-bar-code-based DNA detection with PCR-like sensitivity. *Journal of the American Chemical Society* **126**, 5932-5933 (2004).

105. Thaxton, C. S., Georganopoulou, D. G. & Mirkin, C. A. Gold nanoparticle probes for the detection of nucleic acid targets. *Clinica Chimica Acta* **363**, 120-126 (2006).

106. Zhang, D., Carr, D. J. & Alocilja, E. C. Fluorescent bio-barcode DNA assay for the detection of Salmonella enterica serovar Enteritidis. *Biosensors and Bioelectronics* **24**, 1377-1381 (2009).

107. Mandal, D., Bolander, M. E., Mukhopadhyay, D., Sarkar, G. & Mukherjee, P. The use of microorganisms for the formation of metal nanoparticles and their application. *Applied Microbiology and Biotechnology* **69**, 485-492 (2006).

108. Sastry, M., Ahmad, A., Khan, M. I. & Kumar, R. Biosynthesis of metal nanoparticles using fungi and actinomycete. *Current Science* **85**, 162-170 (2003).

109. Klem, M. T., Young, M. & Douglas, T. Biomimetic magnetic nanoparticles. *Materials Today* **8**, 28-37 (2005).

110. Lang, C. & Schuler, D. Biogenic nanoparticles: production, characterization, and application of bacterial magnetosomes. *Journal of Physics-Condensed Matter* **18**, S2815-S2828 (2006).

111. Bharde, A. A. *et al.* Bacteria-mediated precursor-dependent biosynthesis of superparamagnetic iron oxide and iron sulfide nanoparticles. *Langmuir* **24**, 5787-5794 (2008).

112. Korbekandi, H., Iravani, S. & Abbasi, S. Production of nanoparticles using organisms. *Critical Reviews in Biotechnology* **29**, 279-306 (2009).

113. Turkevich, J., Stevenson, P. C. & Hillier, J. A study of the nucleation and growth processes in the synthesis of colloidal gold. *Discussions of the Faraday Society* **11**, 55-75 (1951).

114. Brust, M., Walker, M., Bethell, D., Schiffrin, D. J. & Whyman, R. Synthesis of thiol-derivatized gold nanoparticles in a 2-phase liquid-liquid system. *Journal of the Chemical Society-Chemical Communications* 801-802 (1994).

115. Brust, M., Fink, J., Bethell, D., Schiffrin, D. J. & Kiely, C. Synthesis and reactions of functionalized gold nanoparticles. *Journal of the Chemical Society-Chemical Communications* 1655-1656 (1995).

116. Daniel, M. C. & Astruc, D. Gold nanoparticles: Assembly, supramolecular chemistry, quantum-size-related properties, and applications toward biology, catalysis, and nanotechnology. *Chemical Reviews* **104**, 293-346 (2004).

117. Guo, S. J. & Wang, E. K. Synthesis and electrochemical applications of gold nanoparticles. *Analytica Chimica Acta* **598**, 181-192 (2007).

118. Ahmad, A., Senapati, S., Khan, M. I., Kumar, R. & Sastry, M. Extracellular biosynthesis of monodisperse gold nanoparticles by a novel extremophilic actinomycete, Thermomonospora sp. *Langmuir* **19**, 3550-3553 (2003).

119. Bharde, A., Kulkarni, A., Rao, M., Prabhune, A. & Sastry, M. Bacterial enzyme mediated biosynthesis of gold nanoparticles. *Journal of Nanoscience and Nanotechnology* **7**, 4369-4377 (2007).

120. Ahmad, A. *et al.* Intracellular synthesis of gold nanoparticles by a novel alkalotolerant actinomycete, Rhodococcus species. *Nanotechnology* **14**, 824-828 (2003).

121. Wen, L. *et al.* Extracellular biosynthesis of monodispersed gold nanoparticles by a SAM capping route. *Journal of Nanoparticle Research* **11**, 279-288 (2009).

122. Du, L. W., Jiang, H., Liu, X. H. & Wang, E. K. Biosynthesis of gold nanoparticles assisted by Escherichia coli DH5 alpha and its application on direct electrochemistry of hemoglobin. *Electrochemistry Communications* **9**, 1165-1170 (2007).

123. Nair, B. & Pradeep, T. Coalescence of nanoclusters and formation of submicron crystallites assisted by Lactobacillus strains. *Crystal Growth & Design* **2**, 293-298 (2002).

124. Lengke, M. F. *et al.* Mechanisms of gold bioaccumulation by filamentous cyanobacteria from gold(III) - Chloride complex. *Environmental Science & Technology* **40**, 6304-6309 (2006).

125. Husseiny, M. I., El-Aziz, M. A., Badr, Y. & Mahmoud, M. A. Biosynthesis of gold nanoparticles using Pseudomonas aeruginosa. *Spectrochimica Acta Part A-Molecular and Biomolecular Spectroscopy* **67**, 1003-1006 (2007).

126. He, S. Y., Guo, Z. R., Zhang, Y., Zhang, S. & Gu, J. W. N. Biosynthesis of gold nanoparticles using the bacteria Rhodopseudomonas capsulata. *Materials Letters* **61**, 3984-3987 (2007).

127. Shankar, S. S., Ahmad, A., Pasricha, R. & Sastry, M. Bioreduction of chloroaurate ions by geranium leaves and its endophytic fungus yields gold nanoparticles of different shapes. *Journal of Materials Chemistry* **13**, 1822-1826 (2003).

128. Mukherjee, P. *et al.* Extracellular synthesis of gold nanoparticles by the fungus Fusarium oxysporum. *Chembiochem* **3**, 461-463 (2002).

129. Mukherjee, P. *et al.* Bioreduction of AuCl4- ions by the fungus, Verticillium sp. and surface trapping of the gold nanoparticles formed. *Angewandte Chemie-International Edition* **40**, 3585-+ (2001).

130. Mao, X. & Liu, G. D. Nanomaterial based electrochemical DNA biosensors and bioassays. *Journal of Biomedical Nanotechnology* **4**, 419-431 (2008).

131. Wang, J. Nanomaterial-based electrochemical biosensors. *Analyst* **130**, 421-426 (2005).

132. Wang, J. Nanoparticle-based electrochemical DNA detection. *Analytica Chimica Acta* **500**, 247-257 (2003).

133. Castaneda, M. T., Alegret, S. & Merkoci, A. Electrochemical sensing of DNA using gold nanoparticles. *Electroanalysis* **19**, 743-753 (2007).

134. Pumera, M. *et al.* Magnetically trigged direct electrochemical detection of DNA hybridization using Au-67 quantum dot as electrical tracer. *Langmuir* **21**, 9625-9629 (2005).

135. Pumera, M., Aldavert, M., Mills, C., Merkoτi, A. & Alegret, S. Direct voltammetric determination of gold nanoparticles using graphite-epoxy composite electrode. *Electrochimica Acta* **50**, 3702-3707 (2005).

136. Kawde, A. N. & Wang, J. Amplified electrical transduction of DNA hybridization based on polymeric beads loaded with multiple gold nanoparticle tags. *Electroanalysis* **16**, 101-107 (2004).

137. Wang, J., Liu, G. D. & Merkoci, A. Electrochemical coding technology for simultaneous detection of multiple DNA targets. *Journal of the American Chemical Society* **125**, 3214-3215 (2003).

138. Zhang, D., Carr, D. J. & Alocilja, E. C. Fluorescent bio-barcode DNA assay for the detection of Salmonella enterica serovar Enteritidis. *Biosensors & Bioelectronics* **24**, 1377-1381 (2009).

139. Zhang, D., Huarng, M. C. & Alocilja, E. C. A multiplex nanoparticle-based bio-barcoded DNA sensor for the simultaneous detection of multiple pathogens. *Biosensors and Bioelectronics* **26**, 1736-1742 (2010).

This chapter is adapted from our recently published work in IEEE Transactions on Nanotechnology and the Journal of Nanoparticle Research:

Edith Torres-Chavolla, Romali J. Ranasinghe, and Evangelyn C. Alocilja. Characterization and functionalization of biogenic gold nanoparticles for biosensing enhancement. IEEE Transactions on Nanotechnology. **2010**. 9(5):533-538.

DOI: 10.1109/TNANO.2010.2052926

Anderson, J. Michael; Torres-Chavolla, Edith; Castro, A. Brian and Alocilja, C. Evangelyn. One step alkaline synthesis of biocompatible gold nanoparticles using dextrin as capping agent. Journal of Nanoparticle Research. **2010**. 13(7):2843-2851.

DOI: 10.1007/s11051-010-0172-3

Chapter 3

Synthesis and characterization of glyco-gold nanoparticles

3.1 Introduction

Gold nanoparticles (AuNPs) are widely used in sensing methods as tracers and transducers. Their unique tunable physicochemical properties, plus their excellent biological compatibility, conducting properties, and high surface-to-volume ratio make them ideal candidates for electronic signal transduction of biological recognition events in biosensing platforms (*1*). Commonly, AuNPs are synthesized by chemical reduction of $HAuCl_4$ under acidic conditions and the introduction of a coating agent (citrate methodology) (*2*). In recent years, alternative biosynthetic approaches have been explored using microorganisms as bio-nano-factories to produce metal nanoparticles as well as alternative biomolecules for coating agents (*3-5*). AuNP biosynthesis procedures include the use of fungi and bacteria strains.

This chapter describes the development of two green-chemistry approaches for the biosynthesis of AuNPs. The first methodology uses alkalothermophilic actinomycetes (*Thermomonospora curvata*, *T. fusca*, and *T. chromogena*) for microbial extracellular biosynthesis of AuNPs. The average AuNP diameter obtained with this methodology was in the range of 30-60 nm and the obtained particles were monodisperse and water soluble. Nevertheless, positive biosynthesis reactions were not consistent between batch-to-batch with the three bacterial strains. Additionally, the particles were not stable for more than one week; they aggregated at room temperature and under refrigerated conditions. Therefore, other alternatives were explored in order to improve the AuNP stability and reduce the batch-to-batch variation of

the synthesis. These evaluations included the use of cell washes instead of the microbial cell pellets for the AuNP synthesis; the use of liquid medium in which the actinomycetes were grown (Hickey-Tresner broth (HT)); and the individual ingredients that compose this medium for the synthesis of AuNPs.

From these evaluations, it was observed that dextrin (one of the ingredients of HT broth) produced reproducible results for the biosynthesis of AuNPs. The second biosynthetic approach described in this chapter generates AuNPs under mild alkaline conditions using dextrin as capping agent and sodium carbonate as the $HAuCl_4$ reducing agent. The particles generated with this methodology were relatively mono-dispersed and water soluble with a range of controllable mean diameters from 5.9 to 16.8 nm ± 1.6 nm. The effect of several factors over the synthesis (pH, temperature, and dextrin concentration) was evaluated in order to optimize the procedure to get robust and consistent results. Furthermore, the produced AuNPs were successfully functionalized with DNA oligonucleotides, and the functionalization efficiency was similar to citrate-generated AuNPs.

The dextrin coated AuNPs obtained with this methodology were stable for more than three months at room temperature (21°C) without protection from light. The optimized one step synthesis methodology is reproducible and robust. The obtained AuNPs can be used to enhance biosensing applications, as transducers or electroactive labels, especially in nanoparticle based electrochemical DNA detection systems. This application is described in chapter 4.

3.2 Materials and methods

3.2.1 Biosynthesis of gold nanoparticles using *Thermomonospora* sp.

3.2.1.1 Bacterial strains and cultures

Three different *Thermomonospora* species, *T. curvata* (ATCC 19995) *T. chromogena* (ATCC 43196) and *T. fusca* (ATCC 27730), were evaluated for the biosynthesis of AuNPs. *T. curvata* has been reported as the type strain of the genus *Thermomonospora*, therefore it was chosen as the main strain for the biosynthesis evaluation. Additionally, *T. fusca* and *T. chromogena* were evaluated for the AuNP production. All strains were purchased from ATCC in lyophilized form and revitalized according to the procedure provided. After culture growth was obtained from the pellet resuspension, two steps of enrichment in broth and agar plates were performed for each strain in order to have stable cultures for storage. The cultures were kept at room temperature in agar slants of the appropriate media (according ATCC specifications) covered by sterile mineral oil for maintenance with monthly transfers. Additionally, glycerol frozen stocks were created for long term storage and kept at -80°C. In order to create a seed culture for the biosynthesis, 10 mL of the appropriate broth (*T. curvata* in Hickey-Tresner broth; *T. fusca* in Tryptone-Yeast-Glucose broth; and *T. chromogena* in Half-strength Nutrient Broth) were inoculated from the agar slants and incubated for 24-48 h at 50°C.

3.2.1.2 Optimization of gold nanoparticle synthesis

The biosynthesis protocol was elaborated based on the aerobic procedure previously published for *Thermomonospora sp.* (*6*) with modifications. Several reaction parameters were optimized including mycelia growth media and pH, $HAuCl_4$ concentration and incubation time. The synthesis procedure can be described as follows: 45 ml of Hickey-Tresner (HT) broth (dextrin 10g/L; tryptone 2g/L; meat extract 1g/L; yeast extract 1g/L; $CoCl_2$ 2mg/L; pH 7.2) were

inoculated with 5 ml of a seed pre-grown culture of *T. curvata* in a sterile 250 ml Erlenmeyer flask. For *T. fusca* and *T. chromogena*, MYGP broth (malt extract 3g/L; glucose 10g/L; yeast extract 3g/L; peptone 5g/L; pH 9) (*7*) was used instead of HT. After inoculation, the flask was incubated at 50°C during 4 days with continuous shaking (100 rpm). After biomass production, the mycelia were washed three times with distilled sterile water (3000 rpm/4°C/10min). The wet mycelia (~ 5 ml) were then transferred into sterile 250 ml flasks containing 50 ml of $HAuCl_4$ solution 2 mM at pH 9 (adjusted using filter-sterile 10% Na_2CO_3). The flasks were then incubated in the dark at 50°C during 5 days with continuous shaking (100 rpm). At the end of the reaction, the suspension was filtered in order to eliminate the mycelia from the system. The obtained solution was then analyzed for nanoparticle characterization.

3.2.1.3 Gold nanoparticle characterization

The AuNP biosynthesis was evaluated using UV/Vis scanning spectroscopy, size distribution by light scattering and transmission electron microscopy (TEM) images. UV/Vis spectra were measured using a UV-VIS-NIR Scanning Spectrophotometer (Shimadzu). Size distribution was obtained with a Zetasizer Nano series (Malvern Instruments). TEM images were collected with a JEOL 100CX Transmission Electron Microscope. A diluted suspension of the obtained AuNPs in distilled water was sonicated for 5 min. 5 µl of the sample was transferred into a formvar/carbon coated copper grid (300 mesh). The grid was left to dry and observed.

3.2.1.4 Glutaraldehyde stabilization

Glutaraldehyde is a common crosslinker for biomolecule functionalization on surfaces and nanoparticles. Therefore, in order to improve the stability of the AuNP, glutaraldehyde was added to the biosynthesis reaction as a capping agent using *T. curvata*. One (1) ml of 50% glutaraldehyde was added before incubation to the $HAuCl_4$ solution with the cell-pellet (10%

glutaraldehyde final concentration) which was prepared using the same procedure described above. After the incubation period, the suspension was filtered and the obtained solution was then analyzed for nanoparticle characterization.

3.2.2 Biosynthesis of gold nanoparticles using dextrin as capping agent

3.2.2.1 Optimization of gold nanoparticle synthesis

A gold chloride ($HAuCl_4$) stock solution (20 mM) was prepared using distilled sterile water and was stored under refrigeration. The dextrin stock solution (25 g/L) was prepared using deionized water and autoclaved prior to use. A mixture of distilled sterile water and dextrin stock solution was added to a sterile 250 mL flask according to the desired dextrin concentration within the 2.5 to 20.0 g/L final working range. A volume of 5 mL of $HAuCl_4$ stock solution was added to the reaction and adjusted to pH 9 using filter-sterile 10% sodium carbonate (Na_2CO_3), the final $HAuCl_4$ concentration in the reaction was 2 mM. Finally, the reaction volume (50 mL) was completed by using pH adjusted distilled water (pH 9). The flask was incubated in the dark at 50°C with continuous shaking for 8 hours. Particle formation was observed through the following stages of color change; clear, purple tint, red tint, and red (520 nm), the same color sequence as citrate reduction (*8*). The effects of pH (from 3 to 11) and temperature (25°C and 50°C) on the synthesized particles were evaluated and compared to sodium citrate generated AuNPs.

3.2.2.2 Gold nanoparticle characterization

The AuNP formation was evaluated using UV/Vis scanning spectroscopy and transmission electron microscopy (TEM) using the same procedure and equipment described before (3.2.1.3).

3.2.2.3 Gold nanoparticle functionalization with DNA probes

In order to evaluate the ability to use the dextrin-coated AuNPs for future sensing assays, thiol-modified oligonucleotides were attached to the AuNP surface using the ligand exchange method for functionalizing citrate-coated AuNPs (*9,10*). An oligonucleotide (sequence 5'-TTA TTC GTA GCT AAA AAA AAA A-3') was used with 5' 6-Carboxyfluorescein (6-FAM; λ excitation = 495 nm, λ emission = 520 nm) and 3' thiol modifications. The oligonucleotide was ligand-exchanged for the capping agent post-AuNP production. The AuNPs were centrifuged into a pellet and separated from the excess DNA ligand, washed three times, and resuspended in dithiothreitol (DTT) buffer. The DTT AuNP-DNA solution was heated for 60 minutes at 50°C in order to ligand-exchange DTT for the thiolated DNA. The fluorescence signal from the supernatant was measured for DNA conjugation efficiency using a 527-547 nm emission filter (VICTOR^3 1420 Multilabel counter, Perkin-Elmer).

3.3 Results and discussion

3.3.1 Biosynthesis of gold nanoparticles using *Thermomonospora* sp.

3.3.1.1 Gold nanoparticle synthesis and characterization

After incubation, the suspension obtained from the microorganisms in which the AuNP synthesis has occurred showed a change from pale yellow to red, which is an indicator of extracellular AuNP production (Figure 3-1). The obtained spectra showed absorption peaks from 530 to 550 nm, which correspond to particles from 30-60 nm. Figure 3-2 shows the spectra from the optimization trials. As it can be observed in the plots, optimal AuNP biosynthesis was obtained using a mycelia growth pH of 7.2; 2mM $HAuCl_4$; and five days of incubation. Particles in the range of 5-15 nm and 30-60 nm were observed with all three *Thermomonospora* species (*T. curvata*, *T. fusca* and *T. chromogena*). Nevertheless, a higher AuNP production yield was obtained with *T. curvata*, as can be observed in the absorbance peak (1.15 A.U.) in Figure 3-2. The absorbance is directly proportional to the AuNP concentration. With *T. fusca* and *T. chromogena*, low production yields were obtained during all the experiments (0.41 and 0.78 A.U. respectively) as can be observed in Figure 3-2.

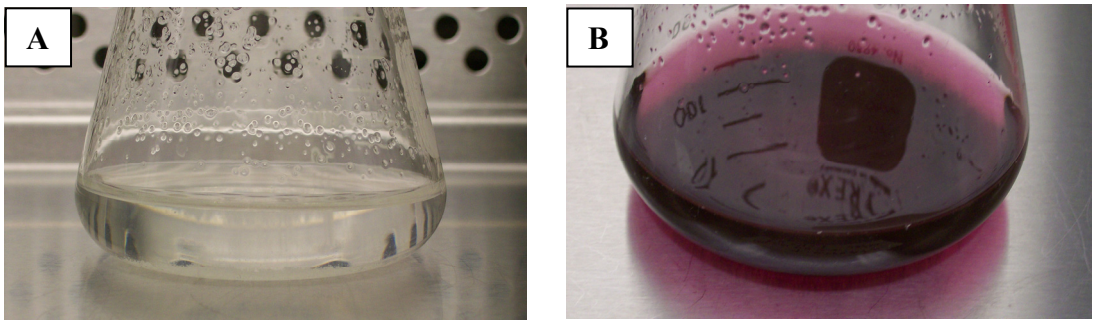

Figure 3-1. Biosynthesis of AuNP using *T. curvata*. Gold chloride solution before the synthesis (A) and after 5 days of incubation (B).

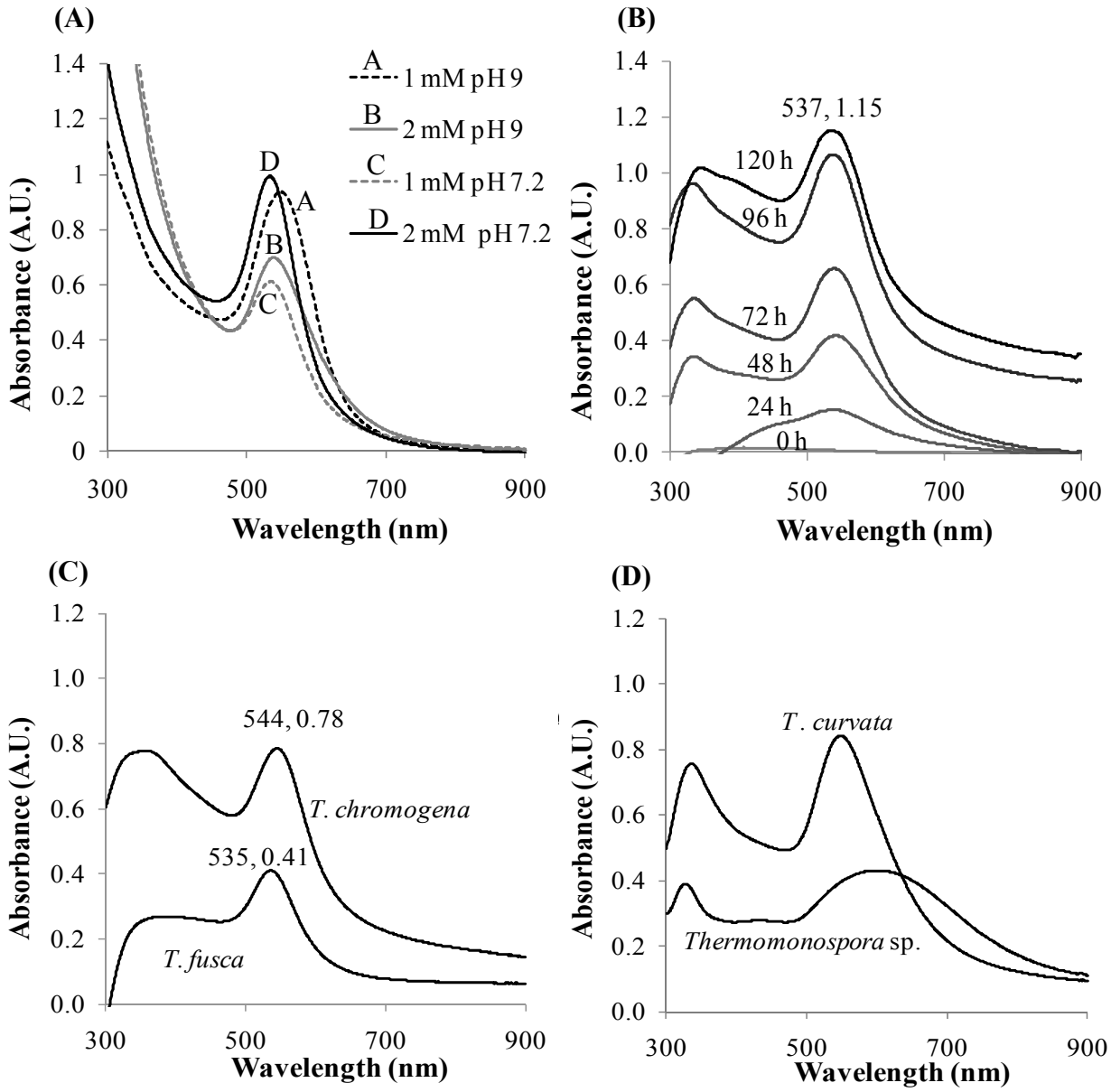

Figure 3-2. UV-Vis spectra of AuNP production. (A) Mycelia growth pH and gold chloride optimization using *T. curvata*. The highest absorption peak was obtained using 2 mM solution of $HAuCl_4$ and pH 7.2. (B) Time monitoring using *T. curvata* biomass and a 2 mM solution of $HAuCl_4$. The highest peak is achieved at 5 days of incubation. (C) and (D) UV-Vis spectra of AuNP production using *T. fusca*, *T. chromogena* and *Thermomonospora* sp (adapted from (*11*)).

From the three bacterial strains evaluated for the biosynthesis of AuNPs, *T. curvata* also showed less batch-to-batch variation in the production yield than *T. fusca* and *T. chromogena*. The particle size distribution also confirmed the obtained average size ranges for all strains (Figure 3-3). The biosynthesis procedure previously published (*6*) used a *Thermomonospora* sp. culture isolated from compost, therefore an additional *Thermomonospora* sp. (DSM 43773) culture was evaluated. The AuNP biosynthesis reactions using this microorganism were negative for all the evaluated trials. Figure 3-2 (D) shows the spectra comparison with a positive reaction using *T. curvata*.

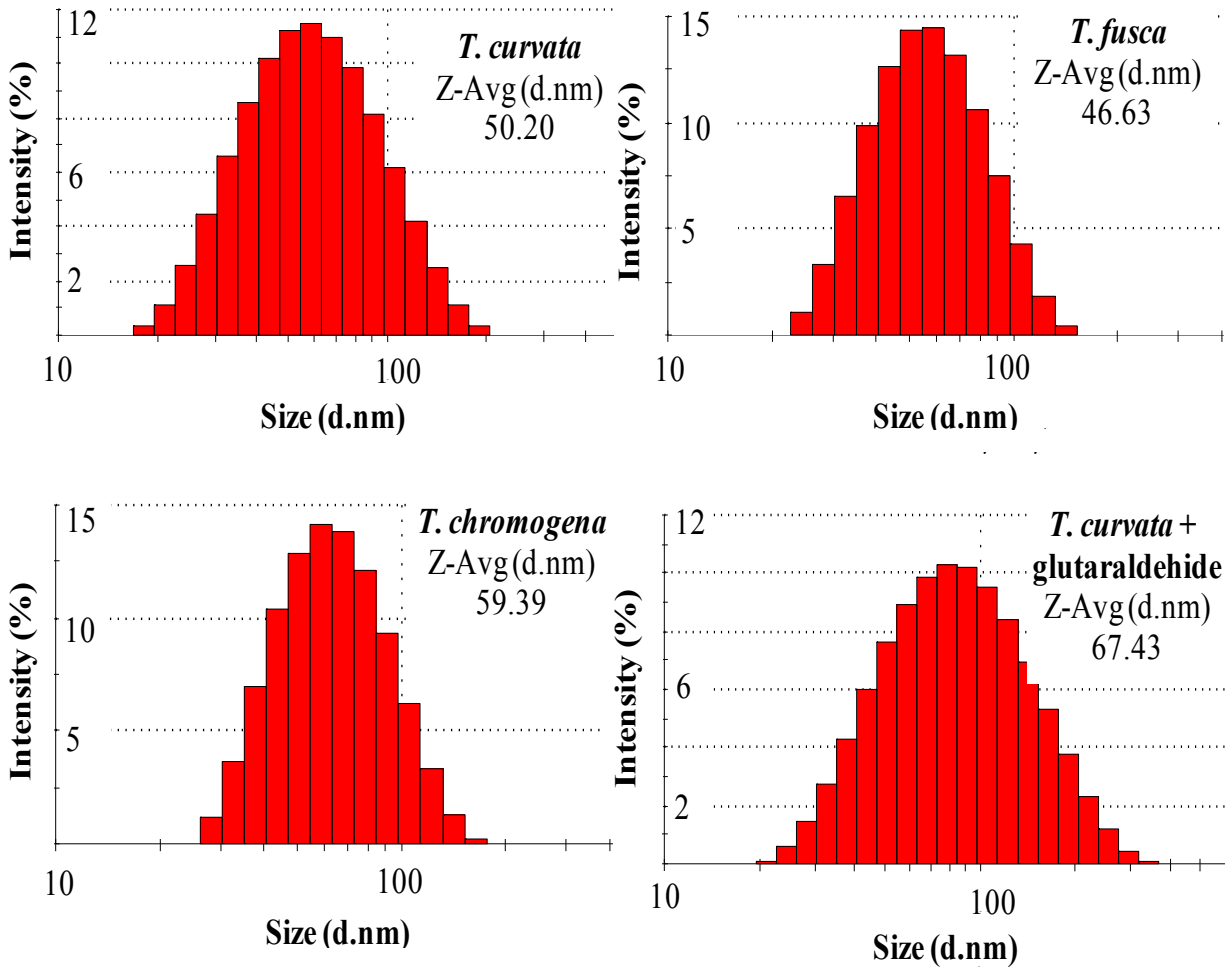

Figure 3-3. Size distribution plots by intensity using light scattering.

Some examples of the TEM images observed from the AuNP biosynthesis using *T. curvata* are shown in Figure 3-4. These images also confirm the average size range obtained with the size distribution and the UV-Vis spectra (Figure 3-2 and 3-3). The main characteristics observed in the produced AuNPs are summarized in Table 3-1.

Table 3-1. AuNP characterization using different *Thermomonospora* species.

Bacteria strain	**Absorbance peak (nm, A.U.)**	**Size ranges[*] (nm)**	**Average size[+] (nm)**
T. curvata	537, 1.15	5-15, 30-60	53
T. fusca	535, 0.41	5-15, 30-60	47
T. chromogena	544, 0.78	5-15, 30-60	59
T. curvata + glutaraldehyde	549, 3.26	30-70	70

[*]The different AuNP size ranges were obtained from the TEM images. [+]The average size (nm) was obtained from the particle size distribution using light scattering.

As mentioned earlier, the first evaluation after biosynthesis is the visual inspection, where a distinctive change in color from pale yellow to bright red is expected when the AuNP synthesis occurs. Therefore, red suspensions were considered positive reactions and the obtained particles were further characterized. One of the major observations in this study was that positive reactions were not consistent between batch-to-batch with the three bacterial strains. Additionally, the particles were not stable for more than one week; they aggregated at room temperature and under refrigerated conditions. To minimize aggregation, glutaraldehyde was added as a protective agent into the system. The optimal pH for the AuNP production was 9. Readjustments of the pH during the biosynthesis were necessary in order to increase stability (minimize aggregation).

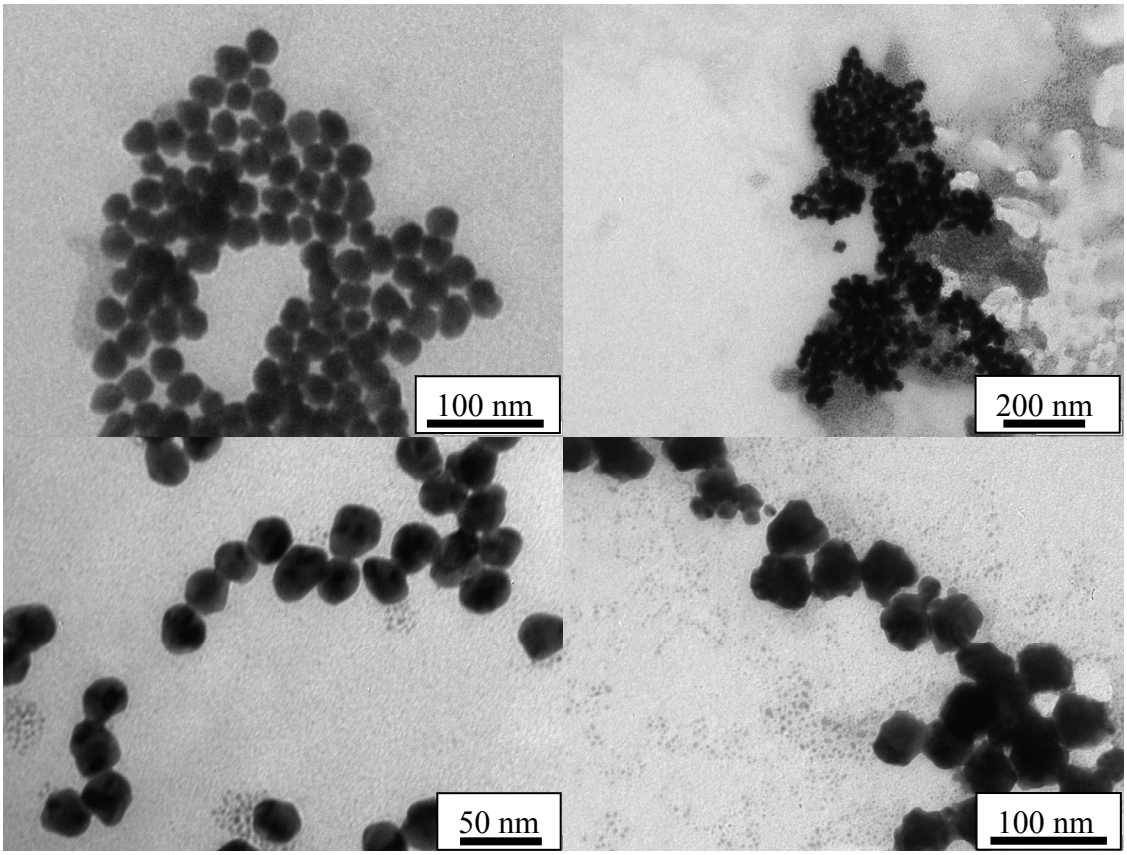

Figure 3-4. TEM images of AuNPs produced using *T. curvata.*

The addition of glutaraldehyde, as stabilizer to avoid aggregation, produced an absorption shift to the right and a higher absorbance with a narrower peak in the spectrophotometric scanning (Figure 3-5). A significantly higher production yield was obtained with the introduction of glutaraldehyde, as can be observed in the absorbance increase (3.26 A.U.). At the end of the reaction, AuNPs were obtained within a size range of 30-70 nm and an absorption peak at 549 nm. The introduction of glutaraldehyde produced more consistent results between batch-to-batch biosynthesis and the particles were stable over a month in refrigeration, compared with AuNPs without glutaraldehyde coating.

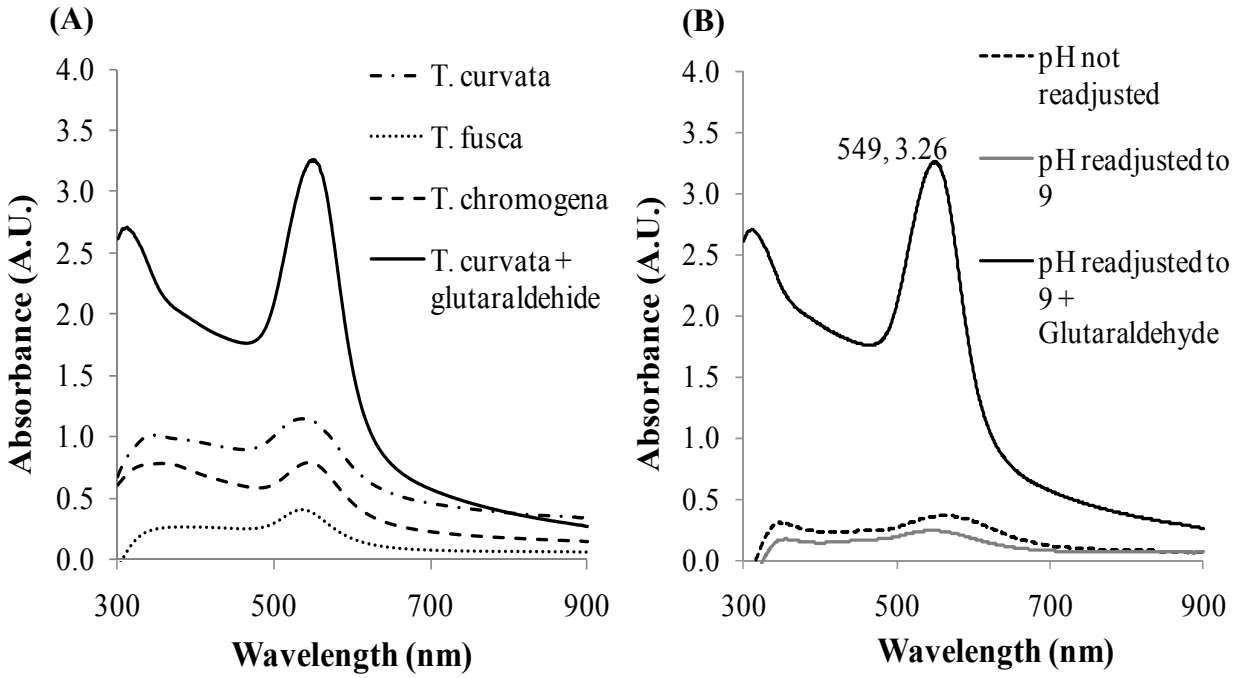

Figure 3-5. (A) UV-Vis spectra of AuNP production using *T. curvata* biomass and glutaraldehyde as capping agent; (B) UV-Vis spectra comparison of AuNP production using *T. curvata*, *T. fusca, T. chromogena*, and *T. curvata* with glutaraldehyde as capping agent (adapted from (*11*)).

3.3.1.2 Biosynthesis using cell washes and nutrient media ingredients

The biosynthesis mechanism for the extracellular production of AuNPs using microorganisms has not been elucidated, and due to the high batch-to-batch variations obtained with the microbial cell pellets, other alternatives were explored. Previous reports have already proposed the hypothesis of an extracellular NADH-dependent reductase that is released to the system (*12*). Other studies have successfully used cell-supernatant instead of cell-pellets to produce AuNPs based on this hypothesis (*13*,*14*). Using the same conditions as previously described, myscelia washes were evaluated for the biosynthesis production instead of cell pellets.

Figure 3-6 (A) shows the UV-Vis spectra characterization. Positive biosynthesis reactions were obtain with all the washes. Furthermore, several experiments were conducted using HT broth instead of water for the biosynthesis reaction, in order to have a favorable media for the mycelia. The characteristic change in color was observed and the synthesis of AuNP was confirmed with spectrophotometry and TEM. The results with these two approaches were more consistent and reproducible and an increase in the absorption peak was observed (Figure 3-6). These observations led to the evaluation of HT broth itself without the use of microorganisms and positive reactions were obtained as well (Figure 3-6 (B)). Negative controls were used for all the experiments, in order to discard the possibility of microbial contamination producing positive reactions where the microorganism was not present.

After the microbial contamination was discarded, the AuNP biosynthesis using HT broth was verified in several trials. UV-Vis spectra and TEM were used to characterize the obtained particles. The absorbance peak was increased and the production yield was reproducible. Therefore, it was concluded that some of the HT broth ingredients could act as reduction agents for the gold chloride and capping agents for the gold nanoparticle formation. Trials with each ingredient and their combination were conducted. Dextrin, yeast extract and tryptone produced a change in color from pale yellow to red and purple (Figure 3-6 (C)). Positive reactions were confirmed using spectrophotometry and TEM (Figure 3-7). From these trials, dextin was selected for further exploration as reduction and capping agent for the production of AuNPs since it showed less aggregation and more stability over time compared with the reactions obtained with the rest of the ingredients (Figure 3-8).

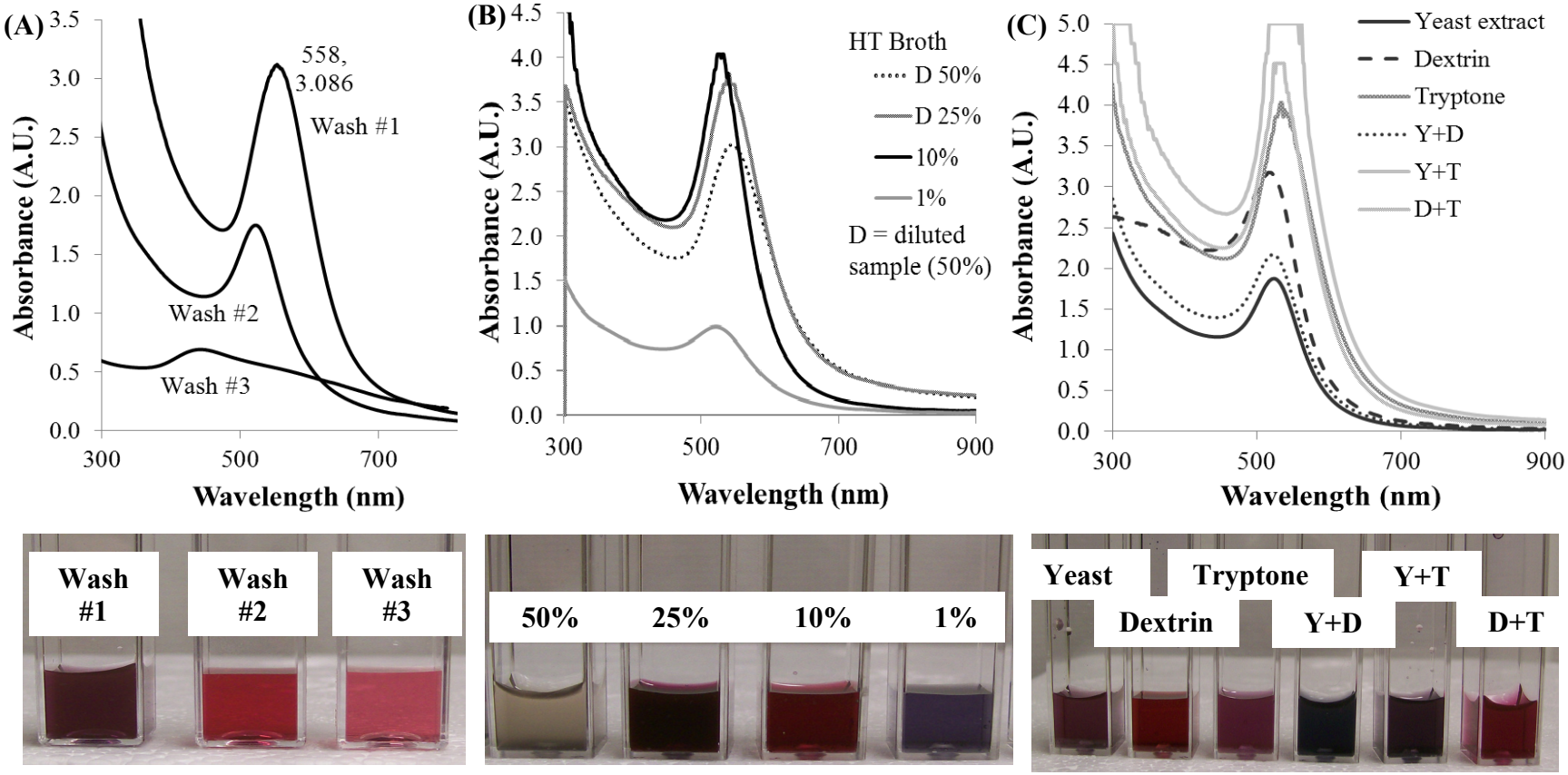

Figure 3-6. UV-Vis spectra of AuNP biosynthesis. (A) Comparison of absorption peaks obtained using mycelia washes instead of cell pellets. Positive AuNP production was observed using the first and second washes. (B) Biosynthesis of AuNPs using HT broth only (with no microbial cells or washes) at different concentrations. (C) Biosynthesis of AuNPs using HT broth ingredients (2.5 g/L) as reduction and capping agents individually and combined for the AuNP production. The images to the left of each UV-Vis spectra profile show the characteristic changes in color for each biosynthesis reaction.

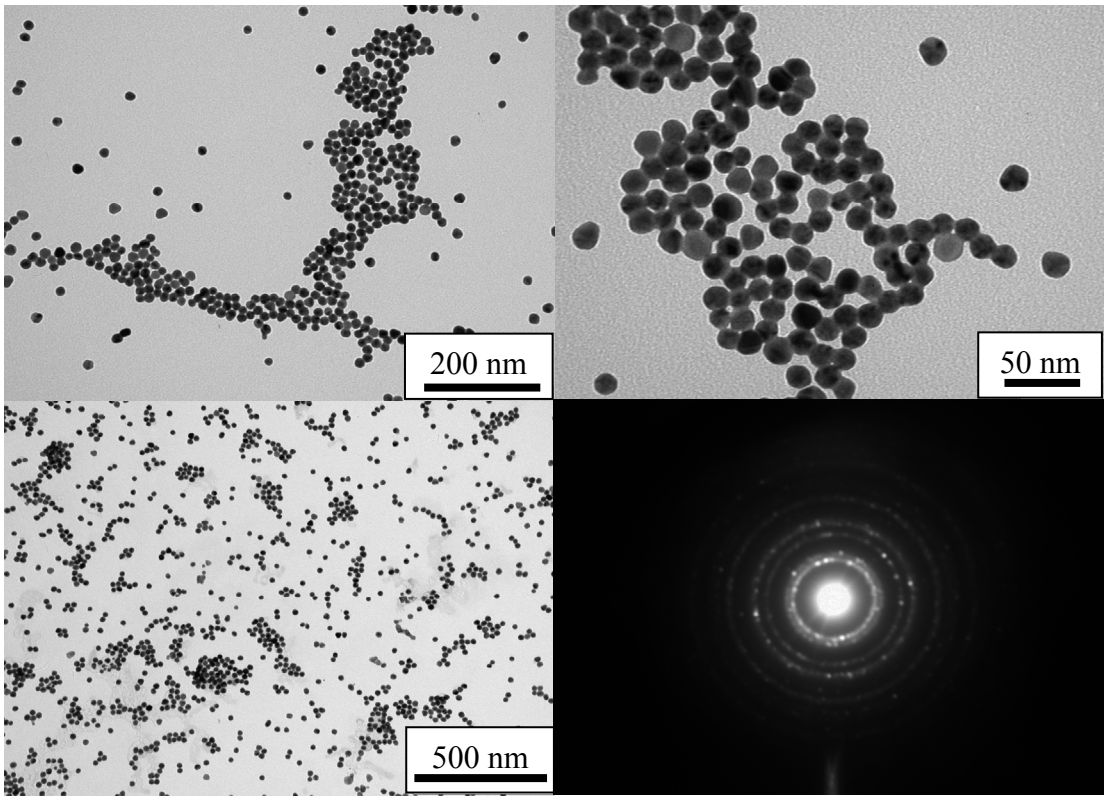

Figure 3-7. TEM images of AuNPs produced using dextrin (2.5 g/L) as reduction and capping agent; and selected area (SA) diffraction pattern from the AuNPs shown.

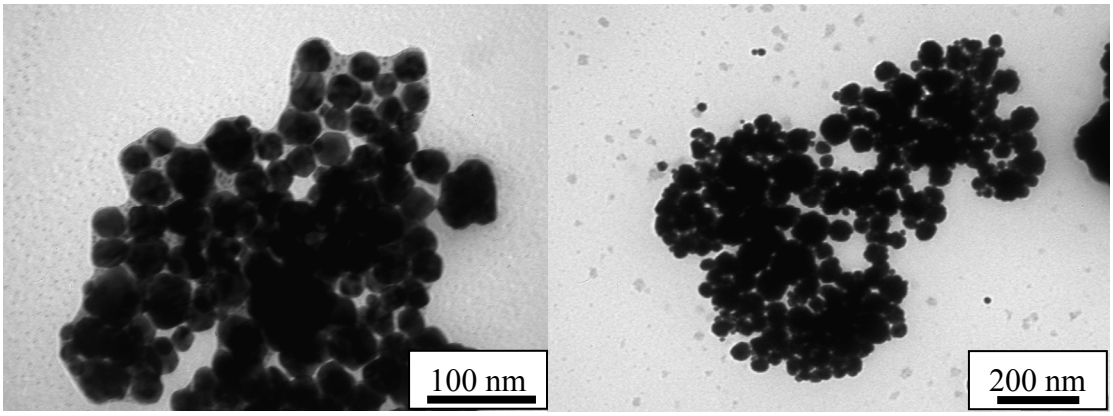

Figure 3-8. TEM images of AuNPs produced using tryptone as reducing and capping agent. The particles show more aggregation and polydispersion when compared to the particles obtained using dextrin (Figure 3-7).

3.3.2 Biosynthesis of gold nanoparticles using dextrin as capping agent

3.3.2.1 Gold nanoparticle synthesis and characterization

AuNPs were successfully synthesized at alkaline conditions using dextrin as a capping agent. Figure 3-9 (A) shows the increase of absorbance at 520 nm with time and the corresponding change in color with time. The particle generation was monitored over 24 hours with UV/Vis spectra. The absorbance peak at 520 nm was observed in all samples after initial red tint through the characteristic red color of gold nanoparticles in the 10-100 nm size range. The AuNP formation was visually observed after 6 hours of incubation. The reaction continued until completion at 8 hours. Figure 3-9 (B) shows TEM images of AuNPs generated at 10.0 g/L dextrin concentration, 2 mM$HAuCl_4$, pH 9.0 and 50°C. Particle formation was not observed when dextrin, pH adjustment, or sodium carbonate was excluded from the synthesis.

3.3.2.2 Effect of dextrin concentration, synthesis pH, and temperature

The ratio of capping agent to particle concentration is a commonly varied factor to control the final size of the particles. The concentration of dextrin was varied from 2.5 g/L to 20.0 g/L to explore the effect of dextrin concentration on particle size. The final size of particles was determined using TEM images (Figure 3-10). It was observed that the particle diameter decreased with increasing dextrin concentration. Particle sizes were 8.6 nm ±1.2 nm, 10.6 nm ±1.6 nm, and 12.4 nm ±1.5 nm for 20.0, 10.0, and 2.5 g/L dextrin concentrations, respectively. Figure 3-11 shows a linear relationship between dextrin concentration and particle size for 2.5 to 20.0 g/L of dextrin.

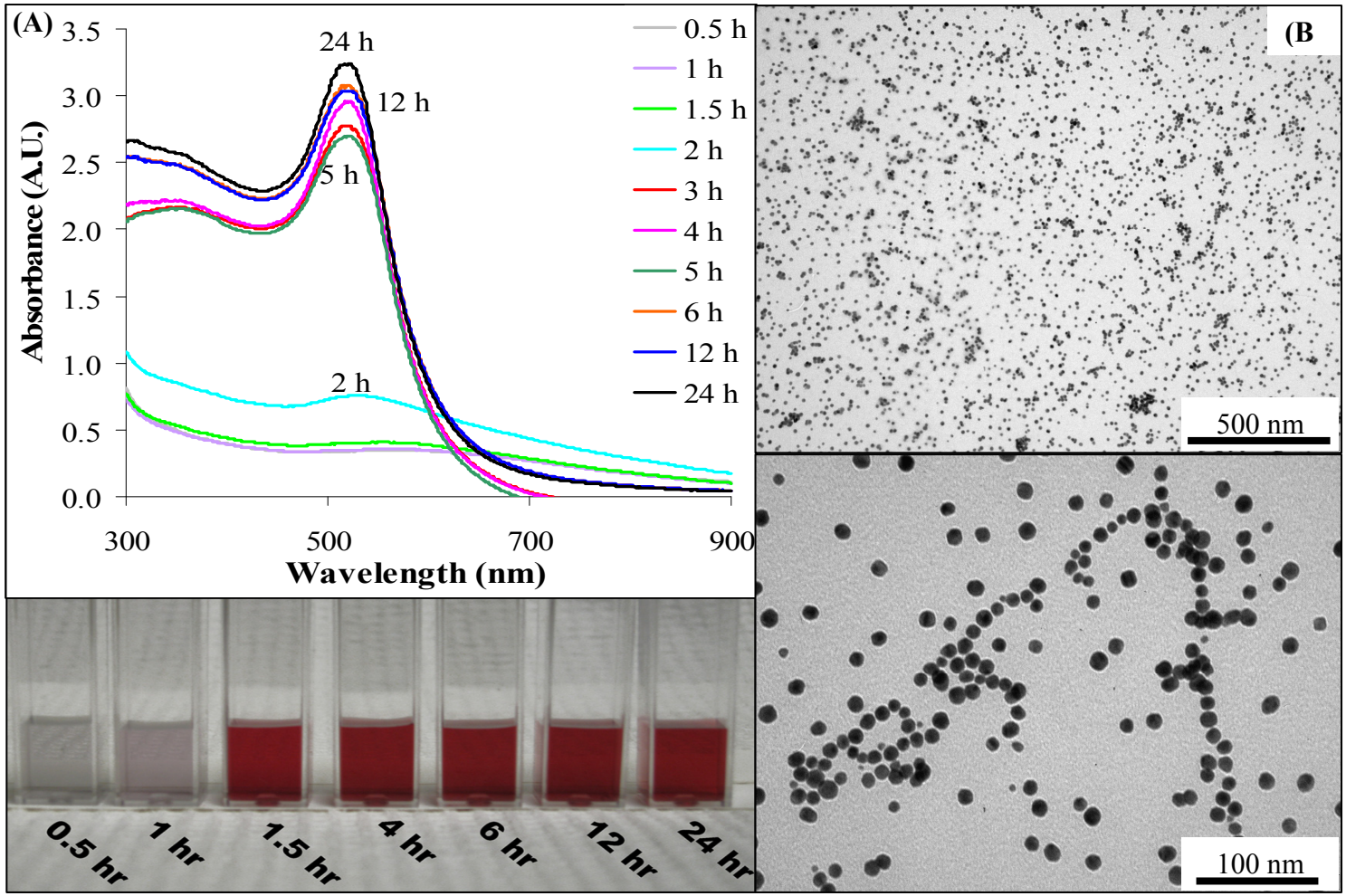

Figure 3-9. (A) Time monitoring UV-Vis spectra of AuNP biosynthesis using dextrin with visual color change over time. (B) TEM images produced at optimal conditions: 50°C, 24 hr, 10.0 g/L dextrin (figure adapted from (*15*)).

The reaction time decreased with increased initial dextrin concentration. Initial particle formation was observed within 5 hours at 2.5 g/L of dextrin, and within 1.5 hours for 20.0 g/L of dextrin indicated by the red color, which became more intense as the reaction completed. UV-Vis spectral data was used to monitor the reactions for completion. All dextrin concentrations between 5.0 and 20.0 g/L showed completion at 6 hours, with 2.5 g/L showing completion at 24 hours.

The size and production rate appeared to be controlled by dextrin concentration. Polte et al. (2010) proposed a four step generation model for citrate coated AuNPs. The alkaline dextrin system presented here appeared to follow a similar mechanism, that is, from reduction, stabilization, exchange (slow growth phase), and finally to capping (fast growth phase). Steps 1 and 2 of our system could be carried out by the sodium carbonate reducing the gold chloride. In the early steps, the oxidized carbonate would be stabilizing the initial AuNP instead of the citrate molecule. As the reaction proceeds into the slow growth phase, step 2-3, the exchange of carbonate for dextrin occurs which explains the extended time it takes for the growth phase to complete, as observed in the transition from the purple tint and the initial red color. Once the system enters step 4, fast growth, dextrin is believed to be the sole capping agent and the disassociation allows for auto-catalytic growth and rapid re-association of free dextrin molecules. Changes in dextrin concentration for this system may explain why rate increased and size decreased with higher concentration. Smaller particle sizes resulted when higher amount of capping agents were used. A greater capping agent concentration can cover greater surface areas and generate smaller sized particles (*16*).

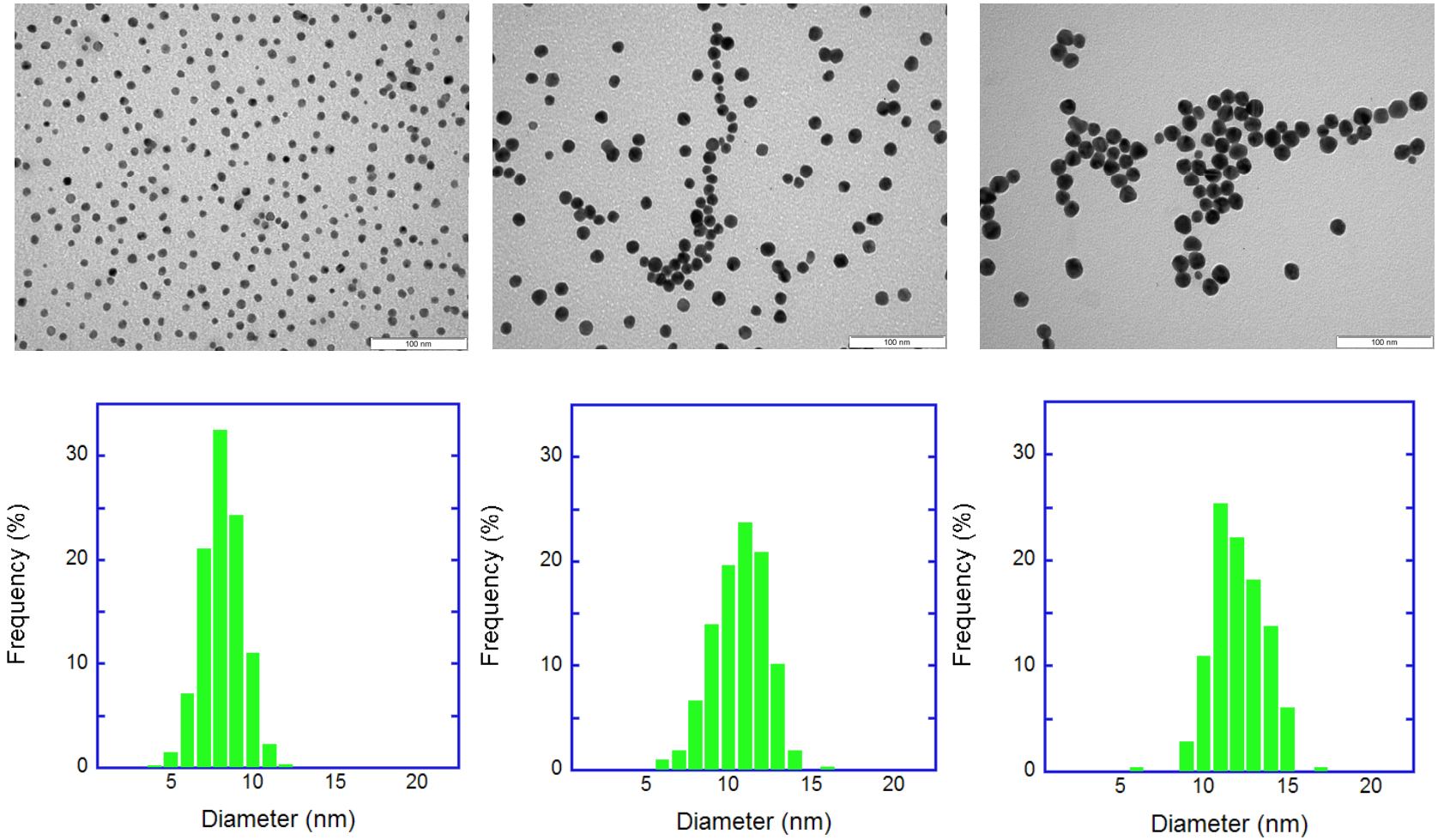

Figure 3-10. TEM images of AuNPs and size distribution using different dextrin concentrations: (A) 20.0 g/L; (B) 10.0 g/L and (C) 2.5 g/L (figure adapted from (*15*)).

In a higher concentration system, dextrin may interact with the carbonate on the gold surface promoting faster carbonate disassociation. As the carbonate disassociates, greater concentrations of free dextrin undergo surface capping more rapidly.

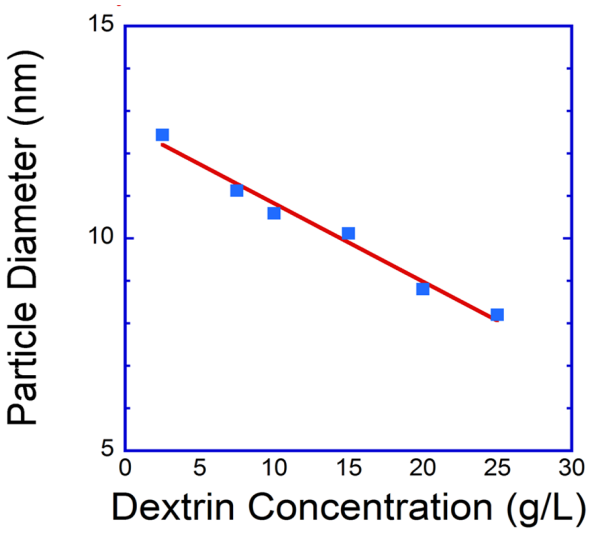

Figure 3-11. Mean AuNP diameter (nm) as a function of dextrin concentration from 2.5 to 25 g/L (from *15*).

Previous reports of sodium hydroxide induced particle formation suggest that hydroxyl ions can reduce Au^{3+} into Au^{0}, but do not participate in the capping and stabilization of the AuNP (*17*,*17*). The pH of the reaction was varied from 3 to 11 to explore the effect of pH on particle formation. The pH reactions were conducted different dextrin concentrations (2.5 - 20 g/L) and 2 mM $HAuCl_4$, and incubated for 24 hours at 50°C. Below pH 7, no particle formation was observed after 24 hours, and at pH 11 the reaction proceeded nearly instantly at room temperature. Negative control with $HAuCl_4$, at pH 9.0 and without dextrin did not yield particle formation after 24 hours nor did solution only adjusted with sodium hydroxide. The use of sodium hydroxide to adjust the pH instead of sodium carbonate produced a purple-black

precipitate with some metallic gold film forming on the glassware. AuNPs with average particle diameters from 7.0 ± 1.2 nm to 16.8 ± 2.3 nm were generated within the biological range of pH 7-10 in 24 hours. Figure 3-12 shows the UV-Vis spectra and the average sizes obtained with different pHs sodium carbonate adjusted and dextrin concentrations.

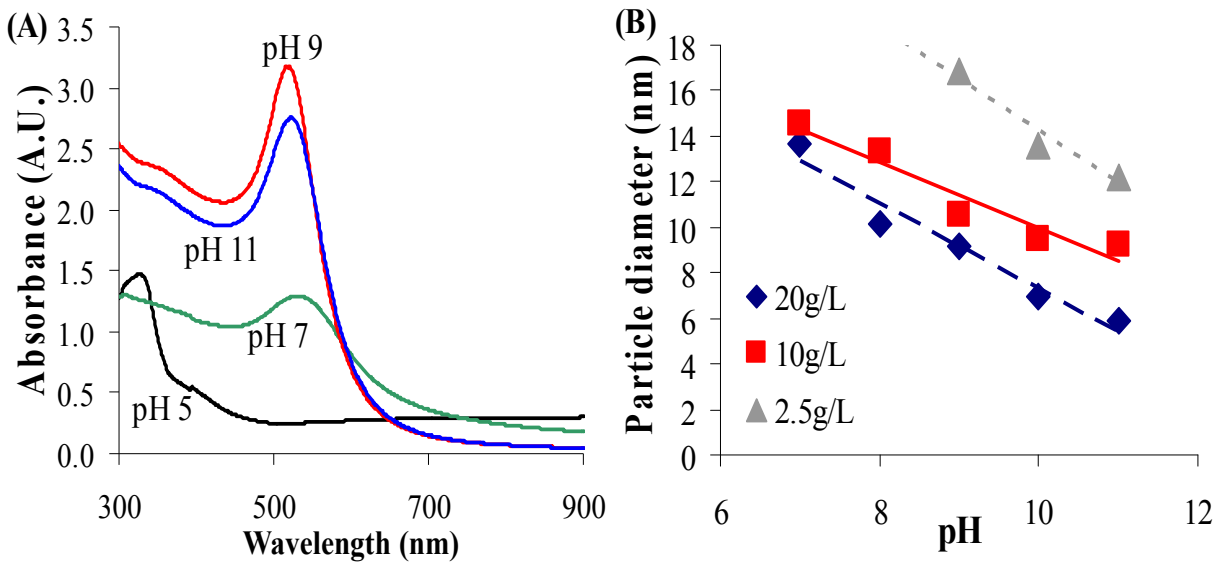

Figure 3-12. (A) UV-Vis spectra obtained using different pHs at 10 g/L of dextrin. (B) Average AuNP diameter (nm) as a function of dextrin concentration (2.5 - 20g/L) and byosinthesis pH (7-11).

By increasing the initial concentration of the reduction agent (sodium carbonate), faster nucleation may explain the observed increase of the reaction rate and observed decrease in the particle sizes. Reactions less than pH 7 did not occur with sodium carbonate as the reduction agent. Carbonate has a pKa 6.33 and 10.35. At pH 9 the predominant form is bicarbonate, at pH 11 slightly more than 65% is carbonate, and at pH 7 virtually no carbonate exists. Carbonate is a more reactive reducing species than bicarbonate and slow carbonate-bicarbonate equilibrium

could account for the longer generation times encountered. This could explain the rapid reaction rate at pH 11, where the carbonate is the predominant specie in equilibrium and why at pH lower than 7 no reaction occurs as nearly no carbonate exists in equilibrium.

The effect of temperature on the AuNP synthesis was explored to determine if the reaction rate or particle size was influenced by this factor. Reactions were carried out at 50°C and room temperature (21°C) during 24 hours for concentrations of 20.0 g/L, 10.0 g/L and 2.5 g/L of dextrin. At 50°C particles were generated in all dextrin concentrations after 6 hours. At room temperature, particle formation using 10.0 g/L of dextrin was complete after 48 hours; using 2.5 g/L of dextrin particle formation was approximately 70% complete after 48 hours. Reaction completion was based on absorbance data. Figure 3-13 shows the UV-Vis spectra obtained over time with both temperatures and the average particle diameter plotted against initial dextrin concentration at varying temperature. The particle size is affected by both temperature and dextrin concentration. The average particle diameter increased with increasing temperature. Particle formation was observed at 100°C in three minutes and completed after 7 additional minutes on the bench top. The particles generated at 100°C were not measured for this study as the reaction temperature was non-favorable for the stability of other possible biological capping agents.

Increases in incubation temperature may increase the rate of disassociation of the capping molecule, dextrin in this study. With higher temperatures, the partially uncapped AuNP is more likely to interact with free gold from solution, and result in a faster growth. A lower temperature reduces the speed of growth and the reaction may not be fully completed, explaining the incomplete reaction at room temperature. This control of size and growth rate through

temperature variation is expected to be a promising method for functionalizing the AuNPs during synthesis.

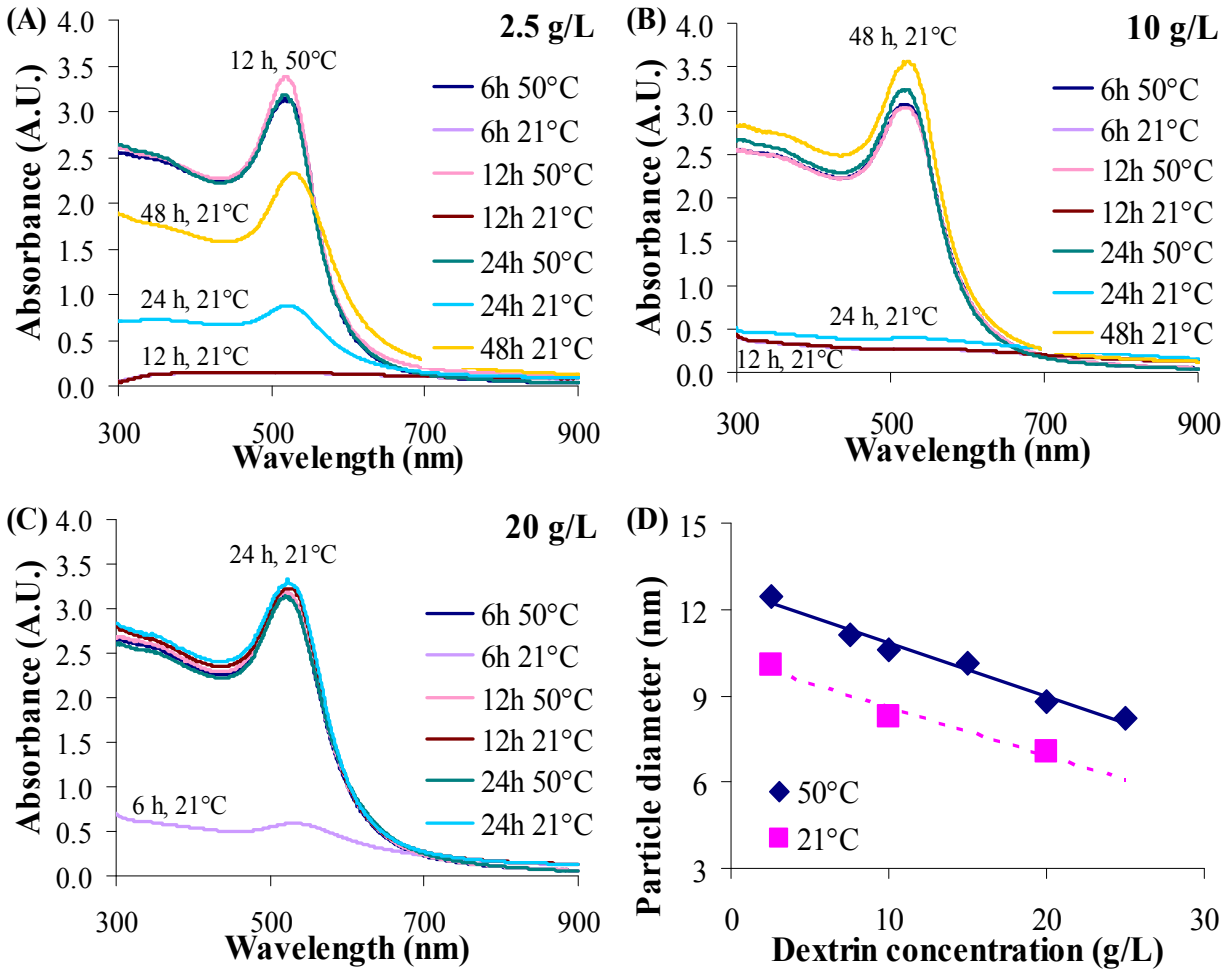

Figure 3-13. (A) to (C) UV-Vis spectra obtained over time using different incubation temperatures and dextrin concentrations. (D) Average AuNP diameter (nm) as a function of dextrin concentration (2.5 - 20g/L) and incubation temperature (21°C and 50°C).

The dextrin coated gold nanoparticles were stable (no aggregation) for more than three months at room temperature (21°C) without protection from light. The AuNPs were sensitive to low pH conditions, and when the system was titrated to pH 3.5-4.0, a quick change in color was

observed to dark purple suggesting aggregation. Complete precipitation of the particles occurred after 12 hours at room temperature. After the color change, a deep purple particulate formed and precipitated. This insoluble precipitate could not be resuspended by pH adjustment or sonication. Dextrin is an oligosaccharide of D-glucose, and D-glucose has a pKa ~12.3. The change in pH reverses the charge of the dextrin capping material thus eliminating the electrostatic interaction between dextrin and the AuNP core. When the particles were pelleted and dried, the resulting pellet could not be resuspended suggesting electrostatic interactions in the aqueous medium are required for stability.

3.3.2.3 Gold nanoparticle functionalization with DNA probes

The capping ligand exchange on citrate generated AuNPs for thiolated-DNA oligonucleotides is one of the more common attachment techniques (*9*). The dextrin coated AuNPs were functionalized as described with thiolated DNA in Hill and Mirkin (2006) and compared against standard citrate reduced AuNPs. Dextrin AuNPs generated at 2.5g/L (size: 12.4 nm) and 10.0 g/L (size: 10.4 nm) were evaluated for ligand exchange capabilities. Both sizes of dextrin coated particles were successfully functionalized with thiol-DNA-6-FAM oligonucleotides. The functionalization results are shown in Figure 3-14.

Direct fluorescence measurement of the 6-FAM is limited because the AuNP core quenches the signal. To measure the attached fluorophore, the DNA-6-FAM was ligand exchanged a second time with DTT to release the thiol-DNA-6-FAM. The recovered fluorescence after the second ligand exchange with DTT comes from the DNA attached to the AuNP cores and demonstrates successful functionalization. The citrate AuNPs were treated with the same ligand exchange procedure. The functionalization efficiency of both sizes of dextrin AuNPs was comparable to the citrate AuNPs. After ligand exchange and release, the citrate AuNPs show

greater capping efficiency only when compared to the 10.4 nm dextrin AuNPs (77% of the citrate signal was recovered). The lower fluorescence recovered with the smaller particles was expected due to less available surface area for attachment (approximate 69% of the citrate particle surface area).

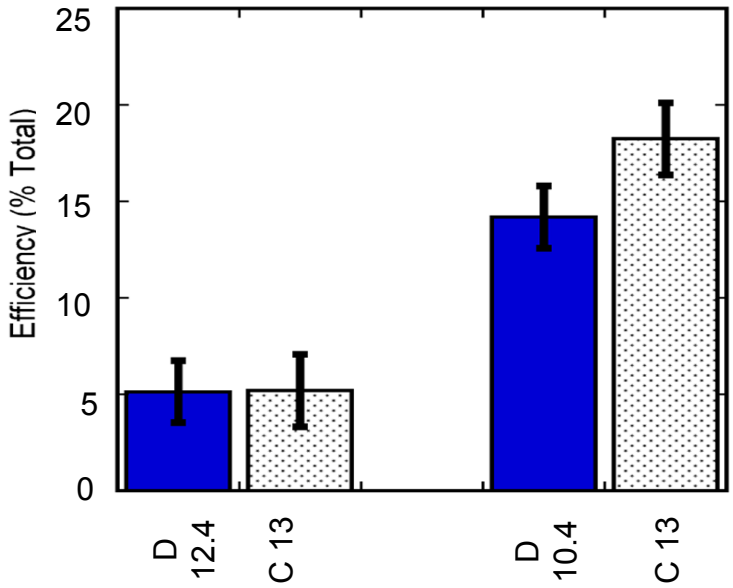

Figure 3-14. Comparative capping efficiencies (percentage of captured fluorescence) of 12.4 nm and 10.4 nm dextrin AuNPs versus 13.0 nm citrate AuNPs. D=dextrin; C=Citrate (from (*15*)).

The functionalization procedure is based on molar concentration, and smaller particles have less surface area for DNA attachment. For the 12.4 nm dextrin AuNPs, the mean capping efficiency is equal to the citrate AuNPs, where the dextrin particles have approximately 90% of the available surface area compared to the 13.0 nm citrate particles. With comparable DNA capping efficiencies, the dextrin AuNPs can be used as an alternative to citrate AuNPs for DNA applications. Another potential application of dextrin AuNPs is the exploration of simultaneous generation and functionalization, greatly reducing the functionalization time of current methodologies.

3.4 Conclusions

In the presented studies, three alkalothermophilic actinomycetes *Thermomonospora curvata*, *Thermomonospora fusca* and *Thermomonospora chromogena* were successfully used as bio-nano-factories for the extracellular biosynthesis of AuNPs following green-chemistry procedure. The obtained particles were in the size range of 30-60 nm and well dispersed in water. In order to improve stability, glutaraldehyde was used to functionalize the AuNP after synthesis. Before the AuNPs can be used for biosensing applications, more characterization of the surface chemistry is necessary in order to elucidate an appropriate functionalization methodology.

The results obtained with the washing steps and the HT broth do not refute the results obtained with microbial cells. Gold nanoparticle synthesis using microorganisms is still driven by the presence of cells and enzymes that are released to the system for the extracellular reduction of gold chloride. The result of this process showed low reproducibility due to the presence of the microorganism itself. For further standardization and optimization, the synthesis pathway needs to be elucidated and characterized in order to determine and isolate the enzymes and/or capping agents that participate in the AuNP formation. To date, several aspects of the biosynthesis of magnetic and conductive nanoparticles using microorganisms remain unknown. The elucidation of the biochemical pathways that lead to the metal ion reduction as well as the characterization of the biogenic nanoparticle surface chemistry are necessary for better understanding and standardization of the biosynthesis.

The alkaline dextrin synthesis generated particles with a diameter between 5.9 and 16.8 nm ± 1.6 nm based on dextrin concentration, pH, and temperature. Optimal AuNP synthesis was at 50°C, pH 9.0, 10.0 g/L of dextrin and 2mM of $HAuCl_4$ and resulted in particles of 10.6 nm ±1.6 nm. The particles remained soluble in water and stable for more than three months at room

temperature. The dextrin capping agent was removed and the particles were functionalized with thiolated ligands (DNA probes). Dextrin coated particles may be used for many biological applications due to the alkaline pH generation conditions. Alkaline generation of dextrin AuNPs provides size control and a sugar capping agent that can be removed for thiolated ligand exchange. The use of a polysaccharide for capping provides a biocompatible coating for potential *in vivo* and *in vitro* use. Finally, the alkaline conditions allow future exploration of simultaneous synthesis and functionalization procedures.

References

3.5 References

1. Baptista, P. *et al.* Gold nanoparticles for the development of clinical diagnosis methods. *Analytical and Bioanalytical Chemistry* **391**, 943-950 (2008).

2. Turkevich, J., Stevenson, P. C. & Hillier, J. A study of the nucleation and growth processes in the synthesis of colloidal gold. *Discussions of the Faraday Society* **11**, 55-75 (1951).

3. Mandal, D., Bolander, M. E., Mukhopadhyay, D., Sarkar, G. & Mukherjee, P. The use of microorganisms for the formation of metal nanoparticles and their application. *Applied Microbiology and Biotechnology* **69**, 485-492 (2006).

4. Mohanpuria, P., Rana, N. K. & Yadav, S. K. Biosynthesis of nanoparticles: technological concepts and future applications. *Journal of Nanoparticle Research* **10**, 507-517 (2008).

5. Sastry, M., Ahmad, A., Khan, M. I. & Kumar, R. Biosynthesis of metal nanoparticles using fungi and actinomycete. *Current Science* **85**, 162-170 (2003).

6. Ahmad, A., Senapati, S., Khan, M. I., Kumar, R. & Sastry, M. Extracellular biosynthesis of monodisperse gold nanoparticles by a novel extremophilic actinomycete, Thermomonospora sp. *Langmuir* **19**, 3550-3553 (2003).

7. Mukherjee, P. *et al.* Bioreduction of AuCl4- ions by the fungus, Verticillium sp. and surface trapping of the gold nanoparticles formed. *Angewandte Chemie-International Edition* **40**, 3585-+ (2001).

8. Polte, J. ê. *et al.* Mechanism of Gold Nanoparticle Formation in the classical citrate synthesis method derived from coupled in situ XANES and SAXS evaluation. *Journal of the American Chemical Society* **132**, 1296-1301 (2010).

9. Hill, H. D. & Mirkin, C. A. The bio-barcode assay for the detection of protein and nucleic acid targets using DTT-induced ligand exchange. *Nature Protocols* **1**, 324-336 (2006).

10. Zhang, D., Carr, D. J. & Alocilja, E. C. Fluorescent bio-barcode DNA assay for the detection of Salmonella enterica serovar Enteritidis. *Biosensors & Bioelectronics* **24**, 1377-1381 (2009).

11. Torres-Chavolla, E., Ranasinghe, R. J. & Alocilja, E. C. Characterization and functionalization of biogenic gold nanoparticles for biosensing enhancement. *Nanotechnology, IEEE Transactions on* **9**, 533-538 (2010).

12. He, S. Y., Guo, Z. R., Zhang, Y., Zhang, S. & Gu, J. W. N. Biosynthesis of gold nanoparticles using the bacteria Rhodopseudomonas capsulata. *Materials Letters* **61**, 3984-3987 (2007).

13. Bharde, A., Kulkarni, A., Rao, M., Prabhune, A. & Sastry, M. Bacterial enzyme mediated biosynthesis of gold nanoparticles. *Journal of Nanoscience and Nanotechnology* **7**, 4369-4377 (2007).

14. Husseiny, M. I., El-Aziz, M. A., Badr, Y. & Mahmoud, M. A. Biosynthesis of gold nanoparticles using Pseudomonas aeruginosa. *Spectrochimica Acta Part A-Molecular and Biomolecular Spectroscopy* **67**, 1003-1006 (2007).

15. Anderson, M., Torres-Chavolla, E., Castro, B. & Alocilja, E. One step alkaline synthesis of biocompatible gold nanoparticles using dextrin as capping agent. *Journal of Nanoparticle Research* DOI: 10. 1007/s11051-010-0172-3 (2010).

16. Wang, Y. & Yang, H. Oleic acid as the capping agent in the synthesis of noble metal nanoparticles in imidazolium-based ionic liquids. *Chemical Communications* 2545-2547 (2006).

17. Zhou, M. *et al.* Minute synthesis of extremely stable gold nanoparticles. *Nanotechnology* **20**, 505-606 (2009).

This chapter is adapted from our recently published work in Biosensors and Bioelectronics:

Torres-Chavolla, Edith and Alocilja, C. Evangelyn. Nanoparticle based DNA biosensor for tuberculosis detection using thermophilic helicase-dependent isothermal amplification. *Biosensors and Bioelectronics.* **2011.** 26(11):4614-4618.

DOI: 10.1016/j.bios.2011.04.055.

Chapter 4

Tuberculosis DNA based biosensor using dextrin coated gold nanoparticles and isothermal helicase-based amplification

4.1 Introduction

The previous chapter (chapter 3) described the biosynthesis and characterization of gold nanoparticles (AuNPs) using sodium carbonate and dextrin as reduction and capping agent respectively. The dextrin coated AuNPs produced with this new alkaline procedure were successfully functionalized with DNA probes. Chapter 4 describes the application of these particles as electrochemical labels on a DNA based biosensor to detect *M. tuberculosis* using thermophilic helicase-dependent isothermal amplification (tHDA). The biosensor is composed of gold nanoparticles (AuNPs) and amine-terminated magnetic particles (MPs) each functionalized with a different DNA probe that specifically hybridize with opposite ends of a fragment within the IS*6110* gene, which is *Mycobacterium tuberculosis* complex (MTC) specific. After hybridization, the formed complex (MP-target-AuNP) is magnetically separated from the solution and the AuNPs are electrochemically detected on a screen printed carbon electrode (SPCE) chip. The developed platform was evaluated using synthetic targets as proof-of-concept. This biosensor system can be potentially implemented in peripheral laboratories with the use of a portable, handheld potentiostat.

4.2 Materials and methods

4.2.1 Thermophilic helicase-dependent amplification (tHDA)

4.2.1.1 tHDA primers and hybridization probes

The tHDA pimers were designed to specifically amplify a fragment of the IS*6110* gene which is tuberculosis (TB) complex specific (GenBank: AJ242908.1). IS*6110* is a 1361 bp repetitive insertion sequence that is usually present 6-20 times in the *Mycobacterium tuberculosis* (MTB) genome (*1,2*). Specific fragments within the sequence (130-500 bp) have been widely used for PCR protocols targeting *Mycobacterium tuberculosis* complex (MTC) species (*1-4*) (MTC includes: *M. tuberculosis*, *M africanum* (subtypes I and II), *M. bovis*, attenuated *M. bovis* (BCG vaccine strain), *M. bovis* subsp. *caprae*, *M. microti*). The tHDA primers were designed considering the optimal conditions for isothermal amplification (Table 4-1 and 4-2) (IsoAmp II Universal tHDA kit, biohelix) using Primer 3 program (http://frodo.wi.mit.edu/cgi-bin/primer3/primer3_www.cgi). The obtained tHDA product (tHDA amplicon) was used as a template for the hybridization assay.

Table 4-1. tHDA parameters.

tHDA Condition	Obtained	Optimal
Amplicon size	105 pb	80-120 bp
Amplicon Tm	74°C	68-75°C
Amplicon GC%	63%*	40%
Primer size	24 b	24-33 bases
Primer Tm	71°C (average)	60-74°C
Primer GC%	62%*	35-60%

*The specific region selected within the IS*6110* has high CG content.

Table 4-2. tHDA primers (105 bp fragment) and amplicon sequence.

105-F 5’ GAG CGT AGG CGT CGG TGA CAA AGG 3’ Length: 24 b (1515-1538). Tm: 71.73. GC%: 62.50
105-R 5’ GCT TCG GAC CAC CAG CAC CTA ACC 3’ Length: 24 b (1596-1619). Tm: 70.78. GC%: 62.50
tHDA amplicon sequence (primer location is highlighted in bold) 1511 5’ctgc**gagcgt aggcgtcggt gacaaaggcc** acgtaggcga accctgccca ggtcgacaca taggtgaggt ctgctaccca cagcc**ggtta ggtgctggtg gtccgaagcg** 3’ 1620

In order to have a synthetic target sequence for tHDA, a longer fragment (190 bp) flanking the tHDA amplicon region was selected. A separate set of primers to amplify this region was generated according to general PCR conditions using Primer 3 (Table 4-3). This synthetic fragment (190 AMP) will be used as target for poof-of-concept evaluations of the tHDA and biosensor.

Table 4-3. PCR primers (190 bp fragment) and amplicon sequence.

190-F 5’ AGG TGG CCA TCG TGG AA 3’ Length: 17 b (1473-1489). Tm: 61.09. GC%: 58.82
190-R 5’ GCT GAT CCG GCC ACA G 3’ Length: 16 b (1657-1672). Tm: 59.85. GC%: 68.75
190 AMP sequence (primer location is highlighted in bold) 1471 5’gg**aggtggcc atcgtggaa**g cgacccgcca gcccaggatc ctgcgagcgt aggcgtcggt gacaaaggcc acgtaggcga accctgccca ggtcgacaca taggtgaggt ctgctaccca cagccggtta ggtgctggtg gtccgaagcg gcgctggacg agatcggcgg gacggg**ctgt ggccggatca gc**gatcgtgg 3’1680

Two different DNA probes were used to specifically hybridize with the fragment generated by the tHDA reaction (Table 4-4). The primers for the 105 bp fragment (target sequence) needed

to be reduced in length to meet the melting temperature (Tm) requirements of the hybridization assay in order to use them as the capture and detection probes. The hybridization assay is conducted 15°C below the Tm (around 45°C), therefore the probe's Tm needs to be 60°C or below. This assay has been designed to work in low temperatures in order to preserve the nanoparticles (*5*). Both probes were designed to hybridize the antisense (complementary) sequence (3' --- 5') of the target and are labeled with a thiolated group at one of the ends that will be used as linker for the particle functionalization.

Thiolation is a common modification for oligonucleotides, it introduces a sulfhydryl reactive group (R-SH) that can be used in the conjugation reaction with nanoparticles (*6*). Between the thiol group (-ss-) and the probe, a poly "A" (12 bases) spacer sequence was included in order to give space for the functionalization and facilitate the correct hybridization to the target sequence. All oligonucleotides were evaluated for specificity using the BLASTN 2.2.25+ (*7*). Primers, probes, and synthetic target were purchased from IDT (Integrated DNA Technologies).

Table 4-4. TB hybridization probes and target sequence.

TB 5'thiol 5'-ss-AAA AAA AAA AAA GAG CGT AGG CGT CGG TGA 3' For MNP Length: 18 b (1515-1532). Tm: 59.9. GC%: 66.7
TB 3'thiol 5' GTG CTG GTG GTC CGA AGC AAA AAA AAA AAA-ss- 3' For AuNP Length: 18 b (1515-1532). Tm: 59.2. GC%: 66.7
Hybridization target sequence (probe location is highlighted in bold) 5' **gag cgt agg cgt cgg tga** 3' 3' **ctc gca tcc gca gcc act** gtt tcc ggt gca tcc gct tgg gac ggg tcc agc tgt gta tcc act cca gac gat ggg tgt cgg cca atc **cac gac cac cag gct tcg** 5' 5' **gtg ctg gtg gtc cga agc** 3'

4.2.1.2 tHDA optimization using a commercially available kit

In order to evaluate the primers designed for the isothermal amplification, a commercially available kit for isothermal amplification was used (IsoAmp II Universal tHDA kit, biohelix). The amplification was conducted following the tHDA conditions for one-step 50µl tHDA reaction using the synthetic target (190 AMP) (1x annealing buffer II, 4mM $MgSO_4$, 40mM NaCl, 3.5µl dNPT solution, 1 ng synthetic target, 75nM primer, 3.5µl enzyme mix). The reaction was covered with mineral oil (50µl) to avoid evaporation and incubated in a regular heating block for 90 min at 65°C (Eppendor Thermomixer R).

4.2.1.3 tHDA optimization using individual reactants

The isothermal amplification reaction was also optimized using individual reactants. The reaction was optimized with respect to type of buffer, salt concentration, target, and DNA concentration; according to previous procedures using individual reactants (*8*, *9*). The reaction was composed of: 1x thermo pol II buffer, 4mM $MgSO_4$, 3mM dATP, 200µM dNPTs, 20 U *Bst* DNA polymerase (large fragment), 100ng thermostable helicase, synthetic target DNA, 75nM forward primer (105-F), 75nM reverse primer (105-F). The total reaction volume was 50 µl and same volume of mineral oil was added to avoid evaporation. The reactions were incubated in a regular heating block for 90 min at 65°C (Eppendor Thermomixer R). After the reaction, the product was purified using a silica membrane column (Miniellute, Qiagen) to eliminate the remaining primers.

4.2.2 Electrochemical detection using SPCE

4.2.2.1 Nanoparticle functionalization

The dextrin coated AuNPs (~12.5nm in diameter) synthetized using the alkaline procedure described in chapter 3 (2.5g/L dextrin, 2mM $HAuCl_4$, pH 9, 50°C, 24 hr) were functionalized with a thiolated probe (TB 3'thiol) following a common methodology applicable for citrate coated AuNPs ligand exchange with modifications (*5*,*10*,*11*). The thiolated DNA probe (5 nmoles) was reduced with 0.1M DTT (dithiothreitol) for 2h at room temperature with constant agitation. This reduction is to assure full reactivity of the thiol group. After the reduction, the DTT was eliminated through a purification step using a Sephadex column (Nap-5, GE Healthcare). One milliliter of the dextrin coated AuNPs (AU=2 at λ520 nm) was mixed with the purified probe solution. The dextin molecules coating the surface of the nanoparticles were exchanged for the thiolated DNA probe over a series of salting steps during two days (*5*). After ligand exchange the particles were stored under refrigeration until use (*11*).

The amine coated MPs (~1 μm in diameter) used in this study were commercially available (Sigma Aldrich Cat No. I7643-5ML) and functionalized with a secondary thiolated DNA probe (TB 5'thiol) using sulfosuccinimidyl 4-*N*-maleimidomethyl cyclohexane-1-carboxylate (sulfo-SMCC) as cross linker (*11*). The thiolated secondary DNA probe (10 nmoles) was reduced with 0.1M DTT for 2h at room temperature with constant agitation. After the reduction, the DTT was eliminated through a purification step using a Sephadex column (Nap-5, GE Healthcare). The amine coated MPs (10mg) were conjugated with 1mg sulfo-SMCC for 2h in 1 ml of coupling buffer (0.1M PBS buffer, 0.2M NaCl, pH 7.2). After the conjugation with the bifunctional linker (sulfo-SMCC) the MPs were washed and mixed with the purified DNA probe solution and incubated for 8 h at room temperature. After functionalization, sulfo-NHS acetate (1mg) was

used to block the unreacted linker groups on the MP surface. After passivation, the particles were washed and stored under refrigeration until use (*11*). The Sulfo-SMCC functionalization is illustrated in Figure 4-1.

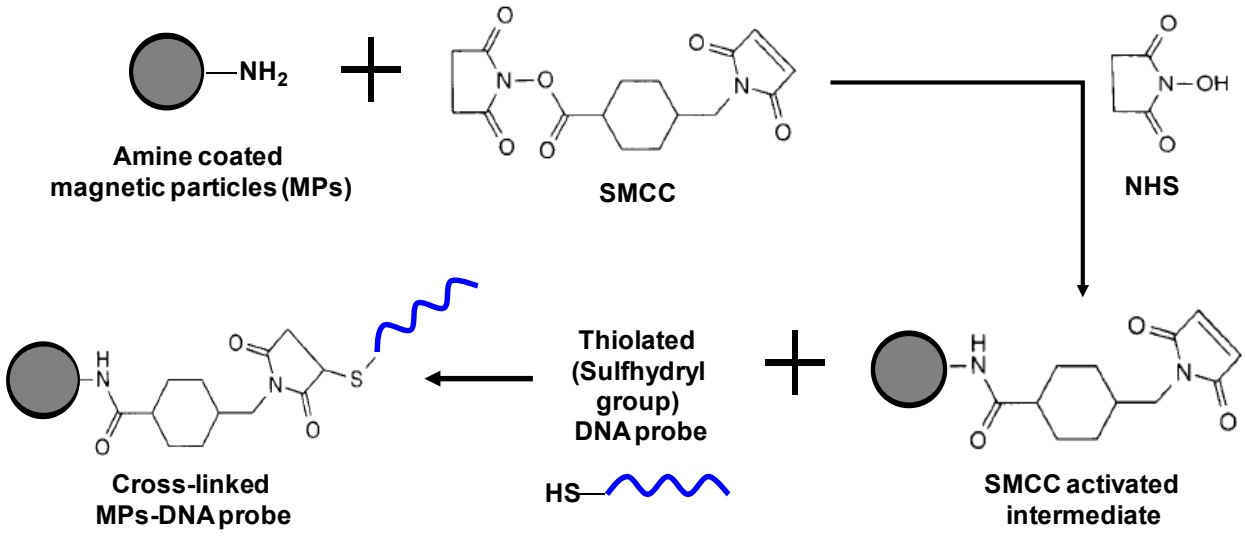

Figure 4-1. Schematic representation of magnetic particle functionalization chemistry using sulfo SMCC as crosslinker between the particles and the DNA probes (adapted from (*6*)).

4.2.2.2 Hybridization assay and electrochemical detection

The product obtained from the tHDA was serially diluted (10 ng/µL – 0.01 ng/µL), denaturated at 95°C for 10 min to separate the double-stranded DNA (dsDNA) into single-stranded DNA (ssDNA). The target DNA (40µl) was mixed immediately with 0.8mg of capture DNA probe (TB 3'thiol)-MPs that were previously resuspended in 160µl of assay buffer (10mM PBS buffer, 0.15M NaCl, 0.1% SDS, pH 7.4). The mixture was allowed to hybridize for 45 min at 44.5°C with continuous rotation to form a MP-target DNA complex (Figure 4-2). After magnetic separation and several washing steps to eliminate the unreacted target, AuNPs (40µL)

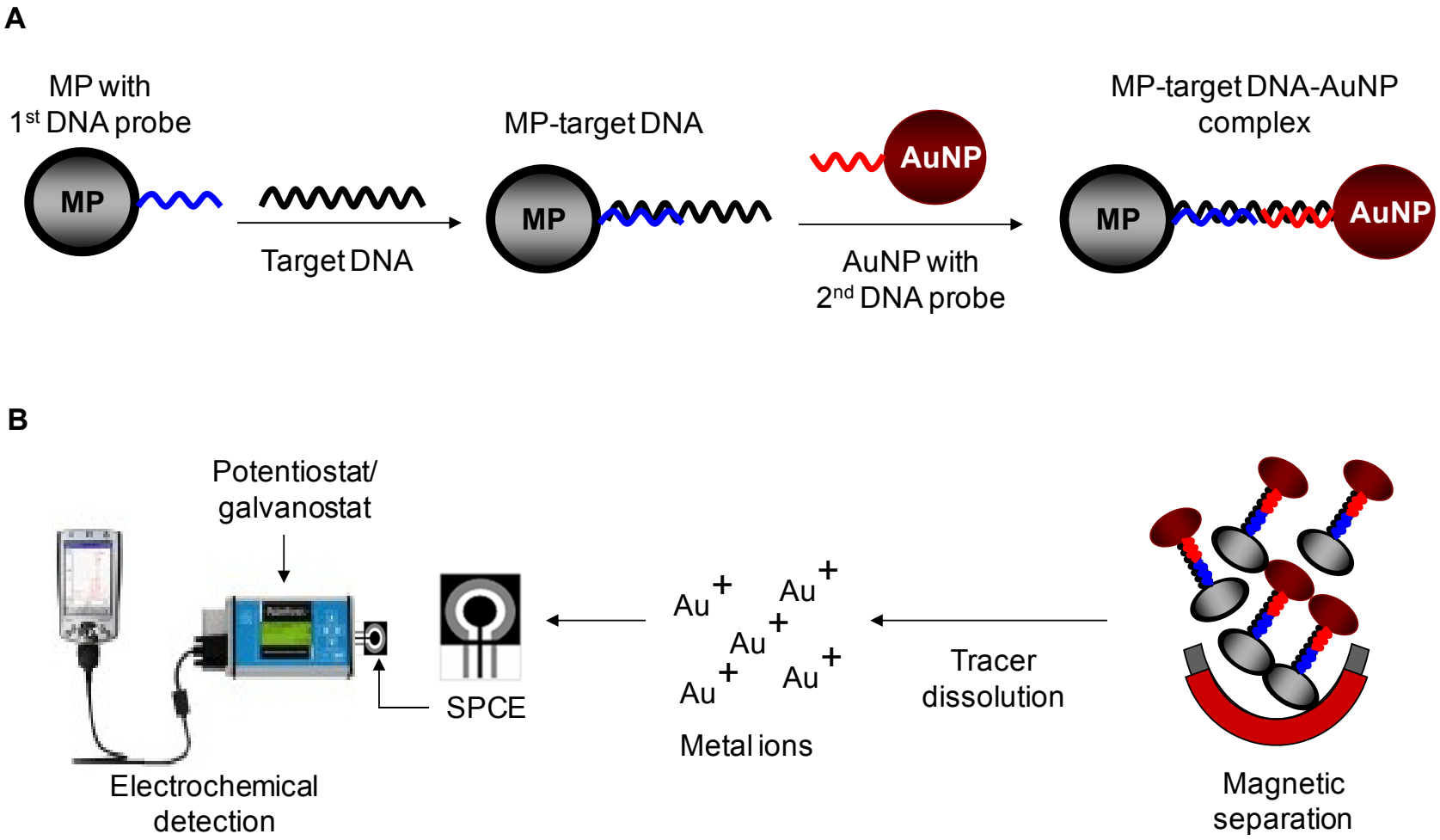

Figure 4-2. Illustration of the electrochemical DNA detection system: (A) formation of complex target sandwich (MP-target DNA-AuNP) (B) Magnetic separation, metallic tracer (Au^{3+}) dissolution and electrochemical detection (adapted from (*12*).

labeled with the reporter probe (TB 5'thiol) were added and incubated for 2h at 44.5°C with continuous rotation to form a hybridized sandwich complex consisting of MP-target DNA-AuNP (Figure 4-2). The sandwich complex was pulled and separated with a magnet. After several washing steps to eliminate the non-hybridized AuNPs, the complex was resuspended in 50µL of water and transferred to a screen-printed carbon electrode (SPCE) (Gwent electronic materials, Ltd.).

The SPCE was composed of working (carbon) and counter-reference (silver/silver chloride) electrodes (Figure 4-3). The solution was allowed to dry onto the carbon electrode for 30 min, and then 50µL of 1M HCl solution was added to dissolve the AuNPs and generate Au^{3+} ions. A constant 1.25 V was applied to the electrode for 2 min to oxidize the gold ions (potentiostat/galvanostat 263A and PowerSuite software, Princeton Applied Research) (Figure 4-2B). Differential pulse voltammetry (DPV) was performed from 1.25V to 0.0V (with a step potential of 10 mV, modulation amplitude of 50 mV, and scan rate of 33.5 mV/s) to generate the voltammogram produced by the reduced gold ions on the SPCE (*11,13*).

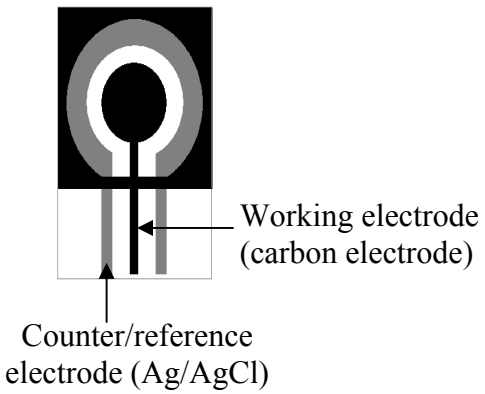

Figure 4-3. Schematic of the $2cm^2$ electrochemical chip containing the screen-printed carbon electrode and Ag/AgCl reference and counter electrodes.

Results and discussion

4.2.3 Thermophilic helicase-dependent amplification (tHDA)

4.2.3.1 Oligonucleotide evaluation using PCR

All oligonucleotides (primers and probes) were evaluated for specificity using the BLASTN 2.2.25+ program (*7*). The results of this evaluation can be found in Appendix B. Table 4-5 presents a summary of the oligonucletide sequences designed for the TB biosensor platform.

Table 4-5. Oligonucleotide sequences summary

Name	Sequence	Binding position*
tHDA Forward Primer (105-F)	5' GAG CGT AGG CGT CGG TGA CAA AGG 3'	(1515-1538)
tHDA Reverse Primer (105-R)	5' GCT TCG GAC CAC CAG CAC CTA ACC 3'	(1596-1619)
Capture Probe (TB 5'thiol) For the magnetic particles.	5'-ss-AAA AAA AAA AAA GAG CGT AGG CGT CGG TGA 3'	(1515-1532)
Reporter Probe (TB 3'thiol) For the gold nanoparticles.	5' GTG CTG GTG GTC CGA AGC AAA AAA AAA AAA-ss- 3'	(1602-1619)

*GenBank sequence: AJ242908.1

In order to evaluate the designed primers, PCR was used to verify amplification for both set of primers (105 and 190 bp). Table 4-6 shows the PCR standard conditions used for this evaluation (*14*). The reactions were conducted in a thermocycler (BioRad) following a standard procedure for amplification with the following program: Initial denaturation (95°C/2min); 25 cycles of denaturation (95°C/1min), hybridization (55°C/1min for 190 bp fragment and 65°C/1min for 105 bp fragment), extension (72°C/1min); and final extension (72°C/5min).

Table 4-6. PCR conditions for both primer sets (190 bp and 105 bp fragment).

Reactant	Final concentration
Buffer	1x
$MgCl_2$	2mM
dNPTs	0.2mM
Forward Primer	0.5uM
Reverse Primer	0.5uM
Target DNA (190AMP)	10ng
Taqpol [5U/ul]	2.5U
mQ H_2O	-----
Total reaction volume	50µl

Successful PCR amplification was visualized using agarose gel electrophoresis (2.5%/50V/60 min) for both set of primers (Figure 4-4). The PCR product obtained for the 190 bp fragment was purified with a mini elute column (Quiagen) to eliminate the remaining primers. This purified product was used as synthetic target input for the tHDA trials. After this initial primer evaluation, the tHDA primers (105 bp) were used for the tHDA optimization.

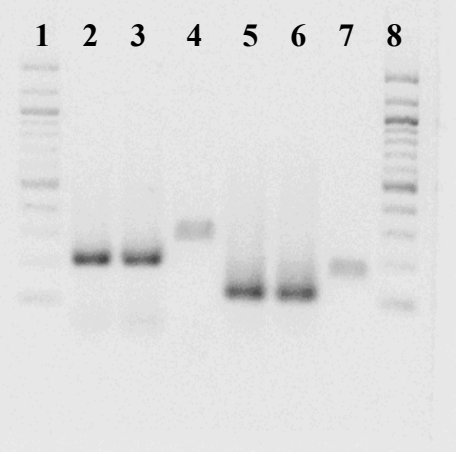

Figure 4-4. Agarose gel electrophoresis showing amplification bands obtained with PCR for both fragments (190 and 105 bp). Lane 1 and 8: 100 bp ladder. Lane 2 and 3: 190 bp fragment. Lane 4: Blank. Lane 5 and 6: 105 bp fragment. Lane 7: Blank.

4.2.3.2 tHDA optimization

Successful amplification was obtained using the designed tHDA primers (Table 4-2), synthetic target DNA and the tHDA kit following the conditions for one-step reaction (90 min of incubation at 65°C) (IsoAmp II Universal tHDA kit from biohelix). Figure 4-5 shows the amplification bands obtained using a regular thermomixer (Eppendorf) which confirms that tHDA reactions can be conducted in a regular thermoblock (or water bath) without the need of a thermocycler. After the primer evaluation with the commercially available kit, the isothermal amplification reaction was also optimized using individual reactants. Table 4-7 shows the obtained parameters for optimal tHDA amplification of a IS*6110* fragment. Figure 4-6 shows successful amplification products (bands) using individual reactants from agarose gel electrophoresis.

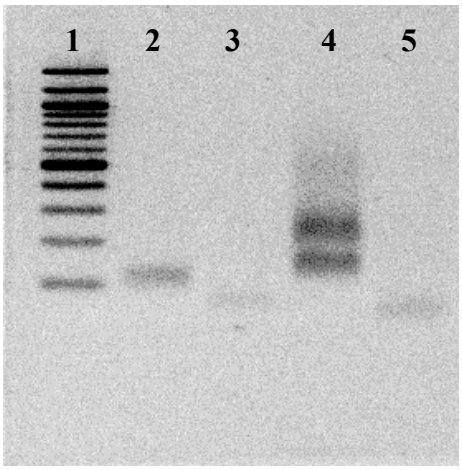

Figure 4-5. Agarose gel electrophoresis showing tHDA bands obtained using the one-step protocol of IsoAmp II Universal tHDA kit (biohelix). Lane 1: 100 bp ladder. Lane 2. 85 bp positive control from the kit. Lane 3: Blank. Lane 4: Synthetic target. Lane 5: Blank.

Table 4-7. Optimal tHDA conditions using individual reactants and synthetic 190 AMP target as amplification input.

Reactant	Amount (µL)	Final concentration
Thermo pol II buffer [10x]	5	1x
$MgSO_4$ [100 mM]	2	4mM
dATP [10 mM]	15	3mM
dNPT's [10mM]	1	200uM
Bst DNA polymerase [8u/ul]	2.5	20 U
Thermostable DNA helicase [50ng/ul]	2	100ng
DNA template 190AMP [10 ng/ul]	1	10ng
Forward primer 105-F [5uM]	0.75	75nM
Reverse primer 105-F [5uM]	0.75	75nM
Water	20	---
TOTAL VOLUME	50	---
Mol Biol mineral oil	50	---

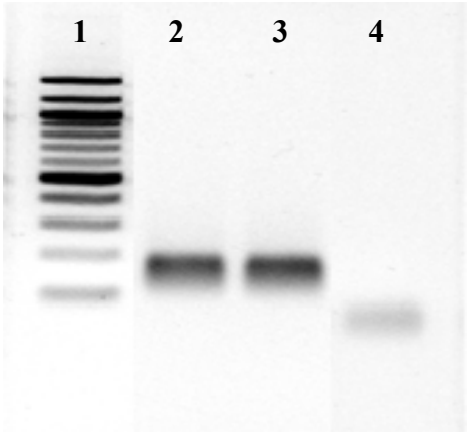

Figure 4-6. Agarose gel electrophoresis showing tHDA bands using individual reactants and the synthetic 190 bp fragment as target input. Lane 1: 100 bp ladder. Lane 2 and 3: tHDA products. Lane 4: Blank.

The target concentration was evaluated using different concentrations (from 100 ng – 1 ng) in order to determine the lower detection limit of the tHDA (product visualization) using synthetic

target (190 AMP) as tHDA input. Figure 4-7 shows the agarose gel electrophoresis image where the change in amplification band with respect to the target concentration can be visualized. The lowest concentration where positive amplification was visualized was 1 ng/µl.

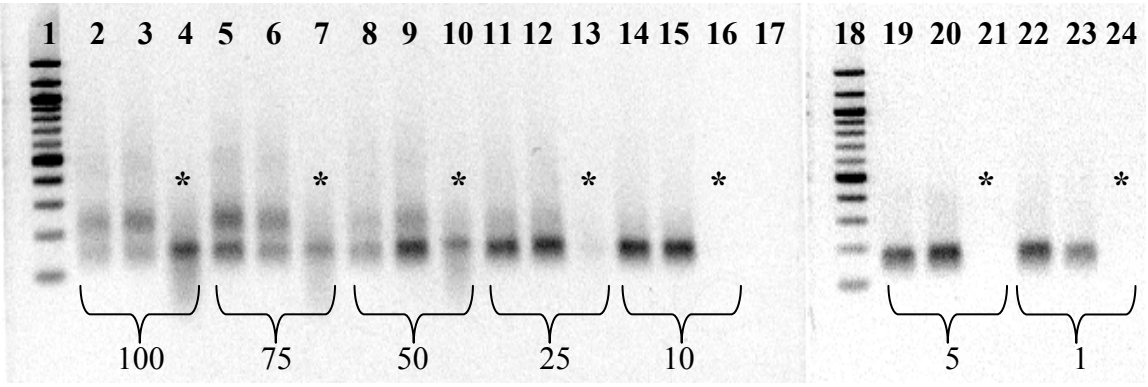

Figure 4-7. Agarose gel electrophoresis showing amplification bands obtained with tHDA using the synthetic 190 bp fragment as target input. The initial target concentration was evaluated from 100 ng to 1 ng. Lane 1 and 18: 100 bp ladder. Lane 17: Blank. The two first lines of each concentration are tHDA products, the third line (*) represents the initial target input for each concentration.

4.2.4 Electrochemical detection using SPCE

4.2.4.1 Optimization of electrochemical detection of gold nanoprobes

One of the parameters that affect the electrochemical detection of AuNPs using SPCE chips is the accumulation time, which is defined as the time from sample deposition on the SPCE surface to electrochemical detection. In order to evaluate this parameter, AuNPs and MPs functionalized with DNA probes were combined in the same concentrations as used for hybridization. Two separate sets of serial dilutions were prepared keeping consistency in the

volume (50µl) used for the electrochemical detection of the hybridized sandwich complex (see materials and methods section 4.2.2.2). One set of dilutions was mixed with 50µl of HCl and immediately deposited on the SPCE surface and the electrochemical gold oxidation and DPV detection was performed following the same conditions described earlier in the materials and methods. A second set of dilutions was deposited on the SPCE, and dried from 30 min to 2 h approximately. After the sample was completely dried, 50µl of HCl was applied to the surface and the electrochemical gold oxidation and DPV detection was performed as described above (Figure 4-8).

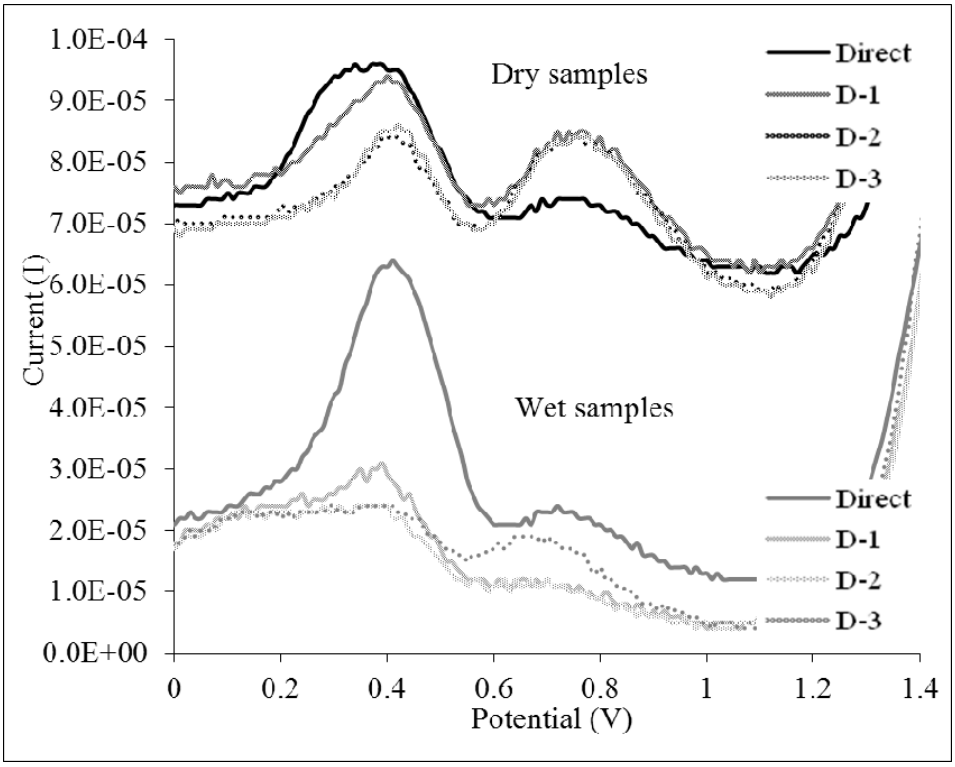

Figure 4-8. DPV response for different gold nanoprobe concentrations on SPCE. Wet samples were detected immediately with minimum or no accumulation time. The AuNP dissolution with HCl was performed in liquid before the sample was transferred to the SPCE. Dry samples were deposited on the SPCE and the HCl was applied after the solution was completely dry. D-1 = 1:10 dilution, D-2 = 1:100 dilution, D-3 = 1:1000 dilution.

From these results it was observed that drying the sample before electrochemical detection produced higher DPV signal. As the accumulation time increases, more AuNPs are adsorbed onto the SPCE surface, more gold ions are available for the electrochemical oxidation and the DVP signal increases. The same experiment was conducted with samples of functionalized MPs and AuNPs that were mixed and refrigerated overnight, in order to determine if the electrochemical response was affected by storage (Figure 4-9). The gold reduction peaks on the stored dry samples were higher than the wet samples obtained on the same day ($1.4x10^{-4}$ and $9.0x10^{-5}$, respectively for the highest concentration). Nevertheless, this type of variation in the shape and height of the current peak was observed between equal trials; therefore, since positive gold reduction peaks were obtained from the stored samples, it could be possible to evaluate samples up to the hybridization point and then store or transport them for of-site electrochemical detection. The variation between dry and wet samples was consistent between same day and stored samples (higher peaks for dry samples).

4.2.4.2 Hybridization assay and electrochemical detection

In order to evaluate the biosensor functionality, citrate coated AuNPs were used during initial runs with PCR products as targets for the hybridization reaction. Direct oxidation of AuNPs onto the carbon electrode surface was optimized at 1.25 V for 2 min obtaining a reduction peak of gold ions between 0.30 and 0.35 V. Figure 4-10 shows the DPV response obtained with different DNA concentrations after hybridization, sandwich complex formation (MP-target-AuNP), magnetic separation and AuNPs dissolution.

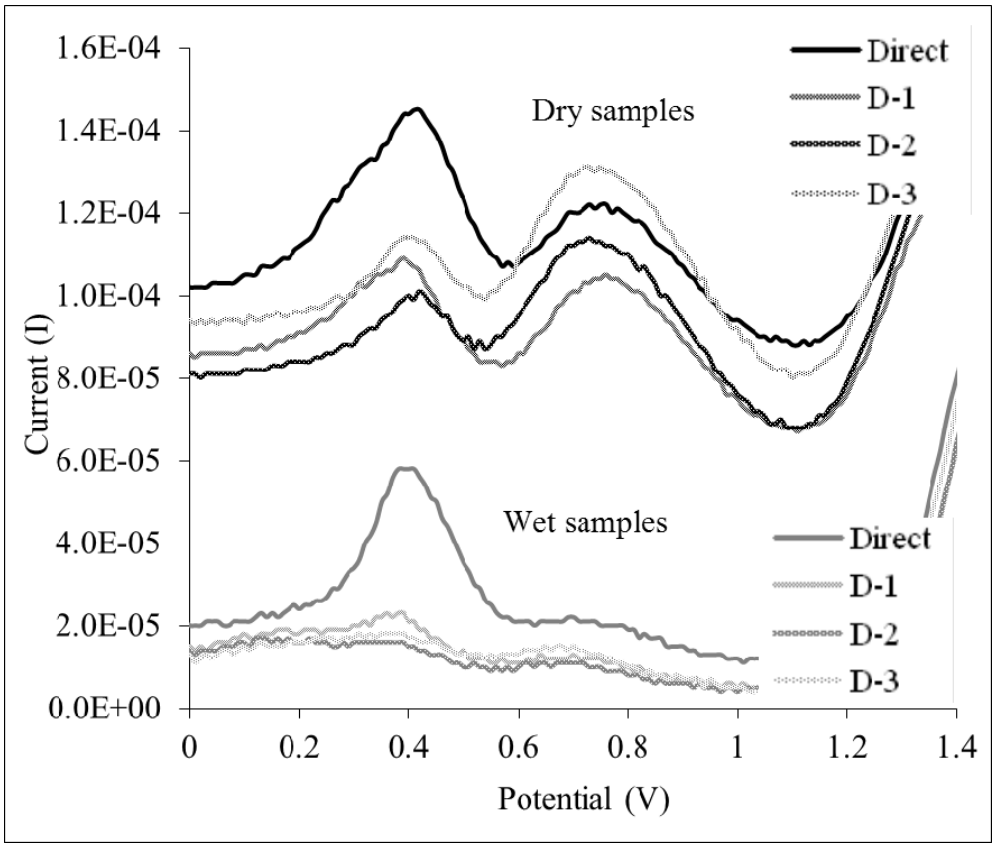

Figure 4-9. DPV response for different gold nanoprobe concentrations on SPCE. The samples were stored overnight before the electrochemical reading.

After the gold was dissolved and oxidized by the acidic solution, the gold ions were reduced by the application of potential between 0.30 and 0.35 V on the SPCE. The electrochemical response (gold reduction peak) was equally proportional to the target concentration for both citrate and dextrin gold nanoparticles. This was expected since there is no remaining capping agent, dextrin or citrate, on the surface of the AuNP after the oligonucleotide functionalization procedure. The particle's coating molecules are exchanged for thiolated DNA probes and the coating material is liberated to the suspension liquid. After functionalization, the particles are centrifuged and washed to eliminate the supernatant with unreacted materials. Since the

elemental gold that is reduced in the electrochemical detection is the same for citrate and dextrin coated AuNPs, there is no effect of the coating material in the system. Figure 4-10 shows an example of the gold reduction peaks obtained for both dextrin (4-10 A) and citrate (4-10 B) coated gold nanoparticles. Even though the shapes of the peak are different, this variation has been observed before between similar trials. The variation could be due to the equipment (potentiostat) or the nature of the electrochemical reaction; but this phenomenon is not observed to be dependent on using either citrate or dextrin coated gold nanoparticles.

After the initial optimization trials with PCR amplified products, the biosensor platform was evaluated using tHDA amplified products as target DNA for the hybridization assay and dextrin-coated AuNPs as electrochemical reporters. Three separate trials were run using four different DNA concentrations (0.01-10 ng/µl) plus a blank with no target DNA. Each sample was run in triplicates. Figure 4-11A shows the DPV response obtained with different DNA concentrations. A linear log-correlation was observed between the target DNA concentration and the gold reduction peak (Fig 4-11B).

The presence or absence of the target was identified with a detection limit of 0.01 ng/µl. Variability in the peak height was observed in different trials between all the target concentrations detected, especially between the two lowest (0.1 and 0.01 ng/µl). This variability may be the result of inter particle distances. At low concentrations, the particles are more dispersed and have more accessible surface area to interact with the acidic solution producing slightly higher reduction peaks. Therefore, the semi-quantitative detection limit obtained using synthetic targets was 0.1 ng/µl. Table 4-8 shows the electrochemical results for different DNA concentrations.

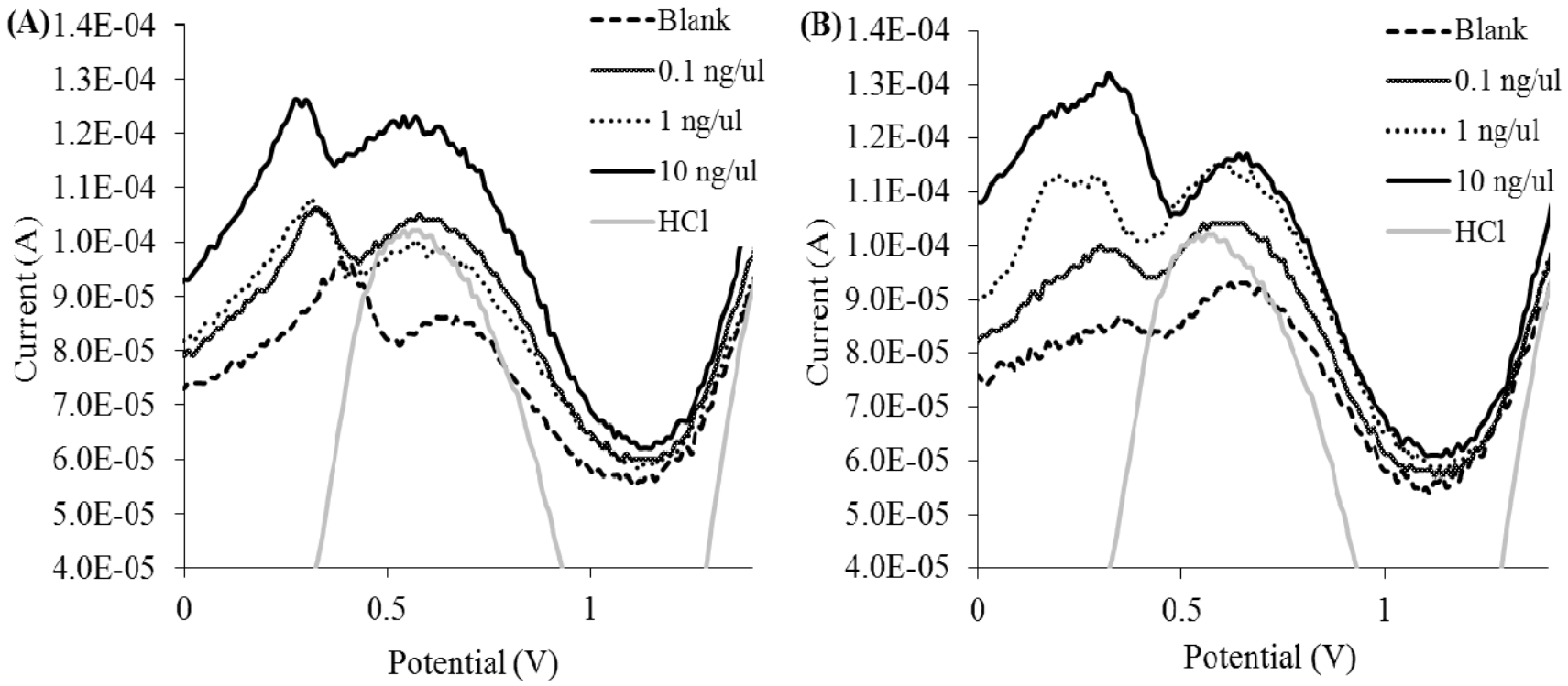

Figure 4-10. DPV response for different DNA target concentrations on SPCE using dextrin coated AuNPs (A) and citrate coated AuNPs (B) as electrochemical labels.

Table 4-8. Mean and standard deviation (STDV) of gold reduction peak at different target DNA concentrations.

	Gold reduction peak @ 0.35 V*					
Target DNA (ng/ul)	Trial 1	STDV	Trial 2	STDV	Trial 3	STDV
Blank	1.06E-04	2.12E-06	1.12E-04	2.25E-05	1.11E-04	7.57E-06
0.01	1.25E-04	5.66E-06	1.29E-04	2.06E-05	1.20E-04	5.29E-06
0.1	1.22E-04	9.16E-06	1.33E-04	1.01E-05	1.15E-04	9.54E-06
1	1.47E-04	1.23E-05	1.77E-04	2.33E-05	1.50E-04	8.54E-06
10	1.63E-04	2.52E-06	1.99E-04	1.46E-05	1.51E-04	6.66E-06

* Each sample was run in triplicates

Statistical analysis (one-way ANOVA) was conducted to evaluate the effect of different target concentrations (tHDA products) on the gold reduction peak (DPV response) using Statgraphics software. Since variation in the peak shape was observed between trials, the current values from 0.3 – 0.4 V were used for the statistical analysis for each concentration. The results from the analysis (Appendix A, Table AA-1) showed that there was a statistically significant difference between the current peaks produced by different target concentrations (P value = 0.0000) with 95% confidence level. To determine which target concentrations produced current peaks significantly different from each other, a multiple range test (LSD) was conducted (Appendix A, Table AA-2 and Figure AA-1). No statistical significant difference was found between the DPV response obtained with 0.01 and 0.1 ng/µl. The rest of the comparisons between blank and each target concentration showed significant difference (Appendix A; Table AA-3). These results confirm our previous observations for the detection limit (semi-quantitative and qualitative).

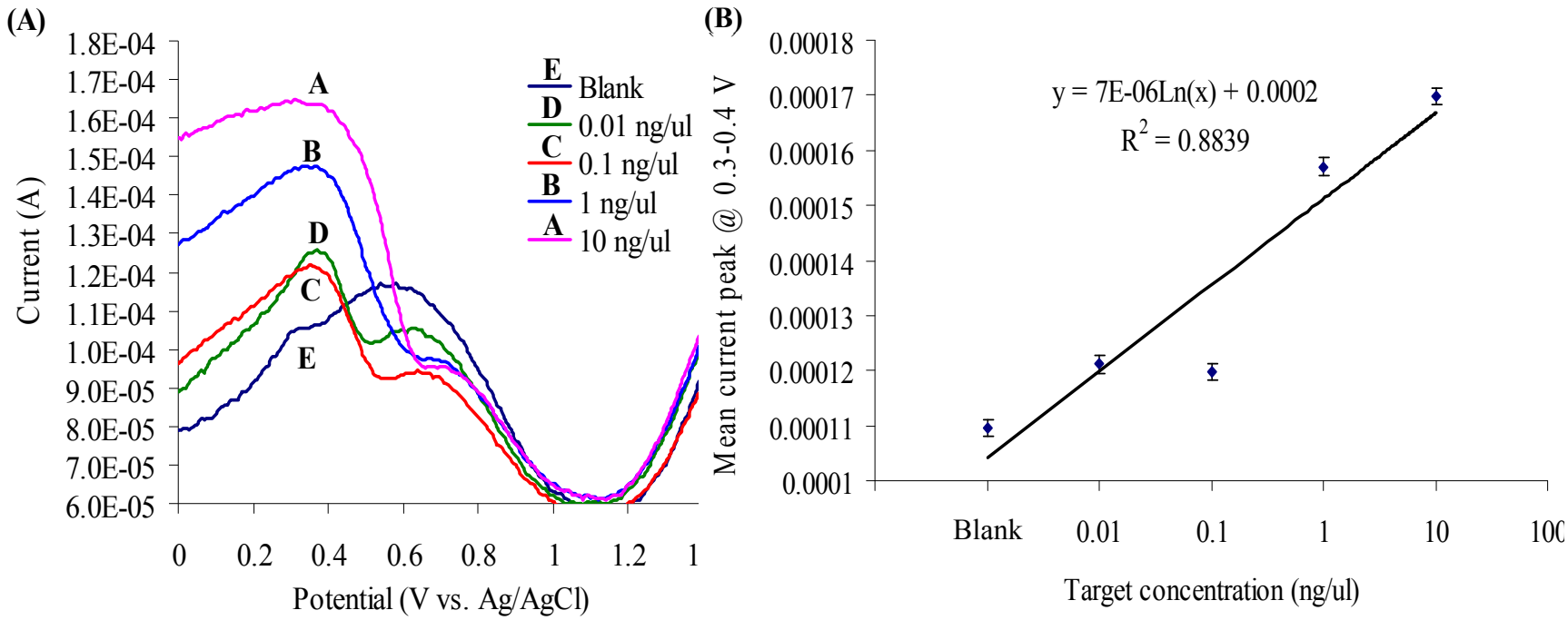

Figure 4-11. (A) Mean DPV response for different DNA target concentrations on SPCE. Each concentration was run in triplicates. The gold reduction peak was observed between 0.30-0.35 V. (B) Logarithmic correlation between the target DNA concentration (ng/µl) and the gold reduction peak (mean from 0.3 – 0.4 V) from three different trials. Each concentration was run in triplicates (adapted from (*12*)).

4.4 Conclusions

The present chapter described the development of a nanoparticle-based biosensor to detect a tuberculosis specific DNA fragment using the electrochemical detection of gold nanoparticles. In order to make the platform more suitable for resource-constrained settings diagnostics, an isothermal amplification reaction was optimized. The isothermal helicase dependent amplification (tDHA) was successfully optimized using individual reactants and a regular heating block, which can be replaced with a water bath. Therefore, a thermocycler is not required for the DNA specific amplification, like in PCR. To the best of our knowledge, this proof-of-concept study is the first application of tHDA instead of PCR for a tuberculosis detection application in a DNA based biosensor platform. A comparison with some DNA based biosensor platforms previously published for tuberculosis detection has been included in Table 4-9. The detection time with the proposed platform, including amplification and hybridization is 6 hours; without considering sample preparation (DNA extraction).

The system developed in this study has comparable characteristics with other biosensors previously developed. The main advantages of the proposed platform are that the detection system is not expensive, it can be portable and there is no need of a thermocycler due to the isothermal amplification. The present study is also the first application of dextrin coated AuNPs as electrochemical labels in a biosensor platform. No difference is observed when using dextrin or citrate AuNPs as electrochemical labels in the detection system.

Table 4-9. Selected papers on biosensor and nanoparticle DNA based systems for *M. tuberculosis* detection (recent publication).

Reference	Specific target (gene)	Biosensor platform/ nanoparticle system	Label/Detection system	Detection time	Detection limit
(*15*)	*gyrB*	Optoelectronic sensor using DNA probes immobilized on gold nanoparticles	Colorimetric (Au-nanoprobe) assay	Assay time: 3 h from sample collection to identification.	50 fmol/µl of synthetic target. Bacterial DNA and isolates from clinical samples were also evaluated.
(*16*)	Not identified	DNA probe immobilized on electrochemically deposited ZnO film on ITO glass surface	MB as electrochemical intercalator. Differential Pulse Voltammetry	Electrochemical response: 60 s. No assay time specified.	1×10^{-13} M of bacterial DNA.
(*17*)	23S rRNA gene and IS*6110*	DNA probes immobilized on magnetic beads and fluorescent QDs (CdSe)	Red fluorescence produced by UV radiation.	Assay time: 2 h (not including DNA extraction)	12.5 ng/µl of unamplified bacterial DNA. Isolates from clinical samples were also evaluated.
(*18*)	IS*6110*	DNA probes immobilized on quartz crystals –gold electrodes	Resonance frequency (piezoelectric)	Not specified.	0.25 µM of synthetic target. Bacterial DNA and isolates from clinical samples were also evaluated.

Table 4-9 (cont'd).

(*19*)	Not identified	Commercially available SPR based portable-multichannel gold sensor system	Surface Plasmon Resonance	Not specified.	30 ng/µl of synthetic target.
(*20*)	IS*6110* and *Rv3618*	DNA probes immobilized on gold nanoparticles.	Spectrophotometry colorimetric (Au-nanoprobe) assay	Assay time: 2 h (without including DNA extraction and amplification)	0.5 pmol of bacterial DNA. Isolates from clinical samples were also evaluated.
(*12*) Present work	IS*6110*	DNA probes immobilized on magnetic beads (DNA separation) and gold nanoparticle complex detected on SPCEs	Gold nanoparticles as electrochemical labels. Differential Pulse Voltammetry	Electrochemical response: 2 min. Assay time: 6 h (not including DNA extraction)	0.01 ng/µl of isothermally amplified synthetic target (190 bp)

Appendices

4.5 Appendices

Appendix A. Statistical analysis of DPV response (gold reduction peak) using tHDA products.

Table AA-1. One-Way Analysis of Variance (ANOVA) for current peak by target concentration.

Source	Sum of Squares	Df	Mean Square	F-Ratio	P-Value
Between groups	2.6459E-7	4	6.61475E-8	292.23	0.0000
Within groups	1.05934E-7	468	2.26354E-10		
Total (Corr.)	3.70524E-7	472			

Table AA-2. Table of means for current peak by target concentration with 95.0% LSD intervals.

Level	Count	Mean	Stnd. error (pooled s)	Lower limit	Upper limit
0.01 ng/ul	88	0.000121159	0.00000160381	0.000118931	0.000123388
0.1 ng/ul	99	0.000119747	0.00000151209	0.000117646	0.000121849
1 ng/ul	99	0.00015704	0.00000151209	0.000154939	0.000159141
10 ng/ul	99	0.000169869	0.00000151209	0.000167768	0.00017197
Blank	88	0.000109511	0.00000160381	0.000107283	0.00011174
Total	473	0.000136402			

Figure AA-1. Means and 95% LSD intervals.

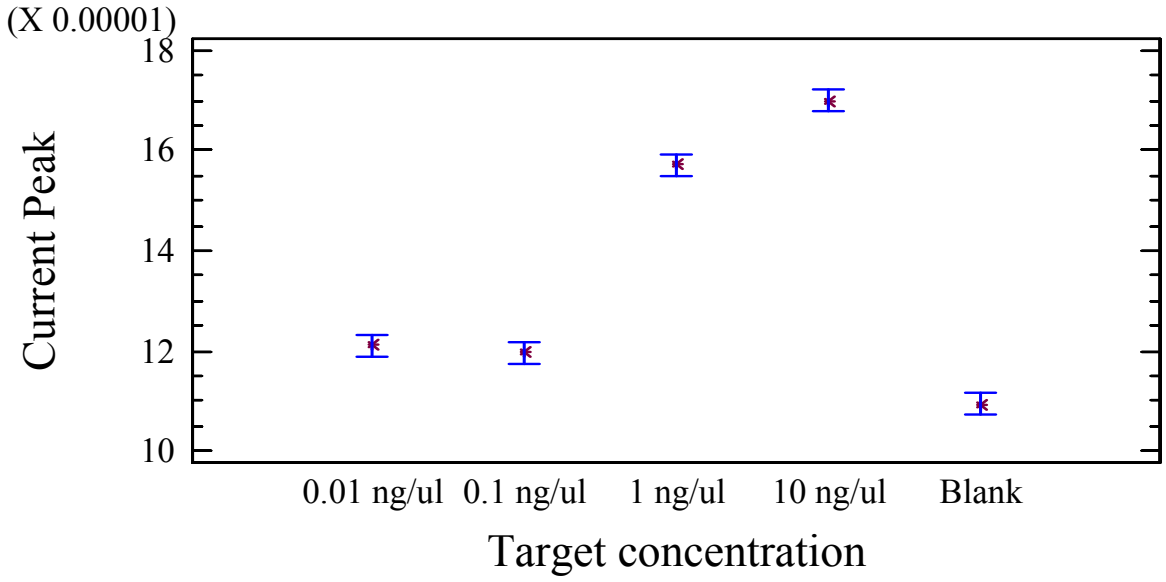

Table AA-3. Multiple range test for current peak by target concentration (Method: 95.0% LSD).

Level	Count	Mean	Homogeneous Groups[&]
Blank	88	0.000109511	X
0.1 ng/ul	99	0.000119747	X
0.01 ng/ul	88	0.000121159	X
1 ng/ul	99	0.00015704	X
10 ng/ul	99	0.000169869	X

Contrast	Difference	+/- Limits
0.01 ng/ul - 0.1 ng/ul	0.00000141162	0.00000433141
0.01 ng/ul - 1 ng/ul	*-0.0000358813	0.00000433141
0.01 ng/ul - 10 ng/ul	*-0.0000487096	0.00000433141
0.01 ng/ul - Blank	*0.0000116477	0.00000445698
0.1 ng/ul - 1 ng/ul	*-0.0000372929	0.00000420208
0.1 ng/ul - 10 ng/ul	*-0.0000501212	0.00000420208
0.1 ng/ul - Blank	*0.0000102361	0.00000433141
1 ng/ul - 10 ng/ul	*-0.0000128283	0.00000420208
1 ng/ul - Blank	*0.000047529	0.00000433141
10 ng/ul - Blank	*0.0000603573	0.00000433141

* Denotes a statistically significant difference.

[&]Within each column, the levels containing X's form a group of means within which there are no statistically significant differences.

Appendix B. Oligonucleotide specificity evaluation using BLAST *(7)* (http://www.ncbi.nlm.nih.gov/)

BLASTN 2.2.25+ Reference: Stephen F. Altschul, Thomas L. Madden, Alejandro A. Schaffer, Jinghui Zhang, Zheng Zhang, Webb Miller, and David J. Lipman (1997), "Gapped BLAST and PSI-BLAST: a new generation of protein database search programs", Nucleic Acids Res. 25:3389-3402.

tHDA primers (105 bp fragment)
105-F 5' GAG CGT AGG CGT CGG TGA CAA AGG 3'
105-R 5' GCT TCG GAC CAC CAG CAC CTA ACC 3'

RID: YUU9HB4P01N
Query ID lcl|36237
lcl|36237
Description None
Molecule type nucleic acid
Query Length 48
Database: All GenBank+EMBL+DDBJ+PDB sequences (but no EST, STS, GSS,environmental samples or phase 0, 1 or 2 HTGS sequences)

Sequences producing significant alignments:	**Score (Bits)**	**E Value**
gb|CP001662.1| Mycobacterium tuberculosis KZN 4207, complete ...	48.1	0.003
gb|HM053707.1| Mycobacterium tuberculosis strain G4B1.2 350 K...	48.1	0.003
gb|HM053706.1| Mycobacterium tuberculosis strain G4B1.2 350 K...	48.1	0.003
gb|HM053705.1| Mycobacterium tuberculosis strain G4B1.2 350 K...	48.1	0.003
gb|GU968453.1| Mycobacterium tuberculosis isolate patient 8 i……..	48.1	0.003
gb|CP001658.1| Mycobacterium tuberculosis KZN 1435, complete ...	48.1	0.003
dbj|AP010918.1| Mycobacterium bovis BCG str. Tokyo 172 DNA, c.	48.1	0.003
gb|CP000717.1| Mycobacterium tuberculosis F11, complete genome	48.1	0.003
gb|CP000611.1| Mycobacterium tuberculosis H37Ra, complete genom	48.1	0.003
emb|AM408590.1| Mycobacterium bovis BCG Pasteur 1173P2, compl.	48.1	0.003
gb|DQ217928.1| Mycobacterium microti insertion sequence IS611.....	48.1	0.003
gb|AF189827.1| Mycobacterium sp. 9502227 direct repeat locus ...	48.1	0.003
gb|AF189829.1|MTDRLN2 Mycobacterium microti strain 16240 dire...	48.1	0.003
gb|AF189826.1|MTDRLM2 Mycobacterium bovis strain 9401854 dire...	48.1	0.003
gb|AF189824.1|MTDRLL2 Mycobacterium bovis BCG strain BCG-Russ...	48.1	0.003
gb|AF189762.1|MTDRLI1 Mycobacterium tuberculosis strain 16319...	48.1	0.003
gb|AF189761.1|MTDRLH2 Mycobacterium tuberculosis strain 94001...	48.1	0.003
gb|AF189757.1|MTDRLF2 Mycobacterium tuberculosis strain 97005...	48.1	0.003
gb|AF189755.1|MTDRLE2 Mycobacterium tuberculosis strain 16923...	48.1	0.003
gb|AF189753.1|MTDRLD2 Mycobacterium tuberculosis strain 94003...	48.1	0.003
gb|AE000516.2| Mycobacterium tuberculosis CDC1551, complete g...	48.1	0.003
emb|AJ879180.1| Mycobacterium tuberculosis Rv1917c gene disru...	48.1	0.003
emb|AJ879179.1| Mycobacterium tuberculosis Rv1917c gene disru...	48.1	0.003

emb|BX248343.1| Mycobacterium bovis subsp. bovis AF2122/97 co... 48.1 0.003
emb|Z48304.1| M.tuberculosis direct repeat cluster DNA 48.1 0.003
emb|BX842579.1| Mycobacterium tuberculosis H37Rv complete gen... 48.1 0.003
emb|BX842580.1| Mycobacterium tuberculosis H37Rv complete gen... 48.1 0.003
emb|BX842583.1| Mycobacterium tuberculosis H37Rv complete gen... 48.1 0.003
emb|BX842581.1| Mycobacterium tuberculosis H37Rv complete gen... 48.1 0.003
emb|BX842577.1| Mycobacterium tuberculosis H37Rv complete gen... 48.1 0.003
emb|BX842582.1| Mycobacterium tuberculosis H37Rv complete gen... 48.1 0.003
emb|BX842578.1| Mycobacterium tuberculosis H37Rv complete gen... 48.1 0.003
emb|BX842576.1| Mycobacterium tuberculosis H37Rv complete gen... 48.1 0.003
emb|BX842574.1| Mycobacterium tuberculosis H37Rv complete gen... 48.1 0.003
gb|AF390039.1|AF390039S1 Mycobacterium tuberculosis strain SA... 48.1 0.003
gb|AF357173.1|AF357173 Mycobacterium tuberculosis isolate DS7... 48.1 0.003
gb|AF357166.1|AF357166 Mycobacterium tuberculosis isolate DS6... 48.1 0.003
emb|Y15749.1| Mycobacterium tuberculosis DNA for partial hr-d... 48.1 0.003
gb|AF181860.1|AF181860 Mycobacterium tuberculosis direct repe... 48.1 0.003
emb|AJ242908.1| Mycobacterium tuberculosis IS6110 genes and p... 48.1 0.003
emb|AJ242907.1| Mycobacterium tuberculosis partial plcD and R... 48.1 0.003
emb|X57835.2| Mycobacterium bovis insertion element IS6110 DNA 48.1 0.003
emb|Y08970.1| M.tuberculosis metB gene interrupted with IS987 48.1 0.003
emb|Y17220.1| Mycobacterium tuberculosis bj locus and (IS6110)2 48.1 0.003
emb|Y17219.1| Mycobacterium tuberculosis bj locus 48.1 0.003
emb|Y15805.1| Mycobacterium tuberculosis DNA for partial hr-d... 48.1 0.003
emb|X98154.1| M.tuberculosis IS6110, right inverted repeat; ipl4 48.1 0.003
emb|Y14614.1| Mycobacterium tuberculosis ipl8::IS6110 IS-like... 48.1 0.003
emb|Y14613.1| Mycobacterium tuberculosis ipl7::IS6110 IS-like... 48.1 0.003
emb|Y14048.1| Mycobacterium tuberculosis IS6110 element and d... 48.1 0.003
emb|Y14047.1| Mycobacterium tuberculosis IS6110 element and d... 48.1 0.003
emb|Y14046.1| Mycobacterium tuberculosis IS6110 element and d... 48.1 0.003
emb|Y14045.1| Mycobacterium tuberculosis IS6110 element and d... 48.1 0.003
gb|AD000019.1|MSGY223 Mycobacterium tuberculosis sequence fro... 48.1 0.003
gb|AD000007.1|MSGY414A Mycobacterium tuberculosis sequence fr... 48.1 0.003
emb|X52471.1| M. tuberculosis insertion sequence IS986 48.1 0.003
emb|X17348.1| Mycobacterium tuberculosis IS6110 IS-like element 48.1 0.003

gb|CP001032.1| Opitutus terrae PB90-1, complete genome 38.2 3.3
ref|XM_001393951.2| Aspergillus niger CBS 513.88 arginine per... 36.2 13
gb|CP002047.1| Streptomyces bingchenggensis BCW-1, complete g... 36.2 13
gb|CP001778.1| Stackebrandtia nassauensis DSM 44728, complete... 36.2 13
gb|CP001821.1| Xylanimonas cellulosilytica DSM 15894, complet... 36.2 13
gb|CP001785.1| Ammonifex degensii KC4, complete genome 36.2 13
gb|CP001349.1| Methylobacterium nodulans ORS 2060, complete g... 36.2 13
ref|XM_001910617.1| Podospora anserina S mat+ hypothetical pr... 36.2 13
emb|CU638744.1| Podospora anserina S mat+ genomic DNA chromos... 36.2 13
ref|XM_001708098.1| Giardia lamblia ATCC 50803 TCP-1 chaperon... 36.2 13
emb|AM270211.1| Aspergillus niger contig An09c0220, genomic c... 36.2 13
ref|NM_066286.2| Caenorhabditis elegans CaDHerin family membe... 36.2 13

ref|XM_753669.1| Ustilago maydis 521 hypothetical protein (UM... 36.2 13
gb|AF226725.1|AF226725 Giardia intestinalis chaperonin subuni... 36.2 13
gb|L14324.1| Caenorhabditis elegans cosmid ZK112, complete se... 36.2 13
gb|CP002743.1| Bifidobacterium breve ACS-071-V-Sch8b, complet... 34.2 51
gb|CP002409.1| Propionibacterium acnes 266, complete genome 34.2 51
ref|XM_003251597.1| PREDICTED: Apis mellifera FCH domain only... 34.2 51
ref|XM_624598.3| PREDICTED: Apis mellifera FCH domain only pr... 34.2 51
emb|FR799566.1| Leishmania mexicana MHOM/GT/2001/U1103 comple... 34.2 51
gb|CP002481.1| Acidobacterium sp. MP5ACTX9 plasmid pACIX901, ... 34.2 51
ref|XM_001398232.2| Aspergillus niger CBS 513.88 zinc finger ... 34.2 51
gb|CP002432.1| Desulfurispirillum indicum S5, complete genome 34.2 51
ref|XM_003000482.1| Verticillium albo-atrum VaMs.102 cyclin C... 34.2 51
gb|CP002040.1| Nocardiopsis dassonvillei subsp. dassonvillei ... 34.2 51
gb|FJ862019.1| Photorhabdus sp. Q614 DNA recombination protei... 34.2 51
gb|CP001977.1| Propionibacterium acnes SK137, complete genome 34.2 51
gb|CP001738.1| Thermomonospora curvata DSM 43183, complete ge... 34.2 51
gb|FJ653663.1| Mycobacterium tuberculosis clone TB4C insertio... 34.2 51
gb|FJ653662.1| Mycobacterium tuberculosis clone TB3A insertio... 34.2 51
gb|FJ653661.1| Mycobacterium tuberculosis clone TB2A insertio... 34.2 51
gb|CP001728.1| Alicyclobacillus acidocaldarius subsp. acidoca... 34.2 51
gb|CP001700.1| Catenulispora acidiphila DSM 44928, complete g... 34.2 51
ref|NG_012492.1| Homo sapiens plectin (PLEC), RefSeqGene on c... 34.2 51
ref|XM_002474692.1| Postia placenta Mad-698-R predicted prote... 34.2 51
gb|CP001614.2| Teredinibacter turnerae T7901, complete genome 34.2 51
ref|XM_002367247.1| Toxoplasma gondii ME49 hypothetical prote... 34.2 51
gb|CP001618.1| Beutenbergia cavernae DSM 12333, complete genome 34.2 51
gb|AC235087.2| Homo sapiens FOSMID clone ABC13-988622F7 from ... 34.2 51
gb|FJ638108.1| Synthetic construct Drosophila melanogaster cl... 34.2 51
gb|FJ633859.1| Synthetic construct Drosophila melanogaster cl... 34.2 51
ref|XM_002136685.1| Drosophila pseudoobscura pseudoobscura GA... 34.2 51
ref|XM_002136687.1| Drosophila pseudoobscura pseudoobscura GA... 34.2 51

References

4.6 References

1. Dalovisio, J. R. *et al.* Comparison of the amplified Mycobacterium tuberculosis (MTB) direct test, amplicor MTB PCR, and IS6110-PCR for detection of MTB in respiratory specimens. *Clinical Infectious Diseases* **23**, 1099-1106 (1996).

2. Eisenach, K. D., Cave, M. D. & Crawford, J. J. *Diagnostic molecular microbiology*. Persing, D. H., Smith, T. F., Tenover, F. C. & White, T. J. (eds.), pp. 191-196 (American Society for Microbiology, Washington, D.C.,1993).

3. Fernandez, J. G. *et al.* Comparison of three immunological diagnostic tests for the detection of avian tuberculosis in naturally infected red deer (Cervus elaphus). *Journal of Veterinary Diagnostic Investigation* **21**, 102-107 (2009).

4. Myeong-Hee, K., Hee-Young, Y., Jin-Tae, S. & Hee Joo, L. Comparison of in-house PCR with conventional techniques and Cobas Amplicor M. tuberculosis kit for detection of Mycobacterium tuberculosis. *Yonsei Medical Journal* **49**, 537-544 (2008).

5. Hill, H. D. & Mirkin, C. A. The bio-barcode assay for the detection of protein and nucleic acid targets using DTT-induced ligand exchange. *Nature Protocols* **1**, 324-336 (2006).

6. Hermanson, G. T. Bioconjugate Techniques. *Academic Press. Elsevier*., Oxford (2008).

7. Altschul, S. F. *et al.* Gapped BLAST and PSI-BLAST: a new generation of protein database search programs. *Nucleic Acids Research* **25**, 3389-3402 (1997). http://www.ncbi.nlm.nih.gov/

8. Lixin, A. *et al.* Characterization of a thermostable UvrD helicase and its participation in helicase dependent amplification. *Journal of Biological Chemistry* **280**, 28952-28958 (2005).

9. Vincent, M., Xu, Y. & Kong, K. Helicase-dependent isothermal DNA amplification. *EMBO Reports* **5**, 795-800 (2004).

10. Anderson, M., Torres-Chavolla, E., Castro, B. & Alocilja, E. One step alkaline synthesis of biocompatible gold nanoparticles using dextrin as capping agent. *Journal of Nanoparticle Research* DOI: 10. 1007/s11051-010-0172-3 (2010).

11. Zhang, D., Carr, D. J. & Alocilja, E. C. Fluorescent bio-barcode DNA assay for the detection of Salmonella enterica serovar Enteritidis. *Biosensors & Bioelectronics* **24**, 1377-1381 (2009).

12. Torres-Chavolla, E. & Alocilja, E. C. Nanoparticle based DNA biosensor for tuberculosis detection using thermophilic helicase-dependent isothermal amplification. *Biosensors & Bioelectronics* **In Press**, (2011).

13. Pumera, M., Aldavert, M., Mills, C., Merkoτi, A. & Alegret, S. Direct voltammetric determination of gold nanoparticles using graphite-epoxy composite electrode. *Electrochimica Acta* **50**, 3702-3707 (2005).

14. McPherson, M. J. & Moller, S. G. PCR. The Basics. *BIOS Scientific Publishers,* New York (2000).

15. Silva, L. B. *et al.* Portable optoelectronic biosensing platform for identification of mycobacteria from the Mycobacterium tuberculosis complex. *Biosensors & Bioelectronics* **26**, 2012-2017 (2011).

16. Das, M., Sumana, G., Nagarajan, R. & Malhotra, B. D. Application of nanostructured ZnO films for electrochemical DNA biosensor. *Thin Solid Films* **519**, 1196-1201 (2010).

17. Gazouli, M. *et al.* Specific Detection of Unamplified Mycobacterial DNA by Use of Fluorescent Semiconductor Quantum Dots and Magnetic Beads. *Journal of Clinical Microbiology* **48**, 2830-2835 (2010).

18. Kaewphinit, T., Santiwatanakul, S., Promptmas, C. & Chansiri, K. Detection of Non-Amplified Mycobacterium tuberculosis Genomic DNA Using Piezoelectric DNA-Based Biosensors. *Sensors* **10**, 1846-1858 (2010).

19. Duman, M., Caglayan, M. O., Demirel, G. & Piskin, E. Detection of Mycobacterium tuberculosis Complex Using Surface Plasmon Resonance Based Sensors Carrying Self-Assembled Nano-Overlayers of Probe Oligonucleotide. *Sensor Letters* **7**, 535-542 (2009).

20. Soo, P. C. *et al.* A simple gold nanoparticle probes assay for identification of Mycobacterium tuberculosis and Mycobacterium tuberculosis complex from clinical specimens. *Molecular and Cellular Probes* **23**, 240-246 (2009).

Chapter 5

Conclusion and Future work

The research presented in chapters 3 and 4 described the design and development of a biosensing platform based on the use of dextrin coated gold nanoparticles as electrochemical labels for the detection of a specific DNA sequence (particularly within the IS*6110* gene) targeting *Mycobacterium tuberculosis*. As part of the sample preparation steps for DNA based biosensors, it is required in most platforms to have a previous step of DNA amplification (most commonly PCR) before detection. PCR-based amplification is performed in a thermocycler, which is an expensive and specialized equipment that is not commonly available in peripheral laboratories of TB endemic countries with limited resources. In the present platform, thermophilic helicase-dependent isothermal amplification (tHDA) was incorporated for this step in lieu of PCR. Successful isothermal amplification of synthetic targets representing a specific Mtb DNA fragment was obtained and the amplified targets where successfully detected using the electrochemical AuNP-based platform.

Dextrin coated gold nanoparticles were used as novel electrochemical labels on the DNA based biosensor platform developed in this dissertation for TB detection. A new alkaline based biosynthesis procedure was proposed to produce dextrin coated gold nanoparticles in a single step reaction. The synthesis procedure was reproducible, the particles were stable for more than three months at room temperature and were successfully functionalized with DNA probes using procedures commonly used for citrate coated gold nanoparticles.

Since synthetic targets were used for the development of this biosensor, the obtained results are on the proof-of-concept level. Further studies of sensitivity and specificity using bacterial DNA and biological matrices (sputum) are necessary in order to address the main issues and constraints of sample preparation (DNA extraction); and optimize the platform using real samples. After this "in-lab" optimization stage with real samples, the designed platform can be evaluated in clinical trials "on-field" for potential use in peripheral laboratories using a handheld potentiostat and a portable PC.

Several methodologies and techniques have been developed for detection of nucleic acids using AuNPs. Most of them have been tested using synthetic or PCR prepared molecules as targets. Few methods have been applied to the detection of DNA directly in clinical samples and most of them involve PCR steps. Most platforms now need to be taken from proof-of-concept to use in real clinical diagnostic situations. Sampling preparation also needs to be addressed, since AuNPs can be susceptible to complex media.

The flexibility of the biosensor platform used has the potential of multiplexing several DNA targets. This opens a possibility to target specific fragments of the *rpoB* gene at the same time to detect rifampicin resistance mutations and presence or absence of Mtb. Multiple specific probes can be labeled using other metal nanoparticles for signal enhancement (cadmium, lead, zinc, etc) besides gold nanoparticles. These protocols are usually based on the capture of metal nanoparticle tracers followed by dissolution and stripping voltammetry measurement of the metal label. Each tracer produces a distinct voltammetric peak, which is useful in the development of multiplex detection systems. These metal traces can be used to label bio-barcode DNA sequences for the electrochemical detection of DNA targets using the sandwich hybridization technique with gold and magnetic nanoparticles.

Another alternative to explore could be the design of isothermal primers and hybridization probes to target transrenal TB DNA fragments and use urine instead of sputum as sample for the TB detection. Transrenal TB DNA has not been validated for TB detection and it is unknown if the DNA fragments found in urine are present in concentrations that will allow detection with the sensitivity available in current detection systems. Nevertheless, the use of urine as specimen for TB detection is a promising and convenient alternative to sputum for point-of-care diagnostic developments.